VSB - Technical University of Ostrava

Faculty of Mechanical Engineering

Department of Robotics

Affordable Active Lower Limbs Exoskeleton for People with Paraplegia

Dissertation Thesis

Study program:	P2346 Mechanical Engineering
Field of study:	2301V013 Robotics
Supervisor:	prof. Dr. Ing. Petr Novák
Ph.D. student:	Ing. Michal Gloger

Ostrava, 2018

Annotation of Dissertation Thesis:

GLOGER, Michal.   *Affordable Active Lower Limbs Exoskeleton for People with Paraplegia*, Department of Robotics, Faculty of Mechanical Engineering, VŠB-TU Ostrava, 114 pages, 108 figures, 31 tables. Supervisor: prof. Dr. Ing. Petr Novák

---

After a broad introduction to the medical and biomechanical background and detailed review of orthotic devices, two newly developed lower limbs exoskeletons for paraplegics are presented in this study.

There was found out the main challenges of designing devices for paraplegic walking can be summarized into three groups, stability and comfort, high efficiency or low energy consumption, dimensions and weight. These all attributes have to be moreover considered and maintained during manufacturing of affordable device while setting a reasonable price of the final product.

A new economical device for people with paraplegia which tackles all problems of the three groups is introduced in this work. The main idea of this device is based on HALO mechanism. HALO is a compact passive medial hip joint orthosis with contralateral hip and ankle linkage, which keeps the feet always parallel to the ground and assists swinging the leg. The medial hip joint is equipped with one actuator in the new design and the new active exoskeleton is called @halo.

Due to this update, we can achieve more stable and smoother walking patterns with decreased energy consumption of the users, yet maintain its compact and lightweight features. It was proven by the results from preliminary experiments with able-bodied subjects during which the same device with and without actuator was evaluated. Waddling and excessive vertical elevation of the centre of gravity were decreased by 40% with significantly smaller standard deviations in case of the powered exoskeleton. There was 52% less energy spent by the user wearing @halo which was calculated from the vertical excursion difference. There was measured 38.5% bigger impulse in crutches while using passive orthosis, which produced bigger loads in upper extremities musculature. The inverse dynamics approach was chosen to calculate and investigate the loads applied to the upper extremities. The result of this calculation has proven that all main muscle groups are engaged more aggressively and indicate more energy consumption during passive walking. The new @halo device is the first powered exoskeleton for lower limbs with just one actuated degree of freedom for users with paraplegia.

Anotace disertační práce:

GLOGER, Michal.   Ekonomicky dostupný aktivní exoskeleton pro dolní končetiny pro paraplegiky, Katedra Robotiky, Fakulta strojní, VŠB-TU Ostrava, 114 stran, 108 obrázků, 31 tabulek. Školitel: prof. Dr. Ing. Petr Novák

První část práce je věnována obsáhlému úvodu do zdravotnické a biomechanické terminologie a detailnímu souhrnnému představení ortopedických pomůcek. Následně jsou představeny dva nově vyvinuté exoskelety aplikovatelné na dolní končetiny paraplegiků.

Bylo zjištěno, že hlavní úskalí konstrukčního návrhu asistenčních zařízení pro paraplegiky lze shrnout do tří hlavních skupin, jako první je stabilita a komfort, druhá je vysoká účinnost a nízká energetická náročnost uživatele a do třetí lze zahrnout rozměry a hmotnost zařízení. Toto všechno je navíc podmíněno přijatelnou výslednou cenou produktu.

Nový ekonomicky dostupný exoskelet pro paraplegiky, který řeší problematiku všech tří zmíněných skupin je představen v této práci. Hlavní myšlenka tohoto zařízení je postavena na mechanismu HALO ortézy. HALO je kompaktní pasivní ortéza s mediálním kyčelním kloubem umístěným uprostřed mezi dolními končetinami. Speciální mediální kyčelní kloub je kontralaterálně propojen s kotníkem soustavou ocelových lanek což zajišťuje paralelní polohu chodidla se zemí v každém okamžiku chůze a navíc asistuje zhoupnutí končetiny. Tento mediální kyčelní kloub je redesignován a v novém provedení je vybaven jedním aktuátorem, nové řešení aktivního exoskeletu dostalo název *@halo*.

Díky tomuto vylepšení lze dosáhnout stabilnější a plynulejší chůze s výrazně redukovanou energetickou náročností uživatele přičemž dochází k zachování nízké hmotnosti a kompaktnosti zařízení. Toto bylo dokázáno během předběžných experimentů se zdravými subjekty, během kterých byla testována aktivní chůze se zařízením vybaveným odnímatelnou pohonnou jednotkou a pasivní chůze se stejným zařízením bez této aktivní jednotky. Nadměrné naklánění se během chůze ze strany na stranu a nadměrná výchylka pohybu těžiště těla ve vertikálním směru byly sníženy o necelých 40% s velmi významně menšími standardními odchylkami v případě chůze s pohonem. Z rozdílu výchylky pohybu těžiště těla ve vertikální poloze bylo vypočítáno snížení energetické náročnosti uživatele o 52% při chůzi s aktivní konfiguraci *@halo*. Při pohybu s pasivní ortézou byl naměřen o 38,5% větší reakční silový impuls v berlích, což znamená nárůst zátěže pro svalový aparát horních končetin. Pro podrobné vyšetření zátěže ramenních kloubů byl aplikován model inverzní dynamiky. Výsledek tohoto výpočtu jednoznačně indikuje agresivnější a hlubší zapojení všech svalových skupin ramenního kloubu a tím vyšší spotřebu energie uživatelem během pasivní chůze. Nové asistenční zařízení *@halo* je prvním exoskeletem svého druhu pro paraplegiky s jediným poháněným stupněm volnosti.

Acknowledgement

" Never say never, but take it easy... "

On the journey to completion of this work I have realised, many amazing and kind people live on this planet and I was lucky enough to meet some of them.

I dedicate this work to a person with the most beautiful character, heart, and soul I have ever encountered, to a person who is here ready to help, give an advice and support me in any instant of my all life,

I dedicate this work to my Mother.

1 Contents

2 List of labels and abbreviations

	DESCRIPTION	UNIT
$\vec{x_i}$	position vector of CoG of ith segment	m
m_{total}	total mass of the subject together with device	kg
m_i	mass of ith segment	kg
$\vec{r}_{SGR}$	position vector from the glenohumeral joint to the marker on the tip of the crutch	m
$\vec{r_i}$	position vector from shoulder joint to the ith segment centre of gravity	m
$\vec{M}_{Ii}$	inertial moment due to ith segment	Nm
$P_{proximal}$	power of the proximal segment of the joint	W
P_{distal}	power of the distal segment of the joint	W
$\vec{v}_{proximal}$	linear velocity of the proximal segment of the joint	$m \cdot s^{-1}$
$\vec{v}_{distal}$	linear velocity of the distal segment of the joint	$m \cdot s^{-1}$
$\vec{\omega}_{proximal}$	angular velocity of the proximal segment of the joint	$rad \cdot s^{-1}$
$\vec{\omega}_{distal}$	angular velocity of the distal segment of the joint	$rad \cdot s^{-1}$
$\vec{\omega}_s$	angular velocity in glenohumeral joint	$rad \cdot s^{-1}$
$\vec{\tau}_S = \vec{M}_S$	moment in a shoulder joint	Nm
$\vec{P}_S$	power flow in glenohumeral joint (shoulder joint)	W
$\vec{\theta}_s$	relative angle vector between upper arm segment and trunk segment	rad
a_i	inertial acceleration of ith segment	$m \cdot s^{-2}$
g	gravitational acceleration	$m \cdot s^{-2}$
$\vec{F}_s$	force vector acting in glenohumeral joint (shoulder joint)	N
$\vec{F}_{GR}$	ground reaction force vector	N
M_{bg}	moment of output shaft from the bevel gearbox	Nm
GRF	ground reaction force	
CoG	centre of gravity	
DoF	degree of freedom	

3 Introduction

3.1 Structure of this work

- *Section 1 – Introduction Chapter*

  Introduction chapter contains medical background and explanation of a terminology used in this work as well as the description of the focus group of the future potential customers. But the main contents of this section is an explanation of the motivation for this work together with the aim and the main objectives and the structure of whole thesis is presented as first.

- *Section 2 - Orthoses and Exoskeletons for lower limbs chapter*

  Main terminology in the field of orthotic devices is discussed here as well as denotation and use of terms "Active Orthosis" and "Exoskeleton". A Broad review of orthoses for lower limbs is in details presented here in order to be able to choose appropriate components and materials for designing new active exoskeletons which will meet the main objectives. As the final part of this chapter all important requirements which the new design of a powered exoskeleton have to meet are summarised and listed in the requirement list.

- *Section 3 – Design of new Exoskeleton Ortholeg 2.0*

  Two new powered Exoskeletons which were designed for the purpose of this study are presented as next. First new exoskeleton Ortholeg 2.0 is presented in this chapter. Exoskeleton Ortholeg 2.0 was designed in the Universidade Federal do Rio Grande do Norte (UFRN), Brazil and some of components were manufactured to test their actual functionality. Manufacturing processes and benefits of this new system are discussed in this chapter.

- *Section 4 - New active exoskeleton @halo and passive orthosis Halo*

  Second new active exoskeleton *@halo* and its passive version *Halo* are presented in details in this section of the work. Exoskeleton *@halo* was developed in the Department of Robotics Science & Engineering of Chubu University, Japan. Mechanical design and control system of novel exoskeleton are explained and described in details in this chapter.

- *Section 5 - Experiments procedure and experimental set up*

  Exoskeleton which meets requirements from the requirement list and which fits better the aims of this work is selected in this section. Exoskeleton *@halo* was chosen as better solution. Walking with active *@halo* device and passive *Halo* orthosis was tested during preliminary experiments. All necessary details about experiments such as experimental set up, experimental trials, data acquisition techniques and description of equipment used during experiments are presented in this chapter.

- *Section 6 - Gait Analysis and evaluation of walking with Halo and @halo*

  Scientific methods of processing and evaluating data from preliminary experiments are discussed in this section. Walking patterns of active *@halo* and passive *Halo* device are compared. Parameters for comparison are step length, velocity, centre of gravity displacement, force impulse in crutches and loads in shoulder joints. Utility of *@halo* device is validated based on this comparison.

- *Section 7 – Conclusions*

Overall contribution of this work for scientific discipline and practise are discussed in this chapter as well as recommendation for further research.

3.2 Motivation

As many as 500 000 people suffer a spinal cord injury every year according World Health Organization (WHO) statistics. People after SCI are two to five times more likely to die prematurely and their economic participation is much lower. Life of people with some form of paraplegia or tetraplegia changes rapidly, school enrolment and employment rate drops significantly with global unemployment rate of more than 60% and substantial individual and societal costs emerge. After such consequences 20-30% of people with spinal cord injury show clinically significant signs of depression, after rapid physiological deterioration psychical state of patient comes as next. This brings negative prognoses for future overall health improvement. Very important aspect at this stage is access to professionals and equipment in the field of rehabilitation and assistance and support services. Talking about rehabilitation technology unfortunately only as low as 5-15% of people in low- and middle-income countries have access to the assistive devices they need. This alarming facts were reflected into WHO`s Global Disability Action Plan where its second objective is:

- *To strengthen and extend rehabilitation, habilitation, assistive technology, assistance and support services, and community-based rehabilitation.*

From this point is obvious, that despite of fact that development in this field is growing, there is still not enough done to cover global needs. This work focuses on people with paraplegia, who end up on wheelchair. In order to carry on in healthy life it is important to undergo regular rehabilitation procedures and try to activate body as much as before trauma, the best way how to achieve that is to put a wheelchair aside. Walking and being able to move from one place to another without wheelchair can be beneficial not only because of increased upright mobility, so to reach hardly accessible objects became possible, but there are many other benefits which can allow disabled people to live healthier life. Advantages discussed in many surveys and studies can be:

- *Reduction of spasticity and potential muscle atrophy by stretching back and legs muscles which are continuously contracted and thigh over time*

- *Improvement of lower extremities contractures leading to deformity and rigidity of joints by augmenting range of motion which keeps joints more flexible*

- *Prevention of Decubitus ulcers caused by prolonged sitting*

- *Overall poise improvement*

- *Possible improvement of functionality of some internal organs e.g.*

    - *augmentation of natural bowel movements and improvement of digestion and stomach functionality*

    - *Improvement of bladder function and decreasing urinary tract infections*

    - *respiratory system and better breathing capability;*

    - *Cardiovascular system by improving circulation of blood in all body*

- *decreasing bone osteoporosis by natural loading of bones*

- *And psychological effect like increased self-confidence and self-esteem and good way how to cope with depression*

Many studies outcomes may speculate unequivocal proofs of such and other benefits. Vast majority of these results are however based on plain surveys not on scientifically proven facts. The most important aspects which are fundamental for promising overall health improvement of paraplegics are frequency and the length of use of orthotic devices which was generally consistent conclusion (M.T. Karimi et al. 2011). The life-long usage of assistive equipment can be the key for happier life with overall physiological and psychological improvement. Long term rehabilitation procedures at hospitals are time consuming and expensive and many patients discontinue attending this sessions in early stages. Unfortunately vast majority of users gave up using assistive technologies like exoskeletons or other orthotic devices outside therapeutic rooms as well. The main problems with orthoses and exoskeletons use are:

- *High energy expenditures, metabolic costs*

- *Mobility speed on wheelchair is incomparably higher than with orthoses*

- *Long and uncomfortable donning and doffing of orthoses, sometimes even not possible without assistance of second person*

- *Big forces applied on upper limb musculature while using crutches*

- *Price of such equipment in case of some actuated configurations*

In order to cope with this situation, there is vital and important to focus on development and manufacturing of such device, which can tackle these problems.

3.3   Aim

Today's products and research in the field of active assistive robotic devices for lower extremities are mostly focusing on adapting normal walking patterns, which means increased number of degrees of freedom. This way we can achieve high stability and low metabolic costs, but price is much higher and design can became bulky (Dollar a Herr 2008). Brief survey, conducted during international championship Czech Open 2015 - Para Table Tennis where were questioned nearly 50 players in category TM1-5 (sitting classes), showed surprisingly very sceptic view of responders on current technology, nearly 80% answers were clearly pointing out imbalance between usefulness (efficiency), price and complexity of devices. This results clearly indicate need of simplification and significant reduction of price in order to increase future demand and interest of users. The aim is rather focus on simple lightweight, compact and economically accessible solutions similar to reciprocal gait orthosis (RGO) or hip guidance orthosis (HGO) (Harvey et al. 1998), (Winchester et al. 1993). RGOs stabilize ankles, knees, hips, and trunk to provide upright posture and due to a reciprocal link between hip joints, more stable walking with reduced metabolic energy consumption can be achieved (Moore a Stallard 1991), (Rose 1979). It was found out coupling contralateral joints is a good way how to increase efficiency of paraplegic walking. A successful walking with these orthoses is however derived from upper body strength. Most of the users failed to continue using these devices outside therapeutic rooms due to inability to control horizontal pelvic rotation and hip flexion, which results in no symmetrical gait with large deviations in stride lengths and velocities. Balance and stability is maintained by use of crutches, this can produce big forces acting on upper limbs. Such excessive load can in case of long term use lead to shoulder pain or the incidence of some diseases. Fear from falling due to low stability was reported as another factor of giving up regular independent walking (M.T. Karimi et al. 2011).

The main aim is to develop affordable actuated exoskeleton for users with complete or incomplete paraplegia which will provide them with smoother walking patterns, increased stability, reduced amount of the force applied on the upper limbs and decreased overall energy consumption. Thus the users can feel safe and comfortable, walk with quick adaptation and less effort and therefor decide to use such exoskeleton regularly in daily life. New device will became every day assistance for maintaining better overall health of paraplegic users by introducing upright mobility in their lives.

3.4 Objectives

The process of determining the main objectives of design of device, was taken entirely from user's perspective. According user's needs we can divide these objectives into four groups:

1. Walking with device must not be toil
    1.1. Efficiency - Energy consumption of users must be reduced to level close to normal walking.
    1.2. Modularity - User can decide whether to use passive or active setting of assistive device.

2. Walking with device should be enjoyable and pleasant. Presence of fear is unacceptable:
    2.1. Stability - Fear from falling significantly reduces desire for everyday regular use.
    2.2. Safety - Safe means mainly increased stability and construction and control without failure.
    2.3. Comfort - Perfect fit and effective force transfers from device to user.

3. Users must be independent, because the independence is as well the purpose of this device:
    3.1. Lightweight, easy to carry, compact device which is quick and easy to
    3.2. Don/Doff directly from a wheelchair are the key elements.

4. Sorry, I am not a millionaire... yet.
    4.1. Economical, affordable solution for everyday use at home
    4.2. Maintenance free and robust design is enclosing the list of important features.
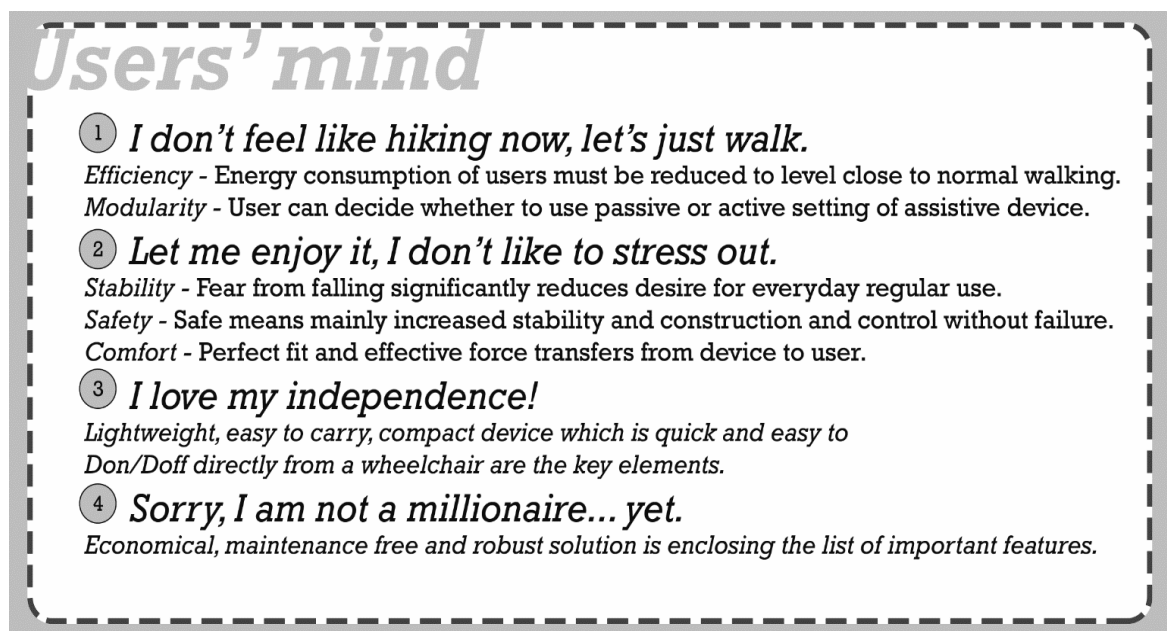

Figure 3.1 The main objectives – Flyer

3.5 Medical Background

Some of the medical terminology used frequently in this work is explained here. This study focuses on biomechanical evaluation of gait patterns, thus it is fundamental to explicitly explain particular terms from medicine related fields.

Anatomy of spine and spinal cord is explained in this chapter as well as common diseases which could lead to paralysis of lower limbs with consequent need for rehabilitation.

3.5.1 Spine and spinal cord

The spine consists of 33 bones build up one on top of the other, see Figure 3.2. Flexible tendons and ligaments are attached to spinal column and connects to strong muscles in order to carry out its main function to support body and protect the spinal cord from its injury. The spinal cord is about 45 cm long and is about thickness of thumb. It runs in the spinal canal from the brainstem to the 1st lumbar vertebra. At the end of the spinal cord, the cord fibres split and continue down through the spinal canal to tailbone before branching off to legs and feet. The spinal cord serves as an information super-highway, relaying messages between the brain and the body. The brain sends motor messages to the limbs and body through the spinal cord allowing for movement. The limbs and body send sensory messages to the brain through the spinal cord about what we feel and touch. Sometimes the spinal cord can react without sending information to the brain. These special pathways, called spinal reflexes, are designed to immediately protect our body from harm. The nerve cells that make up spinal cord itself are called upper motor neurons. The nerves that branch off spinal cord down to a back and neck are called lower motor neurons. These nerves exit between each of vertebrae and go to all parts of body.

3.5.2 Common diseases and reasons for lower limb rehabilitation

There are several reasons for rehabilitation of lower limbs, one of the most common reason is recovering of function after orthopaedic surgeries like arthroplasty e.g. after hip joint replacement patients often start physical therapy straightaway. Besides of diseases of bones, joints and structures connected to them, there are several diseases which may commonly result in functional loss in lower extremities, most common are, (Cuccurullo 2015) :

- *Stroke*

  Sudden local or sometimes global neurologic deficit secondary to occlusion or rupture of blood vessels supplying the brain. AFO greatly improve gait mechanisms and efficiency by preventing the passive or active plantar flexion in swing and stance phases. With use of AFO there is also less need for hip and knee flexion and pelvic elevation to gain foot clearance. An orthosis which can assist in knee extension improves stance stability during the period of decreased muscle tone.

- *Cerebral Palsy (appears in early childhood)*

  Lower limb orthoses can effectively improve the gait of some children with this disease, ankle foot orthoses are often used in this case.

- *Post-polio syndrome*

Postpolio syndrome (PPS) is a neurologic disorder characterized by progressive muscular weakness, pain, and fatigue many years after the acute paralytic infectious disease caused by the poliovirus. Orthoses and assistive devices can help to stabilize the patients' unstable and painful joints and can improve energy consumption of patients during ambulation. With knee-ankle-foot-orthosis (KAFO) and crutches, energy expenditure can be reduced by 25% during ambulation.

- *Guillain-Barrie syndrome*

GB syndrome is disorder in which the immune system of the body attacks some of the peripheral nervous system. Symptoms of this disease include sudden weakness or loss of reflexes and tingling sensations in legs, arms and other parts of your body. AFO orthoses can be used in this case in order to support weakened lower limbs.

- *Transverse myelitis*

Transverse myelitis is a rare neurological syndrome. It is an inflammatory disorder of the spinal cord. KAFO or AFO can be prescribed in case of paraplegia or foot drop which resulted after acute form of disease.

- *Amyotrophic lateral sclerosis (motor neurone disease group)*

This is a specific disease that causes the death of neurons which control voluntary muscles. KAFO may be used to improve locomotor functions.

- *Foot drop*

AFO are usually prescribed to improve gait pattern and support flexion of ankles.

- *Spinal cord injury (SCI)*

SCI is damage to the spinal cord. This disease is one of the most common reasons for lower extremities paralysis, thus will be discussed in detail in following chapter.

3.5.3   Spinal cord injury and the levels of the lesion

The term 'spinal cord injury' refers to damage to the spinal cord resulting from trauma (e.g. a car crash) or from disease or degeneration (e.g. cancer). There is no reliable estimate of global prevalence, but estimated annual global incidence is 40 to 80 cases per million population. Up to 90% of these cases are due to traumatic causes, though the proportion of non-traumatic spinal cord injury appears to be growing according WHO Fact sheet N°384 November 2013.

Symptoms of spinal cord injury depend on the severity of injury and its location on the spinal cord. Symptoms may include partial or complete loss of sensory function or motor control of arms, legs and/or body. The most severe spinal cord injury affects the systems that regulate bowel or bladder control, breathing, heart rate and blood pressure. Most people with spinal cord injury experience chronic pain.

Tetraplegia (or quadriplegia) is impairment or loss of motor and/or sensory function in the cervical segments of spinal cord due to damage of neural elements in spine. Tetraplegia results in impairment of function in arms, trunk, legs, and pelvic organs. Paraplegia is impairment or loss of motor and/or sensory function in thoracic, lumbar, or sacral segments of spinal cord. Trunk, legs, pelvic organs may be involved while having paraplegia, but arm functionality is not affected.

High-Cervical Nerves (C1 – C4)

- damage is the most severe of the SCI
- Paralysis in arms, hands, trunk and legs
- Patient may not be able to breathe, cough, or control bladder or bowel movements.
- Ability to speak is sometimes impaired or reduced.
- Requires complete assistance with activities of daily living, such as eating, dressing, bathing, and getting in or out of bed
- May be able to use powered wheelchairs with special controls to move around on their own

C4 injury
Tetraplegia
or
Quadriplegia

Low-Cervical Nerves (C5 – C8)
Corresponding nerves control arms and hands.

C5 injury

- Person can raise his or her arms and bend elbows. Likely to have some or total paralysis of wrists, hands, trunk and legs
- once in a power wheelchair, can move from one place to another independently

C6 injury

- Paralysis in hands, trunk and legs, typically speak and use diaphragm,
- Can move in and out of wheelchair and bed with assistive equipment

C7 injury

- Nerves control elbow extension and some finger extension, straightening of arm and movement of shoulders is possible.
- Mostly independent with assistive technology
- C8 injury
- Nerves control some hand movement should be able to grasp and release objects
- Mostly independent with assistive technology

C5 injury
Tetraplegia
or
Quadriplegia

Cervical
vertebrae
C1 - C7

Thoracic
vertebrae
T1 - T12

Lumbar
vertebrae
L1 - L5

SACRUM
S1 - S5

Coccyx
C1 - C4
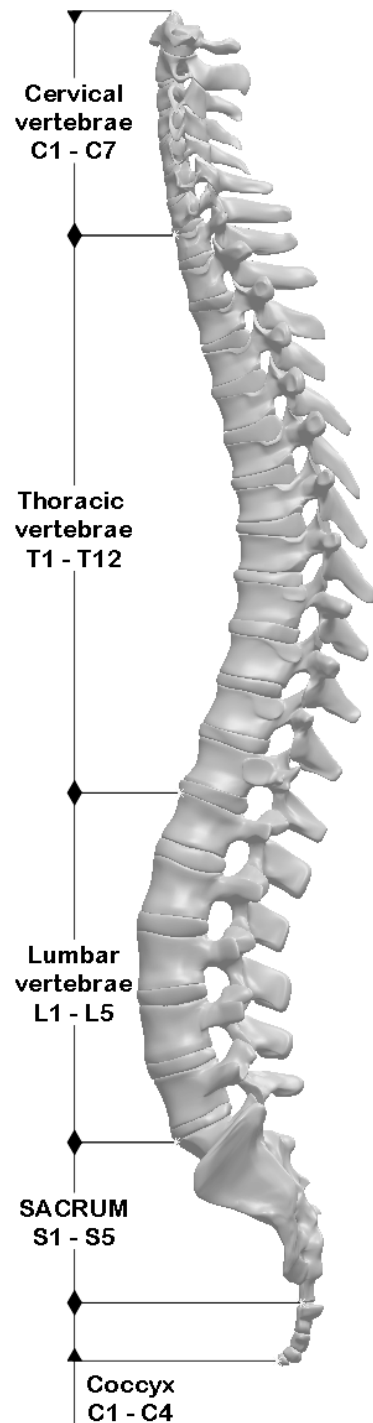
Figure 3.2 Spine

Thoracic Nerves (T1 – T5)

Corresponding nerves affect muscles, upper chest, mid-back and abdominal muscles.

- Arm and hand function is usually normal.
- Injuries affect the trunk and legs
- Can use a manual wheelchair
- May drive a modified car
- Can stand in a special standing frame
- May be rarely able to walk with braces

Thoracic Nerves (T6 – T12)

Nerves affect muscles of the trunk (abdominal and back muscles)

- Normal upper-body functionality n
- Fair to good ability to control and balance trunk while in the seated position
- Should be able to cough productively (if abdominal muscles are intact)
- Can use a manual wheelchair
- Can learn to drive a modified car
- Can stand in a special standing frame
- May be able to walk with braces
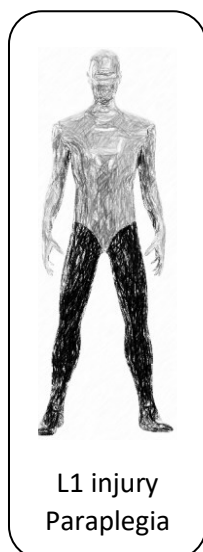
Lumbar Nerves (L1 – L5)

Injuries generally result in some loss of function in the hips and legs. May need a wheelchair but may also be able to walk with braces.

- Injuries result in some loss of function in the hips and legs.
- may need a wheelchair
- Can walk with braces

Sacral Nerves (S1 – S5)

- Some loss of function in the hips and legs.
- Most likely can to walk

T6 injury

Paraplegia

L1 injury
Paraplegia

Cervical vertebrae
C1 - C7

Thoracic vertebrae
T1 - T12

Lumbar vertebrae
L1 - L5

SACRUM
S1 - S5

Coccyx
C1 - C4

Figure 3.2 Spine

16

3.6   Focus Group

The main focus group are the users with SCI T6 – T12 – symmetrical complete and incomplete paraplegia, hemiplegic group of the users however can be considered as well.

As discussed in the previous subchapter there are many more diseases and reasons for lower limb paralysis. This means the end-user group does not need to be such specific and can be widen to any person with lower limb paralysis. The level of paralysis needs to be consulted with doctors and physiotherapists, who can give the best recommendation of proper solution for upright mobility.

3.7   Biomechanical Background

This work focuses on quantitative analysis of the motion based on data collected during walking experiments performed with novel active exoskeleton. This approach requires basic understanding of biomechanical terminology which is presented in this chapter. Definition of space in which experiments were performed, such as planes and coordinate systems are presented here as well as anatomical terms, description of movement of body segments, stride cycle or determinants of gait.
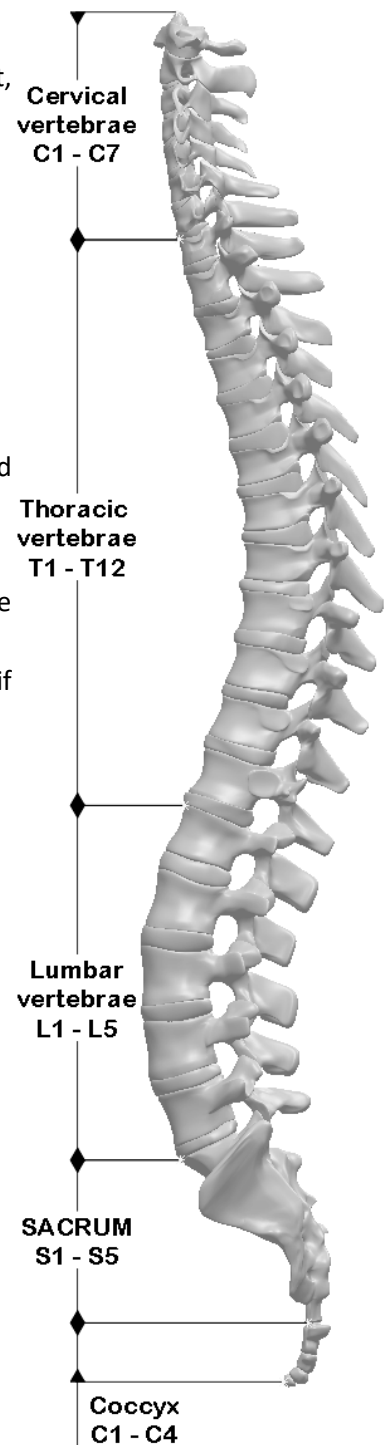
3.7.1   Space definition

Movement during experiments was performed in space defined by planes, global coordinate system and local coordinate systems attached to each body segment.

According general rules we term sagittal plane as travelling plane which direction is defined by anteroposterior axis. If we relate to global coordinate system (GCS), this axis would be in parallel with X axis. Frontal or coronal plane is in which vertical movement is evaluated and direction is defined by vertical (longitudinal) axis witch is in parallel with Z axis of GCS. Transverse or horizontal plane is plane where lateral movement appears which direction is defined by mediolateral or horizontal axis, this axis is in parallel with Y axis of GCS, all planes and GCS is shown on Figure 3.3.

3.7.2   Denotation of Segments

The main segment naming as it will be used throughout all this work is shown on Figure 3.4. Upper limbs consist of upper arms, forearms and hands segments. Upper arms are connected to trunk through glenohumeral joint (shoulder joint), upper arm then performs relative movement with respect to trunk segment. A forearm is connected to the upper arm via an elbow join and a hand to the forearm via a wrist joint. Lower limbs consist of thighs, legs (shins) and feet segments. The thighs are connected to the trunk via a hip joint and perform relative movement with respect to the trunk segment. The Legs are connected to the thighs via a knee joints and the feet via an ankle joint.
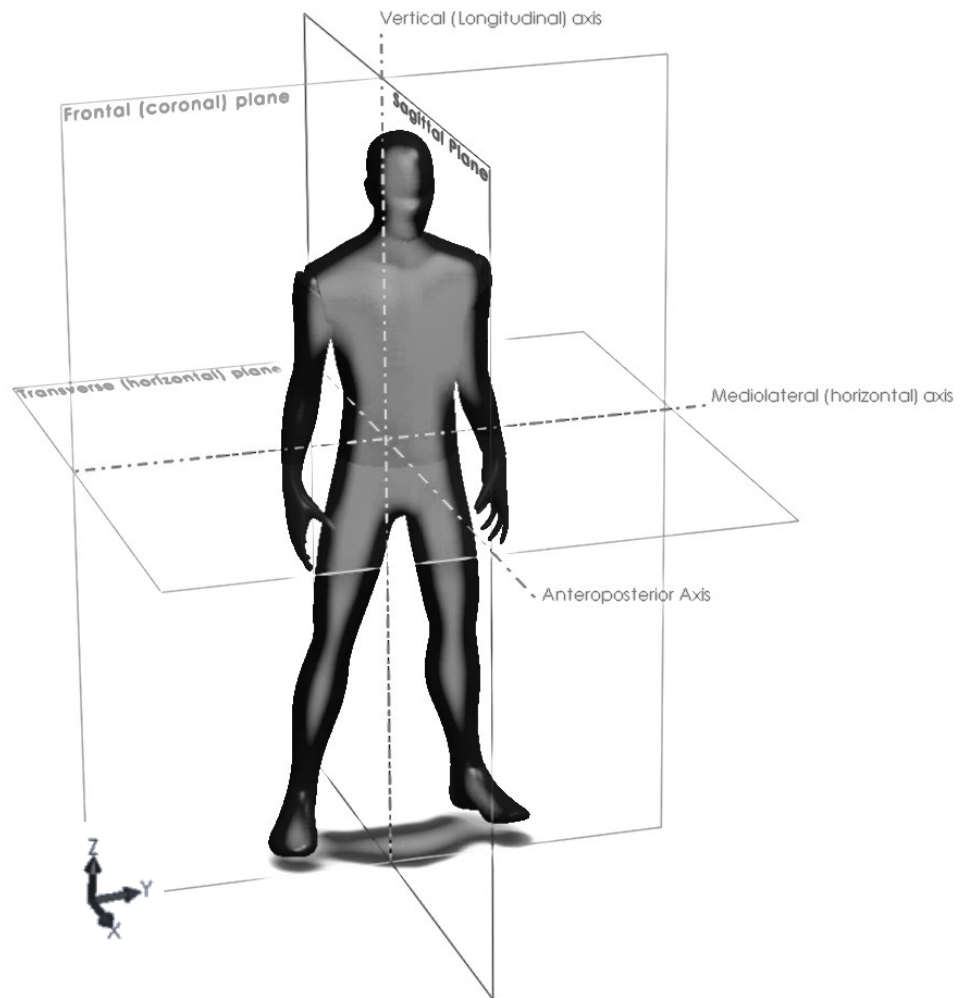
Figure 3.3 Definition of space, denotation of planes and axes
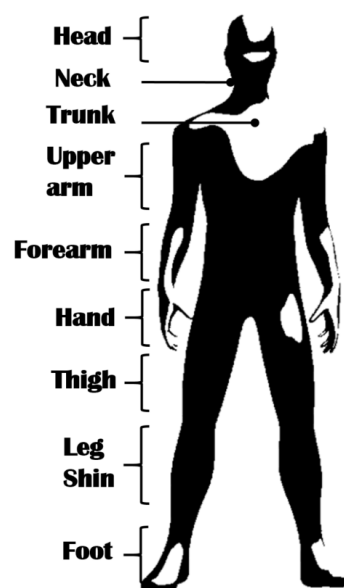

Figure 3.4 Denotation of segments

3.8 Anatomical terms

In this subchapter the most important terms regarding definition of position of segments or anatomical landmarks with respect to reference point of the body are described, (Hamill a Knutzen 2009). Investigation of movement and position of the centre of gravity (COG) of the body is one of the key elements of the analysis chapter of this work, this is why it is fundamental to set the proper naming and terms, which can vary in different literatures, for the graphical representation of these terms see Figure 3.5.

- *Absolute and relative Angles*

First of all in order to discuss joints kinematics, we must define the joint angle. Absolute angle is angle between related axes of GCS and coordinate system of segment (LCS). Angle between two segments LCSs is called relative angle. In the evaluation chapter of this work for instance, there relative angle between trunk and upper arm segments is needed in order to calculate power flow through glenohumeral joint.

- *Movement or position of COG – mediolateral*

In order to describe directions of movement of the COG of body following terminology needs to be defined. The term medial refers to a movement towards mid-axis (vertical axes) or position relatively close to the middle of the body. The opposite of medial movement is lateral. Lateral movement describes motion away from mid-axis or on sides of the body. Lateral position is far from the middle of body. The term **mediolateral** movement of COG describes movement of COG towards and away from the middle of the body or towards sides. This movement occurs in horizontal direction in direction of horizontal (mediolateral) axis. Mediolateral movement is referring to so called **waddling** in following chapters of this work.

- *Movement or position of COG – anteroposterior*

Forward or backward bend result in anterior or posterior movement of COG of the body. This movement occurs in sagittal plane and in direction of anteroposterior axis. In following chapters this movement of COG is called **anteroposterior or sagittal** movement. **Forward progression** is another term which occurs in this study and refers to movement of the COG of body in travelling direction.

- *Movement or position of COG – Vertical elevation*

Superior and inferior are used to describe segment or COG of segment position with respect to body, former is referring to point closer to the top of the body or above the reference and latter is below the reference. Movement of COG of body related to superior and inferior direction is described in following chapters as movement in vertical direction or **vertical elevation**

- *Proximal and distal relative position*

Proximal and distal are used to describe the relative position with respect to a designated reference point. **Proximal** point is the point closer to reference and **distal** is further form the reference. If we take the glenohumeral joint as the reference point, then the wrist joint is distal point and the hand is distal segment, but the elbow joint is proximal point and the arm is proximal segment.

- *Ipsilateral and contralateral location*

The term **ipsilateral** describes activity or location of a segment positioned on the same side as a particular reference point. Actions, positions, and locations on the opposite side can be entitled as **contralateral**.
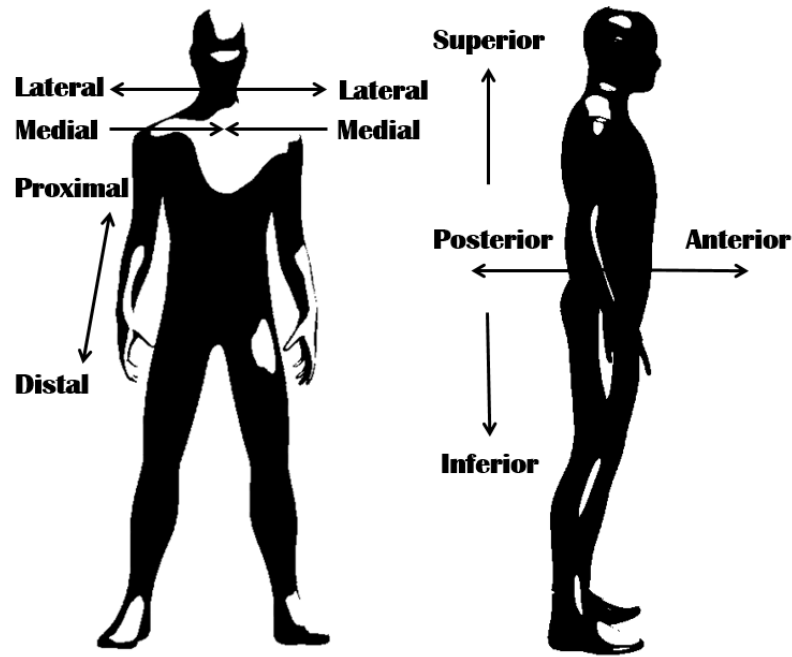
Figure 3.5 Terms defining position of segments or anatomical landmarks

3.8.1 Movement of segments description

I order to be able to investigate movements of the segments and describe their relative positions with adjacent segments, we need appropriate terminology (Hamill a Knutzen 2009), for the graphical representation of these terms see Figure 3.6.

- *Flexion and Extension*

Flexion is movement of two connected segments during which relative angle between these segments decreases. The Upper limbs fundamental position is with arms in relaxed posture at the sides with the palms facing in toward the trunk. The Relative angle between trunk segment and the upper arm is in this moment 180°, while rising arm forward flexion occurs in glenohumeral joint until we reach horizontal position (arm parallel with the ground) when relative angle decreases to 90°. Same with elbow joint, starting angle between upper arm and forearm is 180°. Flexing or banding in elbow joint decreases angle between these two segments. **Extension** is movement opposite to flexion, angle between two adjacent segments is increasing.

- *Abduction and adduction*

Abduction is a movement of the segment to sides out of the mid-axis of the body. Adduction is opposite to abduction, it is a movement towards the mid-axis of the body. Raising an arm to the side is an example of abduction.

- *Medial and lateral rotation*

A rotation can be either medial (also known as internal) or lateral (also known as external). Example of lateral rotation of arm from upper limbs fundamental position is rotating palms from facing in toward the trunk to facing forward.

20
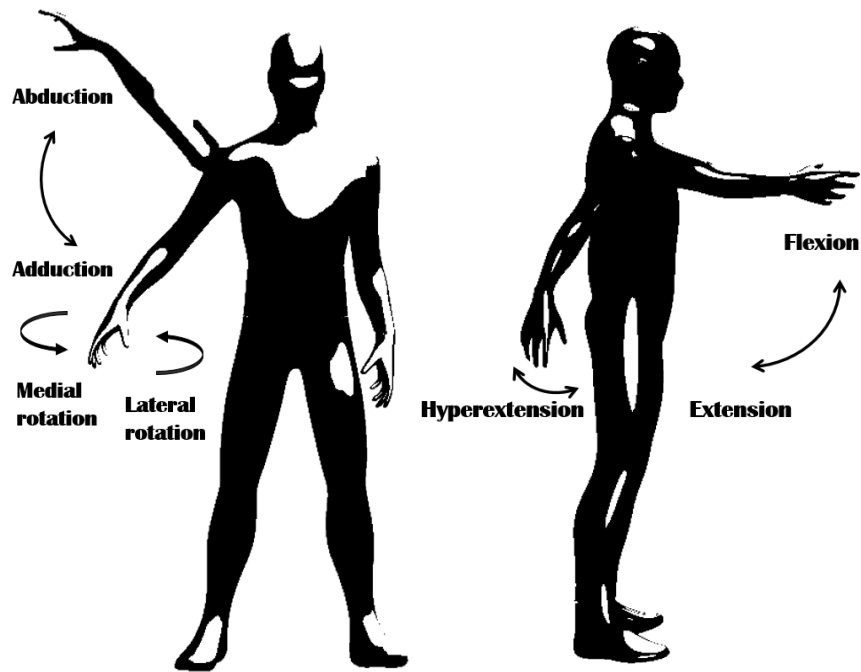
Figure 3.6 Movement of segments description

3.8.2   Gait analysis terminology

The gait cycle consists of one stride. The stride generally begins by one leg initial contact (the heel strike of the stance leg – the first manikin on Figure 3.7 in this case the right leg) following by the loading response through the foot flat until the toe off where midstance begins. Terminal stance follows after midstance and ends by heal strike of swing leg - black left leg. Last part of stance phase is preswing which ends by toe off of stance leg. Swing phase consists of initial swing, mid swing and terminal swing. Initial swing starts just after the toe off of the stance leg. The gait cycle ends same as begins by the heal strike of the same foot. The stance phase is approximately 60% of the gait cycle, leaves swing phase just 40%. This applies to normal slow walking patterns. All attributes of the gait cycle pattern including proper naming of each event during stride is on Figure 3.7.
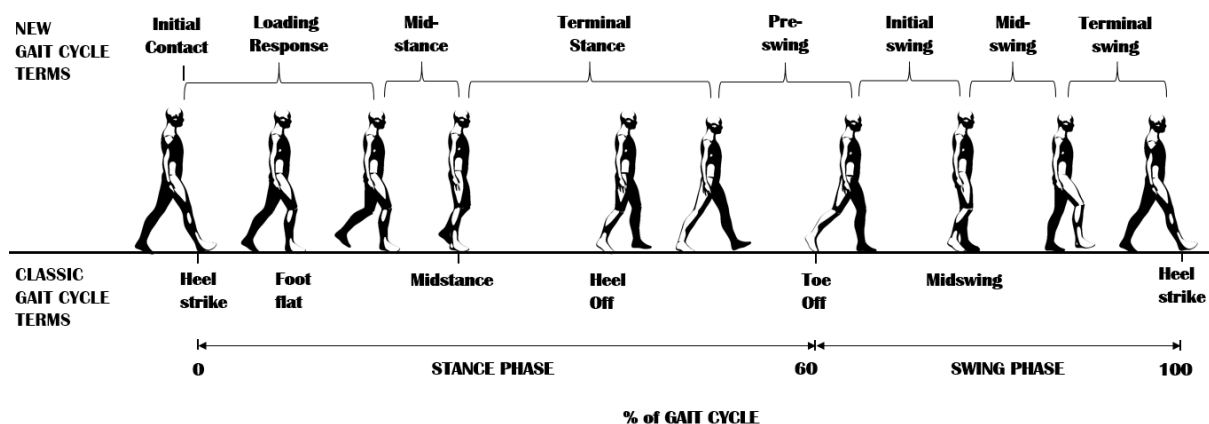
Figure 3.7 Gait cycle phases description and terms

- *Determinants of GAIT*

These factors are applied in normal human gait to minimize the excursion of the body's COG and help produce forward progression with the least energy expenditure.
The six determinants of gait are (Cuccurullo 2015):

    i.   Pelvic rotation

    ii.   Pelvic tilt

    iii.   Knee flexion in stance phase

    iv.   Foot mechanisms

    v.   Knee mechanisms

    vi.   Lateral displacement of the pelvis

i.   Pelvic rotation

The pelvis rotates as we lengthen leg just before load response. Medial rotation of pelvis occurs on the side of the swing leg and reaches its maximum just before heal strike where its value is approximately 4° anteriorly on the swing side and 4° posteriorly on the stance side. In double support phase lower limbs are maximally lengthened and pelvic rotation helps to avoid sudden COG drop.

ii.   Pelvic tilt

The Pelvis drops on the swing leg side by approximately 4°–5° during the midstance. This pelvis movement lowers COG and thus contributes in decreasing COG excursion in vertical direction and helps to avoid sudden COG jump up.

iii.   Knee flexion in stance

Small bending in the knee joint of the stance leg helps to reduce vertical elevation of the COG of body during midstance. The knee flexion in stance is thus decreasing the energy consumption and more over acts as spring-like shock absorber during the heel strike impact.

iv.   Foot mechanisms (ankle plantar/dorsiflexion mechanisms)

Ankle plantar flexion during initial contact prevents sudden COG drop. Controlled dorsiflexion during loading response contributes in smoother progression of COG in vertical direction.

v.   Knee mechanisms

Knee which was slightly bended after loading response and midstance phase extends now in the beginning of terminal stance. This knee extension is followed by ankle plantar flexion, stance leg is straightened which reduces the pelvis drop during swing leg heel strike.

vi.   Lateral displacement of the pelvis

Last important aspect to be mentioned is pelvis lateral displacement. In order to maintain stability during midswing, pelvis moves laterally towards stance leg and moves COG of the body above the base of support.

Determinants 1–5 reduce displacement on the vertical plane. Determinant 6 reduces displacement on the horizontal plane.

- *C posture stable static posture of Paraplegics*

Last to be mentioned in this chapter is special posture, which enables complete paraplegics to stand even without hip support. If the ankles and hips are locked while wearing for instance Scott-Craig orthosis than stable static position can be achieved by leaning the trunk backwards, creating so called C posture, moving the pelvis anteriorly and shifting the COG of the trunk posteriorly.

- *Paraplegic passive walking*

Patients with complete loss of motor control of lower limbs can still walk using special passive orthotic devices if there is a will to do so. The patients can walk with **Scott-Craig** orthoses or **Reciprocal Gait Orthosis (RGO)** and crutches or walker using a swing-to or swing-through patterns and thus ambulate with a **four-point gait.**

Orthoses types, their description and manufacturing processes are explained in details in the following chapter.

4 Orthoses and Exoskeletons for lower limbs

Orthotic devices or braces are those applied externally on injured body parts. This means, orthotic device is not substitution of missing body part, in this case we talk about prosthesis.

The word orthosis is derived from the Greek word "ortho" – to make straight, (Cuccurullo 2015). The word orthosis is singular and orthoses is plural. One of the main tasks of orthotic devices is to straighten bones, but there is much wider variety of reasons why we use such devices. Orthoses for lower limbs can enhance walking performance and assist during daily activities, prevent deformities, relieve pain, protect limbs and spine, control spastic and augment weak muscles or relieve stress in damaged or diseased joints,

Regarding design constraints general rule is applied in all orthotic devices. In order to support and control joints properly three points of pressure principle is needed. This means, orthosis is in contact with wearer`s body in three areas, one principal force is acting in one direction and two counterforces are acting opposite. In case of deformities in wrist (Fw), spine (Fs) or knee (Fk) we can design orthosis using three points of pressure principle according Figure 4.1.
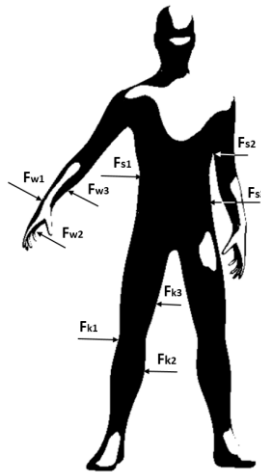
Figure 4.1 Three points of pressure principle – examples for wrist, spine and knee

- *Orthosis vs. Exoskeleton*

Besides of the word – **orthosis** – there is another term – **exoskeleton** – which is used in nowadays. Word Exoskeleton comes from the hard outer shell found on insects and certain animals, this was an inspiration in a process of naming devices which are closely attached to users body and augment users abilities, but would be incorrectly identified as orthoses.

Logical difference between exoskeleton and orthosis for lower limbs can be understood as follows, (Dollar a Herr 2008):

Exoskeleton for lower limbs is defined as a mechanical or electromechanical device that is essentially anthropomorphic in nature, is "worn" by an operator and fits closely to his or her body, and works in accordance with the user's movements. In general, the term "exoskeleton" is used to describe a device that **augments** the performance of an **able-bodied wearer**.

The term **orthosis** for lower limbs is typically used to describe a device that is used to **increase** the ambulatory **ability** of a **person** suffering from a leg **pathology**.

- *Active and passive orthosis and exoskeleton*

Active or powered devices is device which receives an energy from some external source. In case of electromechanical design, this source is battery. In case of pneumatic mechanism, compressed air is needed etc.

The passive devices use an energy accumulated by a user. It can be the energy stored in springs or some mechanisms which use simply gravity or the energy harvested from different parts (joints) of the body.

To conclude, the difference between the terms orthosis and exoskeleton seems to be quite clear. The word exoskeleton however became such popular, that we can't generally follow this division. Many researchers are using name exoskeleton for lower extremities for devices specifically designed for rehabilitation or as assistive walking aids for paraplegics.

Some can say that exoskeleton can be just such device which comply with definition of robotic device, this can be partially true, but unfortunately there are many devices called exoskeletons which does not follow this either.

Because there is no consistent rule, for the purpose of this thesis terminology which comply with following rules will be followed:

- **Powered Exoskeleton**

Powered exoskeleton for lower extremities is anthropomorphic robotic device, which is tend to be universal to fit vast variety of the users, and can be intended to augment the performance of an able-bodied users or daily performance of disabled users, who have to live with disability without much hope for improvement. This device has to be mobile, not fixed or stationary, as for instance rehabilitation robotic devices in rehabilitation centres. Powered exoskeleton for lower limbs can be mobility solution but does not need to be medical device.

- **Active Orthosis**

Active orthosis for lower extremities is powered anthropomorphic device, which is generally designed for specific user. Such orthosis does not need to be robotic device. Active orthoses generally is used for rehabilitation purpose and for users with lower limb paralysis, where an improvement of functionality is expected. Such device is generally categorized as medical device and can be mobility solution.

- **Denotation of device to be developed within this work**

From above description, and from aims of this work, there will be now on used term **Powered EXOSKELETON** for newly invented device.

4.1 Usability of Orthoses

Orthoses are widely used devices not only after trauma like spinal cord injuries or stroke. Orthoses help improve and protect painful or lax joints and correct overall posture by supporting flail joints.

Orthoses become everyday companion for improvement of quality of life. Orthotic devices are prescribed to vast variety of users from small babies, active youngsters to elderly people. All groups have different needs and constraints to design of such devices. Development in this field indicates significant progress in nowadays especially in the field of material engineering and attractive designs.

There is necessary to implement new lightweight materials, in order to relieve loaded muscles and increase flexibility in non-affected parts of body or such materials which can reduce skin infections or pressure soars in portions of body which are in direct contact with device.

Another aspect is appearance. Modern orthoses tend to have futuristic designs using progressive 3D printing or prepreg materials with fibres reinforcement layup technologies. There is increasing demand for such fashion accessory products. It is very important that users feel safe and stable but psychological aspect of wearing orthoses is as well essential in process of accepting this companion in everyday life.

4.2   Materials in orthotics

All different kind of materials are used in manufacturing of orthotic devices. Orthoses generally consists of parts form metal, plastic, see (Showers et al. 1985), rubber, different kind of textiles, composite materials with different kinds of fibres reinforcements and in older orthoses leather was commonly used. Some examples of materials, which can be used are in Table 4.1, as wide range of material modifications exists average values are mostly stated in this table.

Table 4.1 Materials in Orthotics

Material	Type Description	Density [kg/m³]	Tensile strength yield [MPa]	Flexural/ Modulus Elasticity [GPa]
METALS				
Aluminium	2024-T3 * Basic strips	2780	>= 290	73 Mod. of E.
	6061-T6 * Strong alloy for bigger payloads	2700	276	69 Mod. of E.
	7075-T6 * Premium quality big payloads	2810	462	71 Mod. of E.
Stainless Steel	17-4	-	-	-
	303*, 316, 440	8000	240-1280	193 – 200
Titanium	Ti-6Al-4V Strength comparable to steel, but only 60% of the density. More resistant to corrosion.	4430	950	114
Magnesium alloys	Very light weight, not very strong	1780	130	45
PLASTICS				
Poly - propylene	Rigid, impact resistant, Various types	940	32	1,31
Copolymer	Rigid yet flexible	960	30	1,30
LDPE	More flexible and softer	920	10,7	0,217
HDPE	High durability and strength	960	26	1,1
Kydex	Superior formability, even more rigid	1350	39,6	2,48
ABS	High strength and stiffness economical	1006	41	1,86
Iglidur J from IGUS	Low wear and very low coef. of friction	1500	73	2,42 Mod. of E.
COMPOSITE fibres (Used prepreg materials with fibres reinforcements)				
Pre-preg Carbon fibres in epoxy resin*	Bidirectional epoxy M9.6 - 3K 2x2 Twill			
	Bidirectional epoxy M9.6 - 6K 2x2 Twill			
	Unidirectional epoxy M9.6 G300			

*Values depends on number of layers and manufacturing procedure

4.3 Orthoses for lower limbs

As mentioned in the beginning of this chapter, orthoses for lower limbs are generally manufactured and fitted to specific user, with particular disorder. This way mechanical orthotic joints match users anatomic joints and are aligned according them. Load transfer, efficiency and correct performance is increasing with level of manufacturing precision. Designers are usually using 3-point pressure system for proper positioning of limbs in orthosis and it is important to consider this system in prescription procedure. Orthotic devices can be attached to user's body laterally, medially or bilaterally. Lateral and bilateral attachments are widely used and further described in this chapter. Medial attachment may be used only in case of special paired orthoses.

Orthoses can be divided into groups according to which joints or parts of the body they are meant to be determined. We divide orthoses for lower limbs as follows:

- *Orthopaedic shoe*

- *Foot orthoses - FO*

- *Ankle foot orthoses - AFO*

- *Knee ankle foot orthoses - KAFO*

- *Hip knee ankle foot orthoses - HKAFO*

4.3.1 Orthopaedic shoe

The orthopaedic shoe is special footwear solely adjusted to the customer or patient, manually manufactured based on a medical prescription. The task of an orthopaedic shoe is to compensate, suitably for the impediment, or treat in the best possible way individually defined disease and dysfunction of the customer so that he can participate in social life with as little restrictions as possible. Shoe itself is foundation of healthy walking patterns and it is first important element for restoration of correct posture and gait (T. Borchers 2010).

- *Construction of Orthopaedic shoe:*
    - i. Last construction

Classical lasts are made of wood or plastic. Lasts are manufactured with the help of individual measures and according to the desired shoe form. They make visible individual dysfunction of the customer that have treated.

    - ii. Production of upper

An upper is the upper part of the shoe. It consists of several glued together or sewn together parts. It give the shoe its look and its designated use. Here special attention has to be paid to a fashionable esthetic design, so that the customer feels good in his shoe.

    - iii. The midsole

The midsole effects the durability/solidness, the cushioning ability as well as the security (steel sole) of the shoe. It is mostly made of sole leather, rubber, plastic or metal and is inserted between welt and outsole. The outsole, which has direct contact to the environment, is fixed to the welt and mid sole.

iv.   The outsole

The outsole is the top layer of the shoe regarding the manufacturing process and it is the tread area later. It is made of different materials such as for example leather, rubber, or different plastics. (T. Borchers 2010).

Figure 4.2 Manufacturing procedure of shoe, example from Matsumoto Gishi co. Japan

- *Rocker bar and rocker bottom shoes*

Rocker bar: located proximal to metatarsal heads; improves weight shift onto metatarsals.

Rocker bottom: builds up the sole over the metatarsal heads and improves push off in weak or inflexible feet. May also be used with insensitive feet.

4.3.2   Foot orthosis

Foot orthosis is inserted inside the shoe, and usually support foot from heel to metatarsal heads but can be extended as part of insole up to toes. It may be sometimes called orthopaedic insole. Foot orthosis plays an essential role in stabilizing the foot during walking, such stabilization leads to proper joints alignment and correct weight acceptance by lower extremities especially during initial contact and loading response phases of the gait cycle. The manufacturing procedure of such custom orthosis is step-by-step presented in Figure 4.3.

Figure 4.3 Manufacturing procedure of foot orthoses - orthopaedic insole

4.3.3 AFO

The ankle foot orthoses are used to reduce weight bearing and this way prevent deformities or stabilize during walking and thus correct abnormalities. AFOs are widely used orthoses inside therapeutic rooms but as well in daily life due to its undeniably positive impact on corrections in gait patterns and reduction of energy cost during ambulation. AFOs can be static, dynamic or active/powered configurations are recently available as well, (Cuccurullo 2015).

- *Dynamic AFO*

The dynamic AFO is equipped with springs or designed to have a spring-like performance for a dynamic dorsiflexion or plantar flexion assistance and passive contra flexion resistance. Orthosis with dynamic dorsiflexion assistance keeps a foot dorsiflexed during swing phase to increase toe clearance in order to avoid stumbling and increase safety. Orthosis with neutral dynamic plantarflexion helps users with dorsiflexion weakness to walk more naturally and can as well assist knee extension during loading phase in case of slight knee impairment.

- *Active AFO*

Path of least resistance is the way which the body automatically goes during rehabilitation, this is the biggest obstacle in the process of recovering healthy walking. Active AFO comes together with actuator which requires external source of energy (electric or pneumatic). Such active orthoses can be used to support portion of lower body with decreased functionality in order to act against its resistance. For instance active plantarflexion impulse during preswing phase elevates pelvis and helps to decrease or avoid circumduction gait by supporting hip weakness of patients with hemiplegia.

As usual function of orthotic devices AFOs moreover supports ligament instabilities and together with anteroposterior functionality provides mediolateral support as well. As it was already mentioned in previous chapters of this study, AFO is useful for a variety of conditions such as spastic hemiplegia or diplegia caused by cerebral infarction or cerebral palsy.

- *Traditional conventional orthosis*

The Traditional conventional AFO orthosis is generally of bilateral configuration (I.b), II.b and V.a type. This orthoses consists of lather calf bend attached to steel holder. This holder is attached using rivets to metal uprights and these are connected to double-Klenzak ankle joint which allows regulation of range of motion of plantarflexion and dorsiflexion. Stirrups are rotating in this joint and are usually integrated with shoe, see Figure 4.4. There can be springs implemented directly into Klenzak ankle joint or another type of joint can be used here as shown on Figure 4.5.
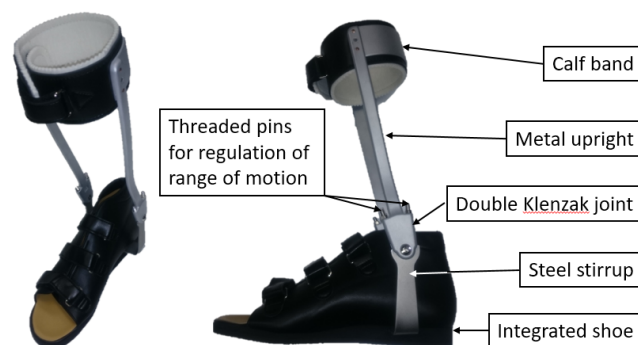

Figure 4.4 Traditional conventional orthosis

Figure 4.5 Traditional conventional dynamic orthosis with Gait Solution spring joint (left) and new modern look (right)

- *Moulded*

The Moulded AFOs are commonly fabricated from preheated thermoplastic materials stretched on patients cast of leg. Preparation of cast, application of heated up thermoplastic material and the final product is illustrated on Figure 4.6. Modern nowadays widely used AFOs are fabricated from a prepreg advanced carbon composites, this AFO orthoses are lightweight as plastic once but have much better rigidity and strength, its only disadvantage price. Such orthosis usually keeps the foot up during swing phase but may reduce heel strike impact forces and increase stability in stance and toe-off, for different types of modern moulded carbon AFOs see Figure 4.7.

Figure 4.6 Process of fabrication of plastic moulded AFO

Figure 4.7 Modern moulded type of AFO - from composite carbon fiber reinforced material

30

- *Broad division of AFOs*

Based on studies of ankle foot orthosis (AFO), (Shorter et al. 2013), (Faustini et al. 2008), (Sawicki and Ferris 2009), (Rouhani et al. 2014), (Bregman et al. 2011), (Kim et al. 2013) prosthesis and all different types of exoskeletons for lower limbs we can summarize types of ankle design as follows according:

I. Symmetry

  a) Bilateral
  b) Unilateral

II. Wearing

  a) External
  b) Integrated
  c) Inserted

III. Actuation

  a) Active
  b) Dynamic
  c) Special

IV. Actuator position

  a) Direct actuation
  b) Non-direct actuation

V. Range of motion

  a) Limited motion
  b) Free
  c) Solid or Static

VI. Feedback

  a) With sensors
  b) W/O sensors

VII. Material composition
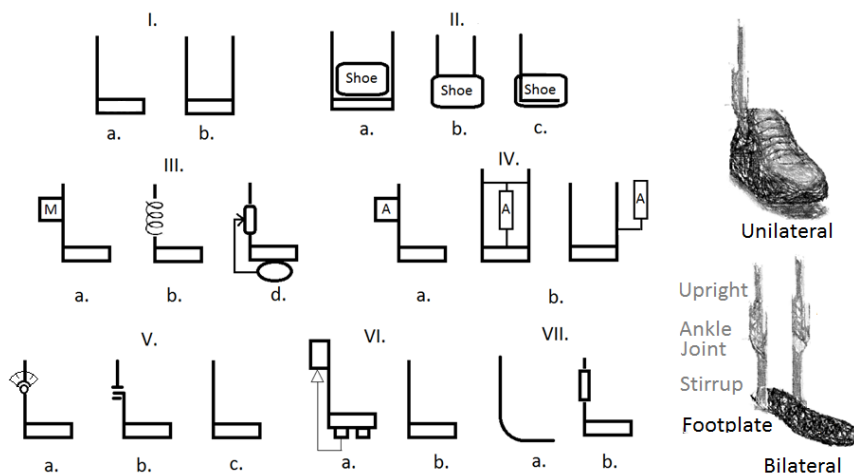
  a) Homogenous
  b) Multi-Material

Figure 4.8 Broad division of AFOs

I. Symmetry
  - Bilateral solution provides with better fixation and stability, but is heavier and bulky.
  - Unilateral solution is compact, lighter, more esthetical, but less stable and rigid.
II. Wearing
  - External is popular with universal powered exoskeletons for its fast donning/doffing.
  - Integrated solution is popular in traditional designs, ugly irreplaceable shoe is disadvantage.
  - Inserted is well accepted by users due to esthetical benefits.
III. Actuation
  - Active AFO is described above, is good for acceleration of rehabilitation process.
  - Dynamic AFO is described above, this type is the most used AFO in the world.
  - Special actuation may harvest energy from different portions of the body or using gravity.

31

IV. Actuator position
- Direct actuation is when an actuator is directly in the axis of actuated joint.
- Non-direct placement of actuator means distribution of energy to the joint through some mechanism.

V. Range of motion (ROM)
- Free motion provides mediolateral stability that allows free motion in dorsi/plantarflexion.
- Solid ankle allows no movement indicated with severe pain or instability.
- Limited motion allows motion to be limited in one or both directions.

VI. Feedback
- Sensor can provide with information which helps evaluate process of rehabilitation or ambulation and protects users against overload or injury, it is normally part of active AFOs.

VII. Material composition
- Homogenous orthoses are usually moulded types from plastic or composite fibre reinforced materials
- Non-homogenous are major group consists of many parts made of different materials.

- *Design elements of AFO*

a. Foot support elements

A foundation of AFO orthosis is the foot support element. This element can be the integrated shoe or sandal or just a footplate inserted into users shoe. Integrated shoes are firmly connected to steel stirrups. Footplates are in case of multi-material AFO combined with steel stirrup or in case of homogenous AFO directly part of stirrup, more about manufacturing procedures of footplates in chapter 3.

b. Stirrups and uprights

Stirrup is a metal attachment riveted to the sole of the shoe; split stirrups allow for shoe interchange solid stirrups are fixed permanently to the shoe and provide maximum stability. Metal upright is rod, which is connected to ankle joint and formed by orthopaedic technician according customers cast shape.

c. Ankle Joints

There are many types of ankle joints in orthotics, but all are basically following principle of Double-Klenzak joint. For understanding how such joint works, see Figure 4.9. Thanks to set screws and pins we can set limits for dorsi/plantarflexion. Springs help to diminish impact forces and prevent drop foot.
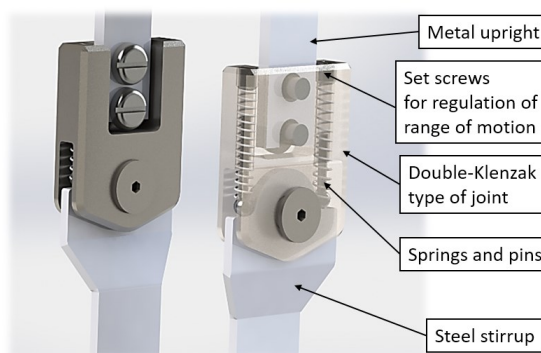

Figure 4.9 Most common AFO ankle joint (double-Klenzak type with springs)

4.3.4 KAFO

Knee Ankle Foot Orthoses (KAFO), see Figure 4.10 is proximal extension of the AFO to control knee motion and alignment. KAFOs with locked knees are used in knee-flexion contractures or during rehabilitation of patients after stroke. KAFOs with locked knees can be used by paraplegics to walk using swing-through gait, such device is known as Scott-Craig orthosis. Different kinds of orthotic knee joints are on the Figure 4.11. KAFO can have same as AFO bilateral or unilateral design.
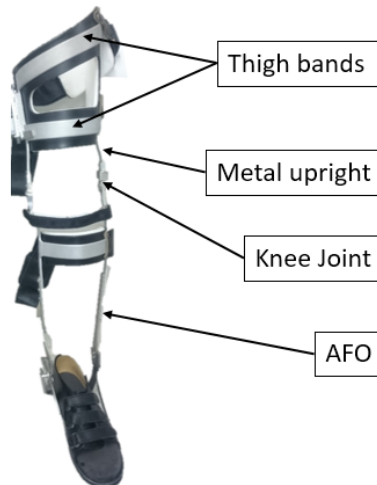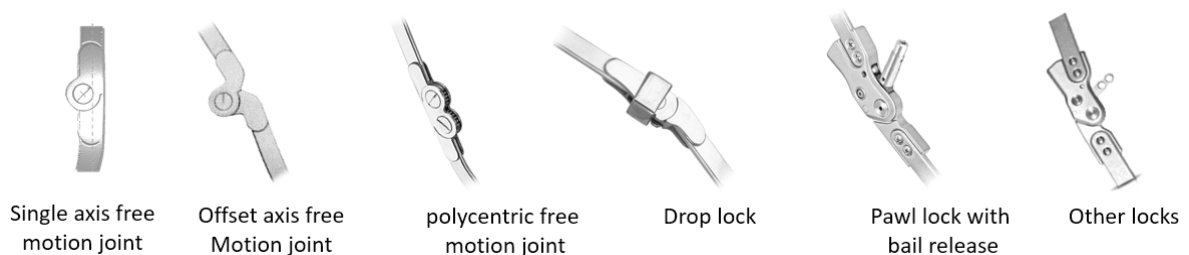

Figure 4.10 KAFO

Figure 4.11 KAFO knee joints

- *Offset axis free motion joint*
  More closely fits to axis of rotation of anatomical joint.
- *polycentric free motion joint*
  Virtual centre of rotation more closely fits to axis of rotation of anatomical joint.
- *Drop lock*
  Metal ring drops over top of the joint such way preventing flexion.
  May be secured by spring and ball.
- *Bale lock*
  Lock is disengaged by pulling bale up. Lock engage automatically when orthoses is extended.
- *Other locks*
  Orthotic knee joints may offer the patient security even though not full extension can be reached, such joints may have several locking positions allowing for instance just limited flexion and extension.

4.3.5   HKAFO

Hip-Knee-Ankle-Foot Orthosis (HKAFO) is KAFO with extended later upright to which hip joint with pelvic band are attached. Hip joint can be same as knee joint. This type of orthoses is used for patients with hip instability and weakness.

4.4   Cuffs, Bands and cushions

Cuffs are moulded from plastic materials. If bigger rigidity is needed than stronger and thinner composite materials can be used, e.g. carbon fibres in epoxy resin.

Proper interface between plastic and metal parts and user's body is fundamental to avoid ulcers, pressure soars or excoriation. Different types of cushion materials are firmly glued to orthoses or removable and washable. Vast variety of new types of fabrics and plastic foams are available on market. Silicon inserts, polyurethane foam or polyamide fabrics are commonly used.

Historically consistent solution for tightening orthoses and 'closing' limbs inside remains Velcro tapes. This universal tape can safely secure the limbs inside orthoses and provides with simple adjustment option. More recent is application of BOA tightening system. The Boa System is custom built for each unique product and use case, they all contain three integral parts: a micro-adjustable dial, super-strong lightweight laces, and low friction lace guides. Each configuration is engineered to optimize fit and provide precision, adaptability, and control.

4.5   Lower limb Passive Orthoses for individuals with paraplegia

Two KAFOs and the swing-through walking gait can be the way for paraplegics to walk. Besides of **two-legs-aligned walking** gear, there are **alternating walking** (first one leg than another) orthoses available. The relationship between the residual function level and the type of orthosis vary depending on whether symptoms of paraplegia are incomplete or complete, the cases of symmetrical paralysis is discussed in this subchapter.

Simple trunk orthosis connected to two HKAFOs (THKAFO) can be prescribed in case of lost flexion in the hip joint (level of paralysis higher than L1). Alternating walking with such device can be rather difficult because of very high variability in step length and large energy consumption, walking with such device is toil. Reciprocal gait orthosis is better to be prescribed for such users.

*We can divide **alternating walking orthosis** as follows:*

I.   Two lateral hip joints

- *RGO (Reciprocal Gait Orthosis)*
    - *Double cable RGO*
    - *Isocentric bar RGO*
    - *ARGO (Advanced RGO)*

II.   Medial single hip joint

    - *Walkabout*
    - *Primewalk*
    - *HALO (Hip and Ankle Linked Orthosis)*

*Characteristics and performance parameters to be investigated – summary:*

- o Stability in anteroposterior and mediolateral direction
- o Energy consumption
- o Temporal parameters of gait – velocity, cadence, stride length
- o Spatial parameters (COG) – waddling, vertical elevation, anteroposterior excursion
- o Determinants of gait – pelvis rotation
- o DON and DOFF of device directly from a wheelchair
- o Dimensions and weight – proportions of device
- o Economically accessible – affordability
- o Appearance and aesthetics of device

4.5.1   RGO

RGO (Reciprocating Gait Orthosis) has two lateral hip joints, bilaterally attached HKAFO (bi-axial system). RGO has contralateral linkage between hip joints – flexion on one side is forcing extension on opposite side. RGOs stabilize ankles, knees, hips, and trunk to provide upright posture and due to a reciprocal link between hip joints, more stable walking with reduced metabolic energy consumption can be achieved (Moore and Stallard 1991), (Rose 1979). It was found out that coupling contralateral joints is a good way how to increase an efficiency of paraplegic walking. Upper body strength however determines a success of walking with these orthoses. There are several types of RGO, double cable RGO, classical isocentric bar RGO and advanced RGO (ARGO), (Baardman et al. 1997). ARGO has single push pull cable system and knee joint with pneumatic cylinder, ARGO is on Figure 4.12.

Advantages and disadvantages of RGO:

- ✓ Temporal parameters
- ✓ Spatial parameters
- ✓ Pelvic rotation 15-20°
- ✓ Trunk support
- ✓ Hip axis alignment
- ✓ Anteroposterior stability

- x Poor lateral stability
- x Hard to don/doff
- x Bulky and heavy
- x Aesthetically unattractive
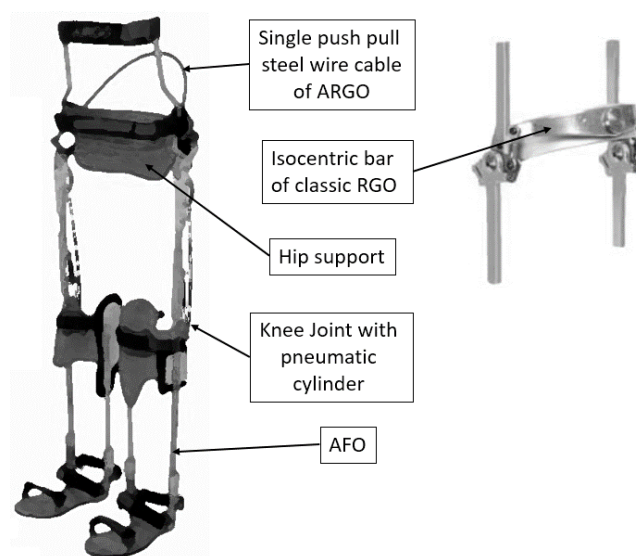
Figure 4.12 ARGO and isocentric bar

4.5.2 Walkabout

Walkabout is the first from the group of single medial hip joint orthosis. This group is characterized by no trunk support. All orthoses consists of two KAFOs connected with different types of medial hip joint. Walkabout is the simplest one with basic hinge type joint with stoppers. Centre of rotation in the hip is shifted below the hip axis and this makes the pelvis rotate more to compensate this shift, (Onogi et al. 2010).

Advantages and disadvantages of Walkabout:

- ✓ Mediolateral stability
- ✓ Easy to Don/Doff
- ✓ Light and compact
- ✓ Affordable solution

- x Anteroposterior stability
- x Energy consumption
- x Spatial parameters
- x Temporal parameters
- x Pelvic rotation
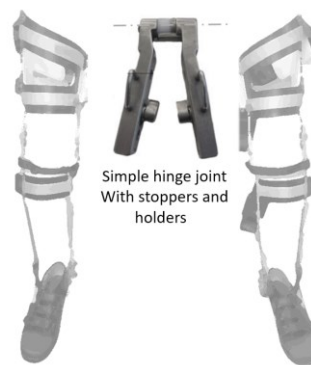
Figure 4.13 Walkabout orthosis - two KAFOs connected by hinge joint

4.5.3 Primewalk

Another single medial hip joint is slider type joint with stoppers - Japanese PRIMEWALK, (Onogi et al. 2010), . Thanks to special curved guide and sliding mechanism virtual centre of rotation is shifted closer to the hip joint. The pelvic rotation is decreased due to this invention, but still not comparable with values of normal walking. Spatial-temporal parameters and energy consumption are better in comparison with Walkabout, but still not satisfactory in comparison with normal walking.

Figure 4.14 Primewalk orthosis, explanation of pelvic rotation and principle of centre of rotation

There are two factors why pelvic rotation still remain, (Genda et al. 2004):

    I.   Lack of assisting mechanism for hip flexion
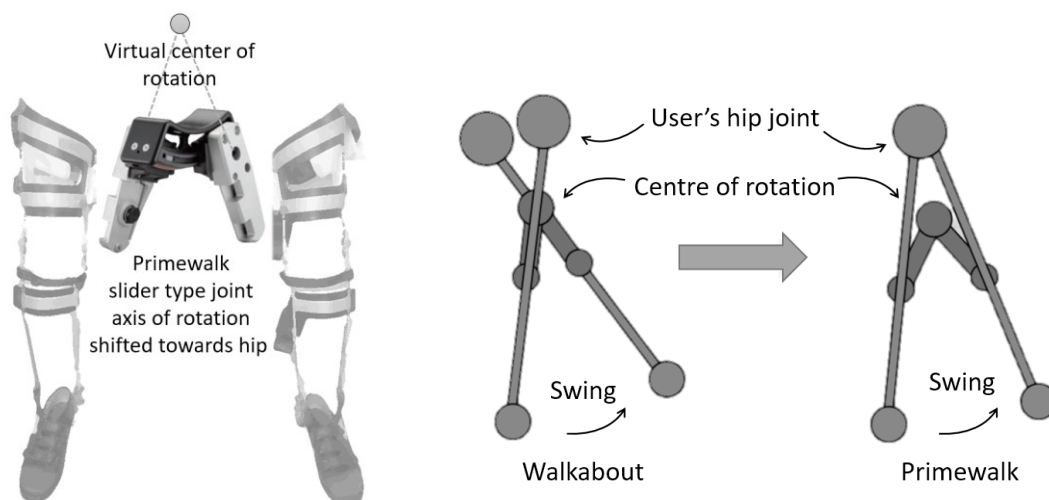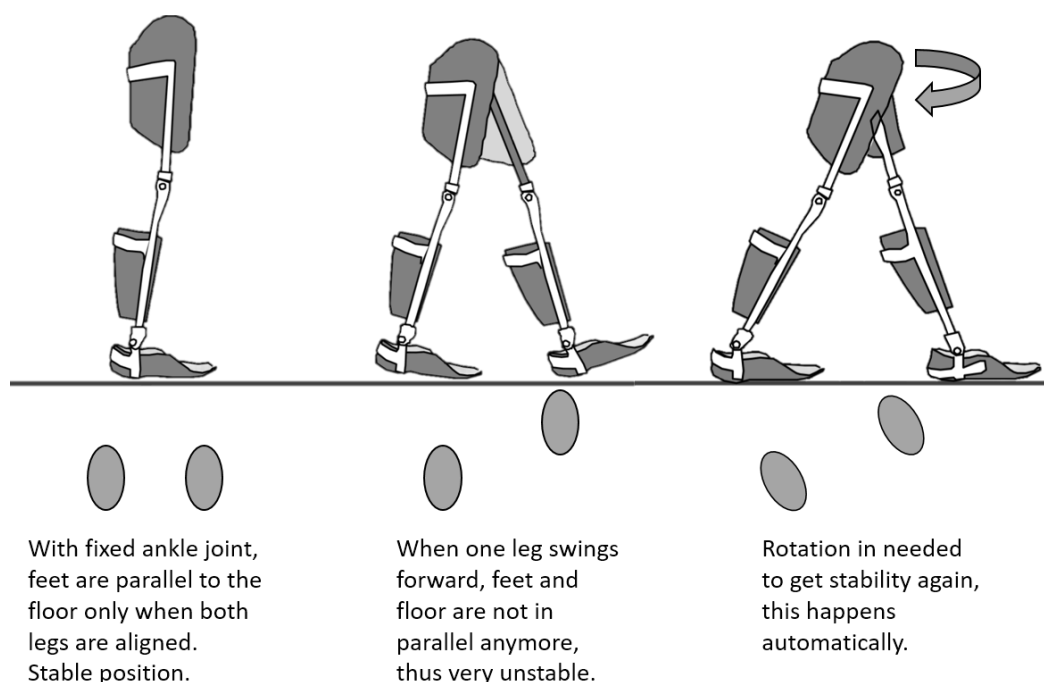   II.   Fixed ankle joint causes instability when the step length become longer, this is explained on Figure 4.15

| With fixed ankle joint, feet are parallel to the floor only when both legs are aligned. Stable position. | When one leg swings forward, feet and floor are not in parallel anymore, thus very unstable. | Rotation in needed to get stability again, this happens automatically. |

Figure 4.15 Why does pelvic rotation still remain with Primewalk?

Advantages, disadvantages and neutral parameters of Primewalk:

- ✓ Mediolateral stability
- ✓ Easy to Don/Doff
- ✓ Light and compact

- x Anteroposterior stability
- x Pelvic rotation

- Temporal parameters
- Spatial parameters
- Energy consumption
- Price

4.5.4   HALO Orthosis

HALO (Hip Ankle Linkage Orthosis) is compact medial hip joint orthosis with contralateral hip and ankle linkage. These two joints are coupled by steel wire rope inserted in pulleys and Bowden. Each hip joint is equipped with one pulley. The dorsiflexion at one foot causes flexion of the opposite hip joint through the wire connected to the pulley. The joints linkage keeps feet always in parallel with the floor to avoid stumbling and assists swinging of the leg. This setting reduces pelvic rotation to a normal level and enables longer and more stable strides (Genda et al. 2004). However, the users have to usually undergo long training periods to master technique of walking, before using HALO orthosis independently.

During development of the HALO orthosis several updates were made, one of them is putting Velcro fastening tapes on back side of thighs and calves to shift support bands on anterior side to make it easy Don/Doff from the wheelchair.

Figure 4.16 HALO orthosis
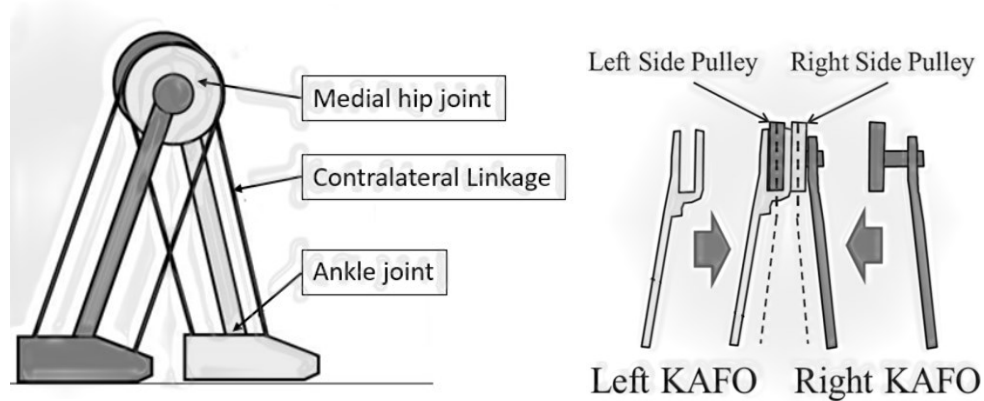
Figure 4.17 HALO orthosis description and principle of HALO joint

- *HALO principle*

Principle of walking with HALO orthosis is shown on Figure 4.18.

When the dorsiflexion of the left ankle occurs, then:

1. The wire connected to the left heel is pulled,

2. the force in wire cause the left pulley at the hip joint rotate,

3. this makes the right leg swing forward with the left pulley.

4. The left leg extends relatively to the right leg and the left pulley rotates,

5. the wire that connects with the right heel is pulled and causes right ankle plantarflexion, thanks to this the right foot is parallel to the ground.

The rotation ratio between hip and ankle joint is set at 2:1 so that the feet are always parallel to the floor.

Figure 4.18 HALO orthosis walking principle

Advantages, disadvantages and neutral parameters of HALO:

✓ Mediolateral stability
✓ Anteroposterior stability
✓ Temporal parameters
✓ Pelvic rotation in normal level
✓ Light and compact
✓ Easy to Don/Doff
✓ Smooth gradual activation of ankle moments
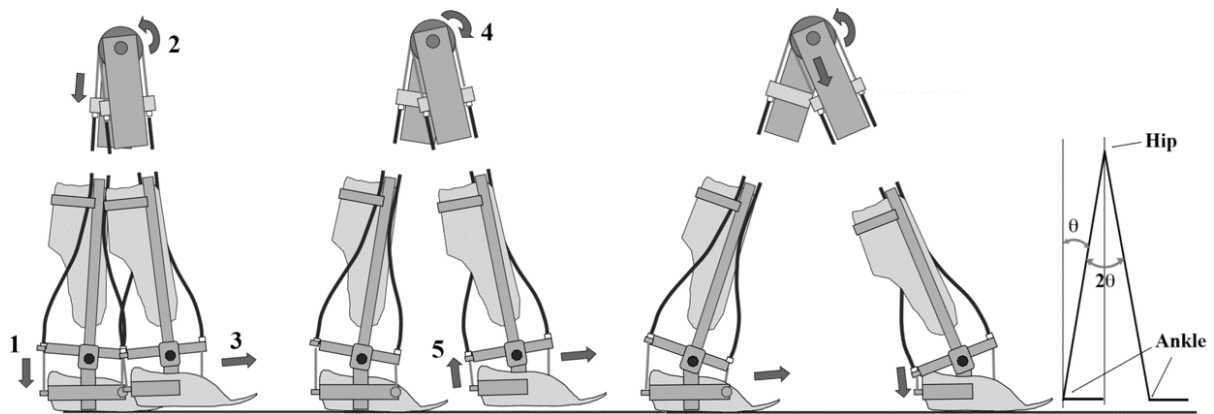
x Complex adjustment system

- Anteroposterior stability
- Spatial parameters
- Energy consumption
- Esthetics (redesign)

4.5.5 Evaluation of passive orthoses

From characteristics and performance parameters, advantages and disadvantages of discussed passive orthoses is obvious dominance of Primewalk and HALO orthoses. Study focusing on comparison of Primewalk and HALO was conducted. Energy consumption, temporal parameters and pelvic rotation were investigated. According this study, the performance of users with HALO orthosis was in all aspects better, see Figure 4.19, (Genda et al. 2010).

Summarized results of comparison:

- Temporal parameters
    - 10 m walking experiment at full speed
        - T9 - HALO - 35.0 m/min - 2.5 x faster
        - T9 - PW   - 14.0 m/min
        - T7 – HALO - 24.8 m/min – 1.7 x faster
        - T7 – PW   - 14.3 m/min
    - Longer strides and cadence
- Energy cost
    - 60% - T9 (PW: 29.0 J/kg/m, HALO: 17.8 J/kg/m)
    - 75% - T7 (PW: 21.4 J/kg/m, HALO: 16.0 J/kg/m)
- Pelvic rotation in the horizontal plane
    - ± 30 for Primewalk
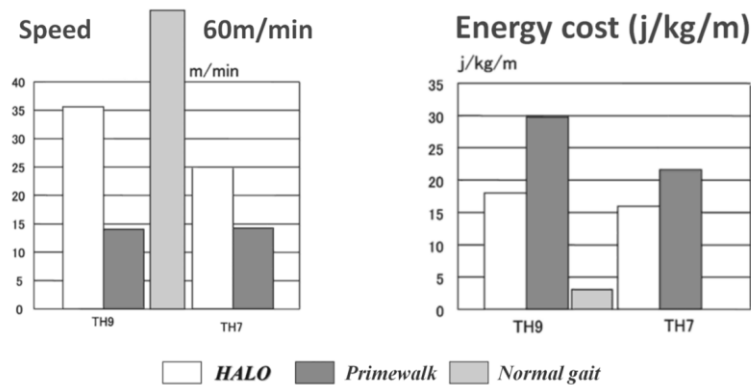   - ± 10 degrees for HALO - within the range of normal gait

Figure 4.19 Speed and energy consumption of HALO, Primewalk and normal walking

4.6 Active Exoskeletons for paraplegics

- ***REX***

The REX for Clinical Use and Personal Use is the premiere commercial exoskeleton for individuals with complete lower body paralysis. The REX is designed to be:

- o *Self-supporting and secure.*

- o *Alleviate complications due to prolonged wheelchair use.*

- o *Developed for Robot-Assisted Physiotherapy (RAP).*

- o *Elevates users from a sitting position into a robot-supported standing position.*

- o *Reduces burden on therapists performing standing therapy.*

- o *One of the most robust and expensive solutions*

For a while exoskeletons that take full control of the gait cycle where receiving a lot of flak for not being as capable as their variable assist counterparts. New research findings in the middle of 2016 have demonstrated, however, that devices such as the REX have a place in the medical industry. It has been discovered that even though the REX moves the rehabilitation participant by itself, it can still provide medical benefits. Exoskeletons that take full control of the user's legs are now starting to be used as a stepping stone towards rehabilitation with variable assist robotics.

- ***Indego®***

The Indego® can be used for therapy as a gait training tool. The Indego Personal can also be employed as a supplementary mobility aid to a wheelchair. In addition to being able to see people eye-to-eye, research using this and other assistive medical exoskeletons has shown a strong correlation between standing up and a multitude of secondary benefits. These positive effects include but are not limited to improved bowel control, increased bone density and reduction in pressure sores. Indego design specifications:

- o *Hip-knee powered exoskeleton*

- o *Li-ion batteries*

- o *Total assembled device weight of 12kg (26lb)*

- o *Modular*

- o *Ability to export data using an iOS app*

- o *Bluetooth connectivity*

- o *Color LED and vibration user feedback (note: Recent independent research has shown haptic feedback to be instrumental in some gait rehabilitation cases)*

- o *Built in functional electrical stimulation (FES) interface (select models)*

- **ReWalk**

Key attributes:

- o *Approved by the FDA for clinical and home use for individuals with spinal cord injury (SPI).*

- o *Battery powered hip-knee exoskeleton.*

- o *Proven to work in clinical, home and city environments.*

- o *Regularly being improved and iterated (the 2016 ReWalk is now 6th revision)*

- o *Controlled by subtle changes in the user's center of gravity.*

- o *Graphical user interphase for the physiotherapist's control.*

- o *Structured training program for the rehabilitation teams purchasing the device.*

The ReWalk Rehabilitation System is optimized for use in a clinical setting. It is used as a tool to augment the capabilities of regular physiotherapy by providing a high number of consistent and reproducible steps. ReWalk Rehabilitation is also used as a stepping stone towards individuals preparing to acquire ReWalk for personal use.

- **ExoGT**

The Ekso GT is a powered hip-knee medical rehabilitation exoskeleton developed by Ekso Bionics. This is the first exoskeleton to be approved by the FDA for those recovering from a stroke. It is also approved for use with individuals with spinal cord injury. The Ekso GT™ is a robotic exoskeleton for comprehensive gait therapy which provides a superior rehabilitation experience for patients and therapists alike. The Ekso GT™ is a tool to supplement professional physiotherapists, not replace them. The use of this exoskeleton allows for a greater number of consistent steps with the appropriate weight shift to be conducted in every rehabilitation session.

The Ekso GT is approved by the FDA for use with:

- o *hemiplegia due to stroke*

- o *SCI at levels of T4 to L5 and levels of T3 to C7*

Design features of the Ekso GT:

- o *Acuated powered hip-knee exoskeleton*

- o *Variable Assist controls, the Esko GT can apply power from 0 to 100% as needed on a step by step basis.*

- o *Adjustable on the fly assistance level and operation mode*

- o *Encourages correct body posture*

41

Figure 4.20 EXO GT, INDEGO, REwalk, REX (from left to right) exoskeletons

- **HAL**

HAL (Hybrid Assistive Limb) from Japanese University of Tsukuba is not device built for people with paraplegia, but due to its progressive PR and success in the field of exoskeletons generally it should not be omitted. HAL is robosuit which function is closest to exoskeleton definition, it was built to extend and amplify human body functions but as well to support rehabilitation and physical training in medical welfare field. Research is being carried out assuming application to heavy work support at factories or rescue activities during disasters, but in hospitals as well. The most characteristic feature of the HAL control method is that the wearer's intention is estimated and assisted by the surface myoelectric potential. In general, there is a time shift called EMD (Electro Mechanical Delay) from the measurement of the surface myoelectric potential until the tension actually occurs in the muscle. Therefore, by measuring the surface myoelectric potential, it becomes possible to predict the intention of the wearer prior to the start of operation and generate the assist torque, thereby realizing a system that moves as desired by the wearer, (Wall et al. 2015)

- **WPAL**

Another device is WPAL, this is tend to be mobility solution (walking assist) for people with paraplegia and has already demonstrated successful clinical trials. WPAL has a total of six actuators symmetrically two in hips, knees and ankles attached medially on two KAFOs connected by medial hip joint. Position feedback control algorithm is tracking joint angles pattern of normal walking as a basic template recorded from healthy subjects. Walking rate, stride and joint angle is set as offset from this basic walking pattern and represents target to be controlled. There were conducted step training, walking training, treadmill walking training, walker assisted walking training with five subjects with paraplegia. As a result, walking distance increased by 5 to 20 times compared with the case without device. Improvement was also seen in PCI (physiological cost index) which is an index of energy consumption during walking, (Hirano et al. 2012), (Tanabe et al. 2013).
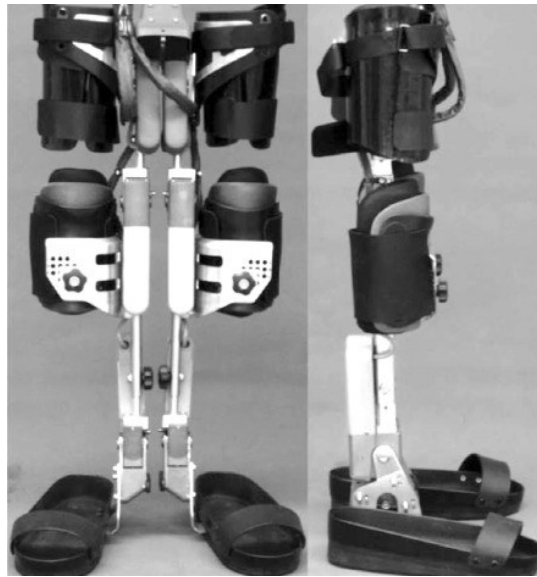
Figure 4.21 WPAL exoskeleton

- **ORTHOLEG 1.0**

Ortholeg is active exoskeleton for lower limbs designed for users of weight between 50 - 60 kg and height 1.55 - 1.65 meters, see Figure 3.1, (Araújo et al. 2015). The prototype is basically a mechanism consists of a set of rigid links joined by rotational joints. Each joint has one degree of freedom and corresponds to human leg structure. Ortholeg first prototype has electromechanical actuators in knees and hips, ankle joint is fixed and does not provide with any degree of freedom. Ankle joints are connected to rigid external soles. Each rotational joint is equipped by Maxon 24volts/150W DC servomotor with encoder and planetary gear box connected by coupling to recirculating ball screw. Torque of motor shaft is transferred to ball screw where transformation of rotational to linear movement is made through nut riding along ball screw axes. Exoskeleton requires usage of crutches.
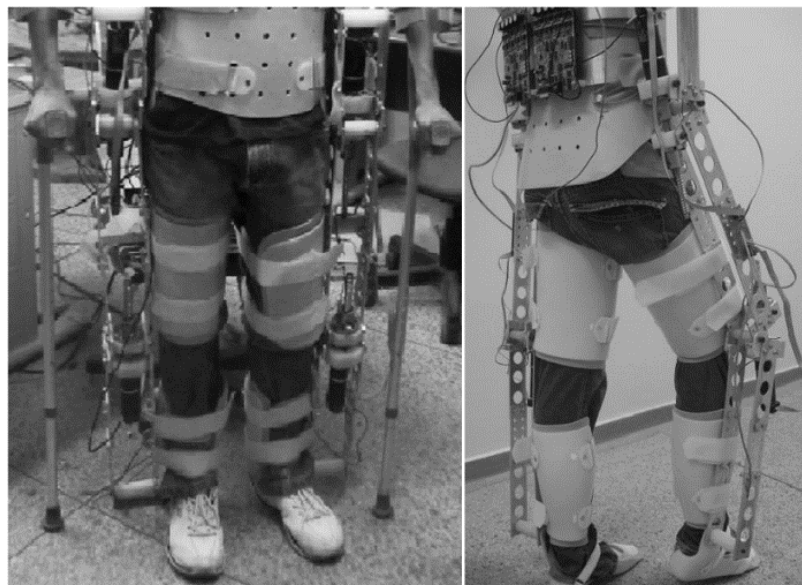
Figure 4.22 Ortholeg – first prototype

4.7   Other Walking assist equipment

In this short subchapter, assistive walking aids are briefly presented (Cuccurullo 2015). Nearly all currently available active orthoses or powered exoskeletons requires some kind of additional walking assist equipment. Generally crutches are the most used and desirable, but some applications which requires wider base of support need walkers to be applied.

4.7.1   Crutches

- *Axillary Crutches*

Components

– Padded axillary piece (on top)

– Two upright shafts

– Handpiece (in middle)

– Extension piece

– Rubber tip

Advantages: inexpensive, adjustable, easier to use

Disadvantages: need good strength and ROM in upper limbs, ties up hands. Increased cardiac/ metabolic demand

- *Forearm Crutches/Lofstrand crutches*

Components:

– Forearm cuff with narrow anterior opening

– Forearm piece bent posteriorly and adjustable

– Moulded handpiece

– Single aluminium tubular shaft

– Rubber tip

Advantages: lightweight, easily adjustable, freedom for hand activities

Disadvantages: needs more strength, requires more skill, and better trunk balance

- *Platform Crutches*

Advantages: Do not need weight bearing through wrist and hand (i.e., fractures, arthritis of wrist or hand. or weakness triceps or grasp)

Disadvantages: awkward, heavy

4.7.2   Walkers

Walkers are recommended for bilateral weakness and/or incoordination of the lower limbs or whole body, or whenever a firm, free standing aid is appropriate (i.e., multiple sclerosis or Parkinsonism) to increase balance and to relieve weight bearing either fully or partially on a lower

extremity (allow the upper extremities to transfer body weight to the floor). Walkers are suitable as well for unilateral weakness or amputation of the lower limb where general weakness makes the greater support offered by the frame necessary (i.e., osteoarthritis or fractured femur) and as general support to aid mobility and confidence (i.e., after prolonged bedrest and sickness in the elderly).

Advantages: Provide a wider more stable base of support. To provide a sense of security for patients fearful of ambulation

Disadvantages: More conspicuous in appearance Interfere with development of a smooth reciprocal gait pattern (e.g., decrease of step length with step-to-gait pattern) Interfere with stair difficult to manoeuvre through doorways or bathrooms.

Types

- – Lightweight walking frame
- – Folding walking frame
- – Rolling walking frame
- – Forearm resting walking frame
- – Hemi-walking frame

4.8   Requirement list

The summary of the driving requirements of design of new exoskeleton based on review of orthotic devices from this chapter and the main objectives of this work is listed in Table 4.2. The price limit was determined from manufacturing costs of orthotic devices for lower limbs and from the fact the final product must be affordable. One of the main objectives is an independent usage of the device including donning and doffing directly from the wheelchair. The user needs to be able to safely manipulate with the device in order to fulfil this objective. Weight limits of the device need to be set firstly to follow ergonomic standards of maximum loads of manual handling for disabled people on a wheelchair (focus group) and secondly to maintain the efficiency of the device (high power-weight ratio). From this two reasons, there is great emphasis placed on lightweight of the exoskeleton. The weight of user limit was derived from the average weight of European man (according to Wikipedia).

Table 4.2 Requirement list

Requirement	Value or description
Mediolateral stability	Walking independently without assistance
Anteroposterior stability	Walking independently without assistance
Price	max € 8000
Weight of device	max 10 Kg
Weight of user	up to 70 Kg
Low energy consumption of user	Evaluated from vertical elevation of CoG
Don/Doff independently from a wheelchair	YES
Modularity	Possibility of switching to passive option

5 Design of new Exoskeleton Ortholeg 2.0

First new exoskeleton Ortholeg 2.0, which was designed for the purpose of this study is presented in this chapter. The project of designing of the exoskeleton Ortholeg 2.0, see was performed in the Universidade Federal do Rio Grande do Norte (UFRN), Brazil and some of the components were manufactured to test their actual functionality. Manufacturing processes and benefits of this new system are discussed in this chapter.
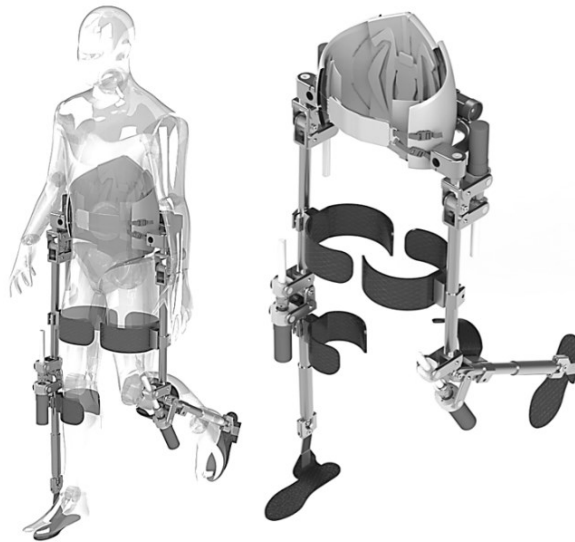
Figure 5.1 Ortholeg 2.0 – CAD model

5.1   Used materials

The main objective of this study is not detailed research in the field of material engineering, but it was significant to study different materials available on market, before actual designing process. Brief summary and description of selected materials with the most appropriate properties was done in previous chapter. Key properties are tensile yield strength, flexural modulus or density. There are more types of materials, suitable for our application, which are currently available on worldwide market.

Figure 5.2 Materials used for manufacturing of Ortholeg 2.0

There were selected and purchased materials from Table 4.1 for new design of Ortholeg 2.0, illustrated on Figure 5.2. Main frame of device and joints are mainly from the aluminium 6061 and 7075. Some parts of fixtures and cuffs (connection parts to users) are made from High Density PE and Copolymer. Support and connection in lumbar region is made from more rigid Kydex. Joints and moving parts of mechanism are equipped by components from plastics Iglidur J with very low coefficient of friction. Components from Prepreg carbon were implemented for better energy transfer between user's body and device.

New Ortholeg is lighter, using modern materials of premium quality. Design using tubes and clamps makes it more compact, modular and secures best-fit for users of variable body proportions. Ankle and knee joint design is described in following sections of this paper.

5.2   Ankle and Shoe insert

Experiments on current design of Ortholeg have conclusively proven urgent need of flexible soles and ankles. Fixed ankle and rigid sole have negative impact on users gait cycle, on wearing comfort and consequently on power consumption of device itself.

Thus study in field of construction of ankle which provides users with some degrees of freedom was triggered and in addition different sole materials, shapes and wearing options were probed.

Ortholeg was designed for paraplegic users, which continues to be main requirement. As already mentioned, rigid passive design is not in consideration (concept V.c. on Figure 4.8 can be excluded). Solution should be furthermore very economical and universal so all users from different social backgrounds can afford it. Expensive customised homogenous 'one piece' AFOs does not comply with this criteria (concept VII.a. on Figure 4.8 can be excluded). Sensory subsystem is not considered in this stage of the project but design should include possibility of future implementation of such components (concept VI.a. on Figure 4.8 can be excluded). We are trying to develop as light device as possible, motors in ankle are excluded, (concept III.a. on Figure 4.8 can be excluded).

Furthermore only these types of the ankle joints from Figure 4.8 which comply with the mentioned requirements were considered and following three different concepts of ankle joint were designed and moreover analysed.

A. Achilles Spring (bilateral, non-direct, semi-active)

B. Adjustable symmetric joints (bilateral, direct,semi-active)

C. Adjustable one-side joint (unilateral, direct, semi-active)
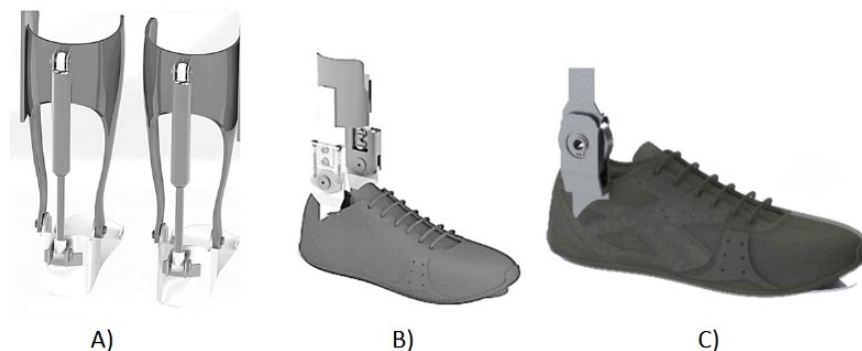
Figure 5.3 Variants of ankle joint design

Analysis of the best design for our device was conducted concerning following criteria, manufacturing and overall price, user-friendly design, variability and adjustability, reliability, weight and size, wearing comfort and safety issues. Upon of results from value analysis and discussions with experts from field of orthopaedics and prosthetics was chosen adjustable unilateral joint, which final design arise from merging B. and C. concepts from Figure 5.3 as the best solution for Ortholeg 2.0, see Figure 5.4. Adjustable ankle joint contains compression springs. These springs job is to lift foot during swing phase. Parameters of springs were calculated using segment method, if we consider weight of one foot 1.38 kg, compression springs with force around 35N in full compression can be used.

Figure 5.4 Final solution of ankle Joint

5.3 Manufacturing

Shoe insert was manufactured from prepreg carbon in combination with stainless steel stirrup. A prepreg consists of a combination of a matrix (or resin) and fibre reinforcement, in our case primarily carbon fibres. This material was chosen because it's ready to use in the component manufacturing process without any other special expensive machinery. Prepreg has very good ratio resin to reinforcement thanks to automatic manufacturing processes of plies, which makes this material the best option for our lightweight device. Prepreg is available in UD (unidirectional) form and in bidirectional fabric form. Unidirectional prepreg has very good mechanical properties in one direction but weakens unequally in perpendicular direction. Fabrics consist of at least two threads which are woven together and have equal properties in both directions. Shoe insert which was manufactured from fibre-reinforced composites was necessary design so that the fibre orientation produces optimum mechanical properties, this can be approach only by appropriate layup of different types of prepreg materials.

According mechanical and physical properties stated by manufacturer of purchased material and maximum ground reaction force (GRF), (Marasovič et al. 2009), we made similar virtual model using structural analysis simulation tools integrated in CAD software and simulated real component in order to determine necessary thickness for our application, see Figure 5.5. Software can only simulate isotropic materials, since structure manufactured from prepreg is never isotropic, rather anisotropic, the results are never same. This approach was carried out I order to roughly estimate number of layers, and spot weakest points which needs to be strengthened by using for instance unidirectional prepreg or thicker and stronger fabrics. This procedure is planned to be improved and upgraded in future deigning works

We chose combination of Bidirectional 3K and 6K 2x2 Twill and UD G300 preprag carbon in epoxy resin with excellent mechanical properties, moderate tack, good toughness, 30 days out-life at 20°C, 3 months storage at 4°C and stability for up to one year at -15°C. Chosen resin can be cured at temperatures from 120°C to 150°C in just vacuum bag.

Mechanical Properties of Epoxy resin:

- *Tensile strength, psi 8300 +/- 400*

- *Tensile modulus, Msi 0.46 +/- 0.02*

- *Flexural strength, psi 14600 +/- 400*

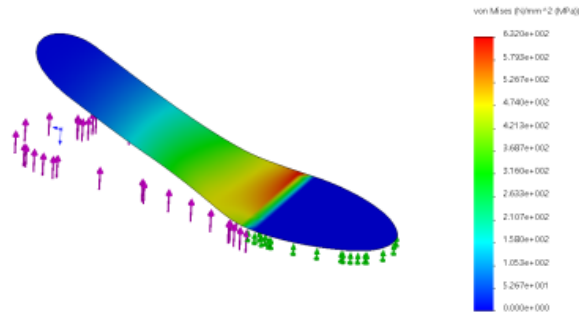- *Flexural modulus, Msi 0.50 +/- 0.02*
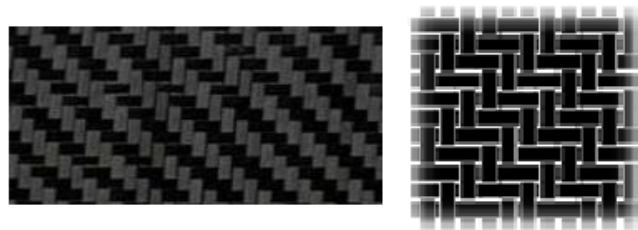

Figure 5.5 Structural analysis of shoe insert

Figure 5.6 Bidirectional 2x2 Twill prepreg carbon

Manufacturing in close cooperation with external company was triggered after selection of appropriate materials. There were tested different layups In order to achieve the best energy transfer between user and device and after experiments with manufactured shoe inserts there was chosen the best layup for our application, final layup is described in tab.2 After layup is done, all mould with prepreg carbon and stirrup is inserted into oven and cured on 120°C for 4-8 hours.
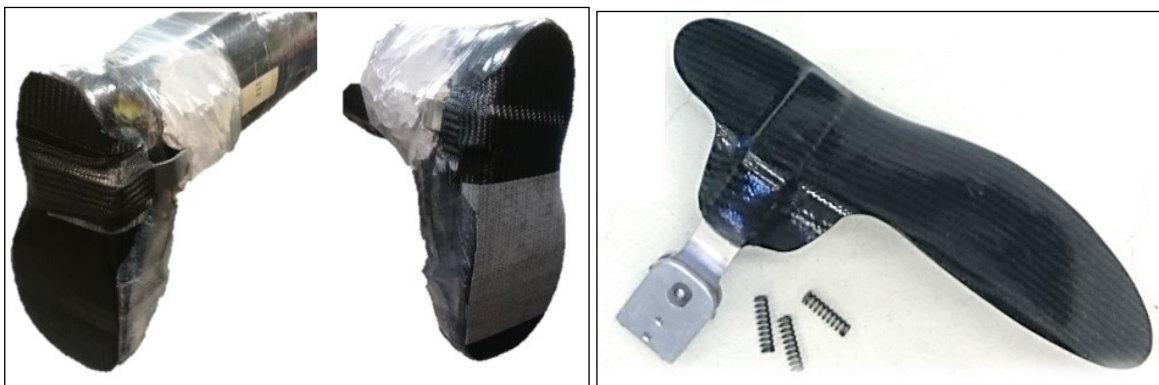

Figure 5.7 Process of manufacturing and complete cured ankle-foot component

Table 5.1 Manufacturing procedure of shoe inserts

Plies		Material	description
1	▦	Bi-direct 6K 2x2 Twill	full sole ply directly on foot mould
2	‖‖‖	UD G300	short ply in place where stirrup will be positioned
3	▦	Bi-direct 6K 2x2 Twill	short ply in place where stirrup will be positioned
4	extra resin	epoxy resin	stronger conjunction with stirrup, epoxy is soaked is steel surface
5	Stirrup	Stainless steel	Steel surface is roughened by grinding and drilling for better connection with prepreg resin
6	▦	Bi-direct 3K 2x2 Twill	full sole ply lay over steel stirrup
7	‖‖‖	UD G300	short ply in place of biggest stress concentration from CAD simulation
8	▦	Bi-direct 6K 2x2 Twill	full sole ply as final layer

5.4 Modular knee

Knees were designed such way to provide user with the possibility of easy configuration between actuated, semi-actuated and passive joint. In standard assembly, knees and hips are equipped with servomotors connected to steep threaded spindle or trapezoidal lead screw spindle same structure as in old design. On these rotating spindles are riding plastic threaded nuts from Iglidur J. In order to use electrically non-actuated version just four screws need to be unscrewed. There will be spring applied in knee joint witch accumulated energy will always return leg in upright position. These configurations allow us to test the differences between actuated and non-actuated gait cycles.
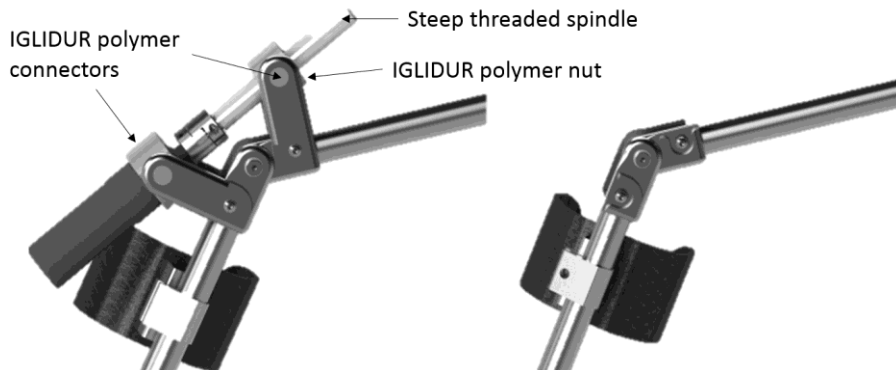

Figure 5.8 Modular knee joint

5.5   Electronics

Ortholeg 2.0 has same electronics as old version. Brushless DC motors (Maxon RE40, 150W) are connected to each hip and knee joints. The number of rotations performed by the motor is controlled by the motor controller (AX3500 Board). Controller keeps sending electrical current to rotate motor's shaft until its encoder (connected to the AX3500 board) indicates value close to the desired one. This values are generated by a central computer (raspberrypi) according to a specific angle joint reference, also connected to the motor controller. When some force pull back the moving link against its on-going direction, the board generates more current to bypass that force and keep the movement going. Because this electrical power source comes from a portable battery, as more the desired movement is slowed by an external force, as faster the battery will run out of power. Control elements and batteries will be located in backpack of spinal brace, which is one of the main, so called best-fit, elements securing exoskeleton on user's body, located on waist of user, see Figure 5.9.

5.6   Best-fit enhancements

Wider range of users can use Ortholeg 2.0 thanks to new adjustable elements, which were implemented in order to get as universal, modular, comfortable and user friendly device as possible, see Figure 5.9.

- *Fixtures*

There are four fixtures made from prepreg carbon for shins and thighs. Manufacturing process of fixtures is same as for shoe inserts. There is small aluminium piece integrated for thread to be drilled in order to attach clamps.

Fixtures can be easily positioned by simple unbuckle clamp connectors, thus user can wear this fixtures comfortably.

- *Adjustable height*

For different height of users there is possibility to adjust length of shin part.

- *Adjustable width*

It is important Ortholeg 2.0 fits as close to users' body as possible especially around waist. There is sliding adjustable back part in lumbar area. Slider is equipped with treaded rod connected to wheel for comfortable regulation which is easily done by user.

- *Brace*

Sinal orthosis with 0° of lumbar support curvature is just excellent component for easy wearing with maximum comfort. Lumbar universal orthosis is connected to Ortholeg construction through back part support which is made from Kydex polymer, see Figure 5.2.

340 +50/-50

SPINAL ORTHOSIS
WITH BACKPACK
FOR BATTERIES
AND ELECTRONICS

FIXTURES

ADJUSTABLE
HEIGHT 1080 +/- 50
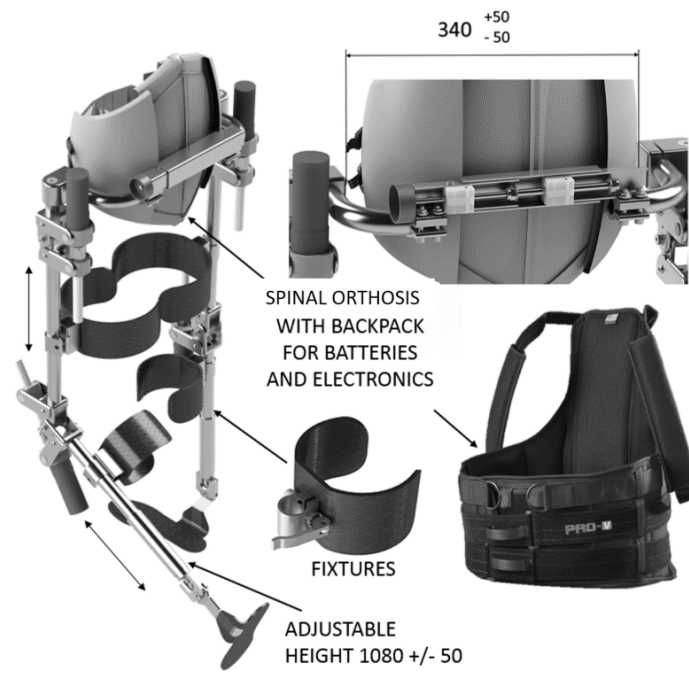
Figure 5.9 Best-fit enhancements

6 New active exoskeleton *@halo*

Second new active exoskeleton *@halo* and its passive version *Halo* are presented in this section. This part of work was performed in the Department of Robotics Science & Engineering of Chubu University, Japan. Mechanical design and control system of novel exoskeleton are explained and described in details in this chapter.

6.1 *Halo* - device update

HALO is a passive medial-hip-joint orthosis which consists of two KAFOs (Knee Ankle Foot Orthosis) connected by the special medial hip joint. The main idea of HALO is to harvest energy from ankle torque in order to assist swinging of contralateral leg and in addition avoid stumbling during walking. This is achieved by connecting the left and right ankle with hip joint using a pair of pulleys and steel wires in Bowden. The pulleys rotate on one shaft connecting left and right KAFO. The pulley which is paired with left ankle is connected to the right KAFO and vice versa,(Genda et al. 2004),for complete explanation of functionality see chapter 4.

The benefits in comparison with other passive orthoses were presented in the Chapter 4. Passive orthoses HALO was chosen for further development, thanks to these advantages. In order to improve some of the parameters such as energy consumption of users and stability, redesign of HALO was done and HALO joint was updated, see Figure 6.1. New *Halo* is passive orthosis with small bevel gearbox implemented on a shaft in between pulleys. This update provides with an available input shaft, for an additional possibility to actuate hip axis, see Figure 6.2.

As it was already explained in the chapter 4 ankle joint and hip joint are interconnected by steel wire rope. The ratio of the radius of rotation of the hip joint and the ankle joint is 1:2, which means any torque applied in the hip joint is two times of this value in the ankle joint in case an efficiency of the steel wire rope in Bowden is considered to be 100%. Due to friction of the wire rope in the Bowden losses are expected. The efficiency of such mechanism is normally between 70-90%, due to nearly straight line between hip and ankle (no loops or bends), we estimate the efficiency to be around 85%.

Figure 6.1 HALO orthoses (on the right) and new Halo with bevel gearbox (on the left)
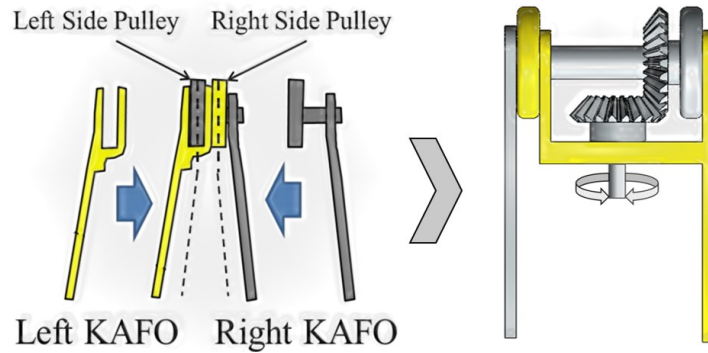
Figure 6.2 Hip joint update

6.2 Moments in ankle and hip joint while walking with Halo

Moments in lower limbs joints were calculated using inverse dynamics model from data from preliminary experiments. The results were compared with calculations done by (Genda 2010).

Two graphs in Figure 6.3 explains moments in the hip and ankle joint. The left graph compares HALO with normal walking and the Primewalk orthosis. The moment in the dorsiflexion direction increases immediately at the beginning of the stance during normal walking. Using HALO orthosis, the dorsiflexion moment is received throughout the stance period, and its dorsiflexion moment is gradually increasing from the mid-stance period, this is smoother trend than in the case of Primewalk.

The right graph shows moment in the hip joint and explains how ankle dorsiflexion moment assists swing of the contralateral leg. The moment received from the contralateral ankle at the initial stage of the stance acts in the flexion direction and is not assisting the hip joint extension movement. In the first half of the swing, the moment received from the opposite ankle acts in the flexing direction and assists the hip flexion movement (swinging of the free leg).
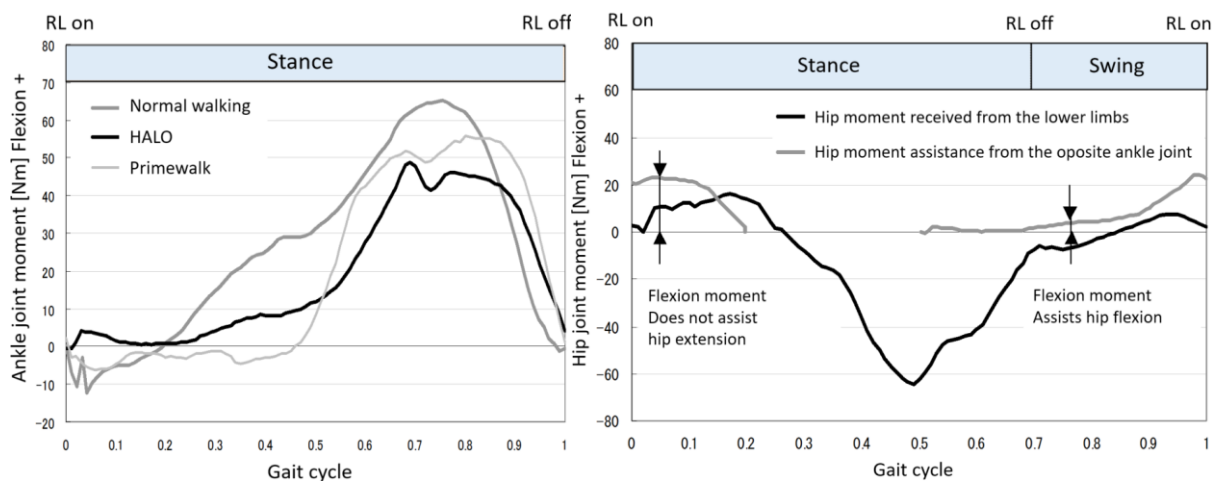

Figure 6.3 Ankle and hip joint moments during walking with HALO according (Genda 2010)

6.3 Calculation of hip and ankle moments by inverse dynamics

Moments in the ankle and the hip joint can be calculated using inverse dynamics after obtaining ground reaction forces data, position vectors and accelerations of each joint (ankle, knee and hip) and centre of gravity (COG) of each segment (foot, leg, and thigh) from experiments. Free body diagram of the foot with all necessary information for inverse dynamics analysis is in Figure 6.4.
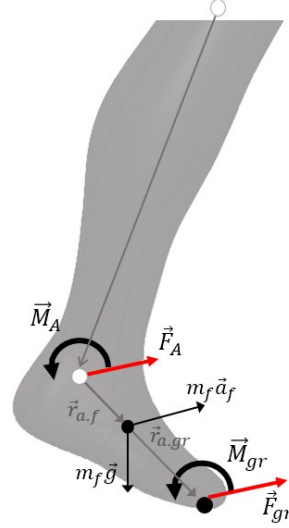

Figure 6.4 Free body diagram of the foot for inverse dynamics analysis

The equation for calculation of moments in the ankle joint is on (6.1).

$$\vec{M}_a = \vec{r}_{a.gr} \times \vec{F}_{gr} + (\vec{r}_{a.f} \times m_f(\vec{g} - \vec{a}_f)) + \vec{M}_{gr} - \vec{M}_{Ia} \qquad (6.1)$$

Where the ground reaction force $\vec{F}_{gr}$ was obtained from measurement, m_f is foot mass, a_f and g are inertial and gravitational accelerations, $\vec{r}_{a.gr}$ is position vector from the ankle joint to the centre of pressure (black spot) and $\vec{r}_{a.f}$ is position vector from the ankle joint to the foot segment centre of gravity, $\vec{M}_{Ia}$ is inertial moment due to foot segment and finally $\vec{M}_{gr}$ is moment measured by footplate.

The generalized equation for calculation of moment in the hip joint is on (6.2), this equation can be used for any last joint of three serially inked segments, in this case, it is foot, leg and thigh segment, more about inverse dynamics model is discussed in a Chapter 8.

$$\vec{M}_H = \vec{r}_{h.gr} \times \vec{F}_{gr} + \sum_{i=1}^{3} \vec{r}_i \times m_i(\vec{g} - \vec{a}_i) + \vec{M}_{gr} - \sum_{i=1}^{3} \vec{M}_{Ii} \qquad (6.2)$$

Where m_i is i^{th} segment mass, a_i and g are inertial and gravitational accelerations of ith segment, $\vec{r}_{h.grf}$ is position vector from the hip joint to the centre of pressure and $\vec{r}_i$ is the position vector from the hip joint to the ith segment centre of gravity and finally $\vec{M}_{Ii}$ is inertial moment due to i^{th} segment.

A comparison of the results of maximal moments in the hip and ankle joints during preliminary walking experiments (both subjects) with new *Halo* orthosis how it was calculated and according (Genda 2010) is listed in Table 6.1. Moreover, an average of the angular velocities of the hip and ankle joint were obtained from the Cortex software.

Table 6.1 Comparison of the results of maximal moments and angular velocity in the hip and ankle

	max. calc. moment subject 2 [Nm]	max. calc. moment subject 2 [Nm]	max. moment Genda et al. [Nm]	calculated speed [rpm]
Ankle	51.5	54.7	≈48	12.5
Hip	47.5	49.9	≈63	21.2

6.4 Mechanical design of powered exoskeleton *@halo*

New *Halo* design together with an actuator unit is called *@halo* (active hip ankle linkage exoskeleton). The new mechanical design is modular. Users can decide and easily switch between active or passive setting by unplugging the actuator unit. A detailed description of the prototype of *@halo* exoskeleton is in Figure 6.5 and two models of *@halo* joint are presented in Figure 6.6. Right model of the joint represents simplified structure for better understanding of its functionality. 3D Models consist of white and black parts firmly assembled in two units or blocks which are mutually rotating.

Black block (dark parts) consists of gearbox 1 case (cut section view) connected to the motor with gearbox 2, KAFO connector 1 with Bowden holder 1 and pulley 1. Motor with planetary gearbox 2 is connected via shaft coupling to a shaft on which rotates spiral bevel pinion. KAFO connector 1 is the interface plate of the right KAFO. Bowden holder with holes for the steel wire is attached to this plate. Pulley 1 on the left side of the joint is through the steel wires linked to the left ankle and in addition, serves as the gearbox 1 case cover, which are firmly screwed together. Bevel gearbox 1 case is stiffening construction and augmenting rigidity of the main shaft, its compact cylindrical shape fits perfectly into the hand, thus serves as a grip for easy manipulating with the exoskeleton.

White block (light parts) consists of the main shaft which is connected to a bevel gear. The spiral bevel gear is then firmly screwed to a pulley 2. This pulley is then linked to the right ankle. The main shaft is firmly attached at the end with KAFO connector plate 2. Bowden holder 2 is connected to this plate and serves as a slideway. Holder was manufactured from POM plastic material, but self-lubricating iglide® polymer from company Igus was tested for better performance. *@halo* joint main parts were manufactured from Aluminium 7075-T6, this material has superior properties and can sustain high payloads thanks to its high tensile strength.

The device weight is 6.8 kg (without electronics). New *@halo* hip joint weight is 1.9 kg. The height of the device is adjustable, according to users' body proportions.

6.4.1 Selection of servomotor

As it is explained in the Chapter 5, motor assistance is activated between double support and heel off during preswing phase, this indicates just partial assistance of the actuator for push off from the ground. Users are partially supporting this movement by crutches. This means, an important and driving element for the selection of appropriate motor is the ankle moment value. Ankle moment should be according to the results from Table 6.1 between 51 to 55 Nm in order to be able to overcome initial resistance and fully assist in forward progression. The moment of output shaft from the bevel gearbox M_{bg} should be about 32 Nm obtained from the ratio between the ankle and the hip 2:1 and efficiency 85% according (6.3).

$$M_{bg} = \frac{55\,Nm}{2 \cdot 0.85} \cong 32Nm \qquad (6.3)$$

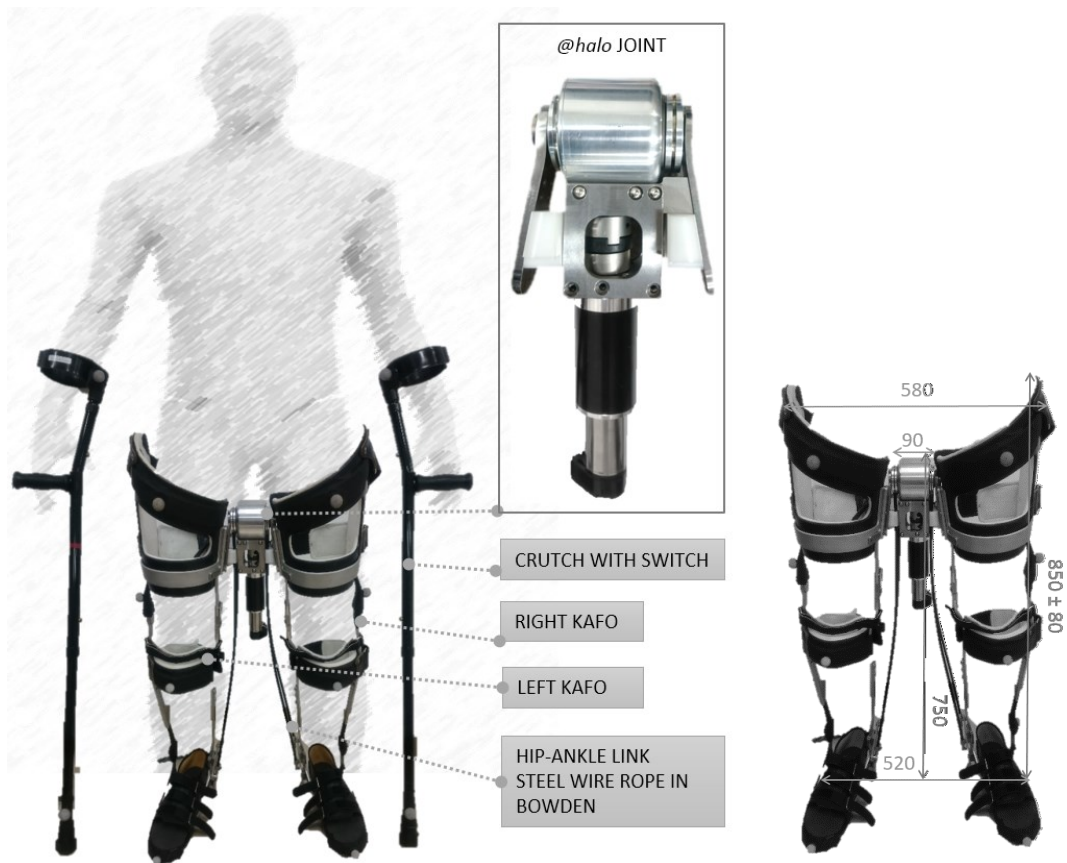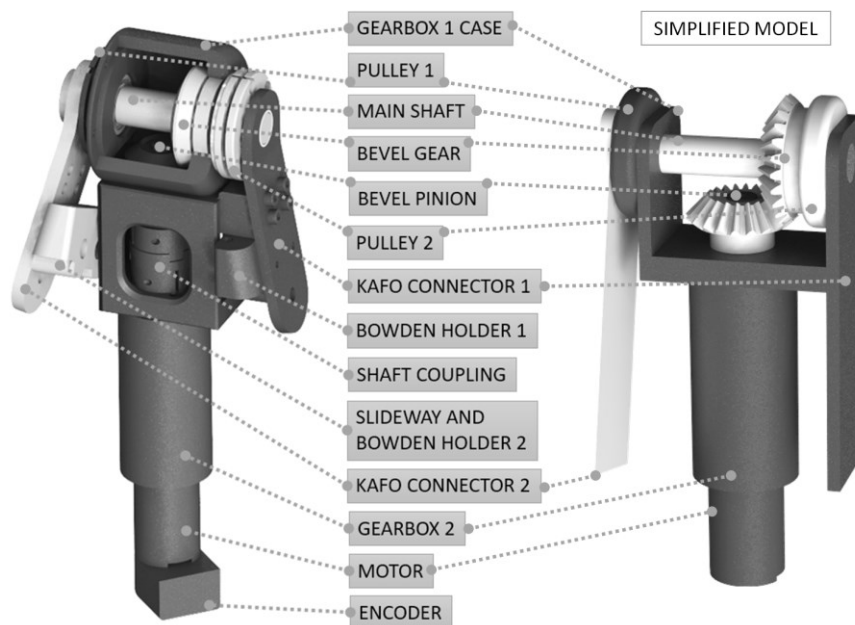*Figure 6.5 New @halo exoskeleton and @halo joint*

Figure 6.6 @halo joint model in section view and simplified model

A servomotor combining the DC motor EC-powermax30 from Maxon and the planetary gearhead GP42C was purchased for this application. The total weight of servomotor is about 0.75 [kg] and the total length of the combination (gearhead + DC motor + encoder) is about 152 [mm].

57

- *Selection of the motor*

According to calculated torque, required for powering ankle joint DC motor EC-powermax30 from Maxon was chosen due to its satisfactory nominal speed and torque, see motor data in Table 6.2 and operating range of motor in Figure 6.7.

Table 6.2 Motor maxon data (EC-powermax30)

Power [W]	100
Nominal voltage[V]	24
No load speed [rpm]	17800
Nominal speed [rpm]	16700
Nominal Torque (max. continuous torque) [mNm]	63.3
Nominal current (max. continuous current) [A]	5.45
Stall torque [mNm]	1280
Torque constant [mNm / A]	12.8
Max permissible speed	25000
Terminal inductance phase to phase [mH]	0.0295
weight [g]	165

- *Selection of the Gearhead*

Planetary Gearhead GP 42 C Ø42 mm, 3 - 15 Nm, Ceramic Version from company maxon was chosen for its high reduction ratio and satisfactory intermittent torque at gear output.

Table 6.3 Planetary gearhead GP 42 C

Reduction	546:1
Absolute reduction	546
Mass inertia [gcm^2]	15
Max. motor shaft diameter [mm]	10
Max. continuous torque [Nm]	15
Max. intermittent torque at gear output [Nm]	22.5
Max. efficiency [%]	64
weight [g]	560

- *Selection of the encoder*

An incremental encoder (HEDL 5540) from the company Maxon is used for detecting the rotation angle of the actuator. Incremental encoders are inexpensive due to their simple structure, but calibration is needed when turning on the power to detect relative values. Specifications are shown in Table 6.4.

Table 6.4 incremental encoder (HEDL 5540)

Pulses per revolution - E_{ppr}	500
Channels	3
Maximum frequency [100Hz]	100
Maximum angular acceleration [rad/s^2]	25000

- *Calculation of output torque and speed*

Calculation of the output torque and speed of the chosen actuator is summarized in Table 6.5.

Table 6.5 output torque and speed summary

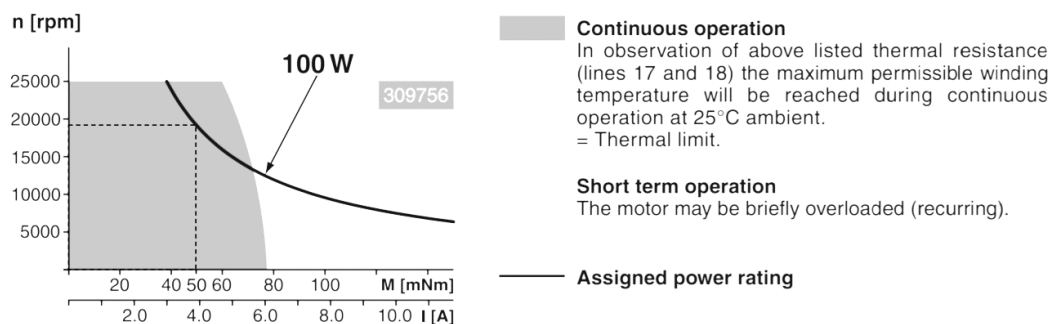|	gear ratio i	efficiency η [%]	torque output [Nm]	speed output [rpm]
Bowden-wire	2	85	54.7	12
Bevel gear	1,5	98	32	24
Gearhead	546	65	21.8	36
Motor	---------------	90	0.063	19656

Figure 6.7 Operating Range of motor (EC-powermax30 - from Maxon motor datasheet)

6.4.2 Selection of bevel gears

Bevel gears were calculated using software Mitcalc where input values are listed in Table 6.6.

Table 6.6 input values for calculation of bevel gears

basic input parameters		Value
Transferred power	Pw [kW]	0.08
Speed (Pinion / Gear)	n [rpm]	36
Torsional moment (Pinion / Gear)	Mk [Nm]	21.8
Transmission ratio / from table	i	1.5

KSP Nissei ground spiral bevel gears were selected for right angle distribution of the moment to the hip joints. There was necessary to order secondary manufacturing operations for this gear set before assembly. All specifications are presented in Table 6.7, Table 6.8 and Figure 6.8 (from KHK STOCK GEARS website).
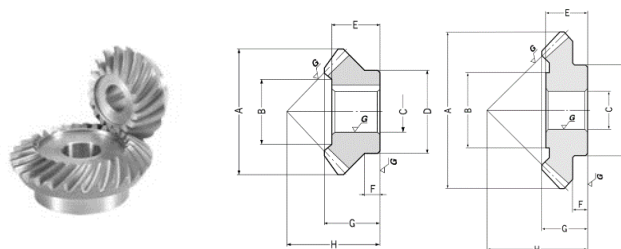

Figure 6.8 KSP Nissei ground spiral bevel gears

Table 6.7 KSP Nissei ground spiral bevel gears characteristics

Characteristics	value / description
Precision Grade	JIS B 1704 grade 0
Gear teeth	Gleason
Pressure angle	20
Helix angle	35
Material	SCM415
Heat treatment	Carbonized
Tooth hardness	60~63HRC
Shaft angle	90

Table 6.8 KSP Nissei ground spiral bevel gears specification

	Direction of Spiral	Module	No. of teeth	Pitch dia	Face width	Outside dia. A	Holding surface dia. B	Bore CH7
KSP0481.5GU P	L	2	16	32	9	34	17.6	12
KSP0481.5GU G	R	2	24	48	9	48	30.4	15

6.4.3 Couplings

Oldham coupling clamping type (MCOCWK38-12-12 - both sides keywayed) with additional set screws on top of the groove were selected to couple motor output shaft with the bevel pinion shaft. Important parameter of the coupling are listed in Table 6.9.

Table 6.9 parameters of coupling

parameters of coupling MCOCWK38-12-12		Value
Allowable Torque	Mk [Nm]	28
Max. rotational speed	n [rpm]	5800
Allowable angular misalignment	[°]	3
weight	[Kg]	240

6.4.4 Steel wire rope calculation

Powered exoskeleton *@halo* is acting on the ankle joint by moment 54.7 [Nm] as it was calculated earlier in this chapter. This big moment is producing pulling force in the steel wire rope of ankle-hip link mechanism. The steel wire rope is acting on rotation radius 0.05 [m]. The maximum pulling force acting on the wire is 547 N. Since the allowable tension of the steel wire rope (7 × 7 type thickness 2.0 mm) is 3234 N, it can be said that the durability is sufficient. The most critical point is pressed wire ending, see Figure 6.9, this part was however tested by years of usage of passive HALO orthosis and the allowed pulling force limit was set to 784 N. This means, such way of securing the steel wire rope is sufficient. Nonetheless, other more durable techniques may be used in case of further development.
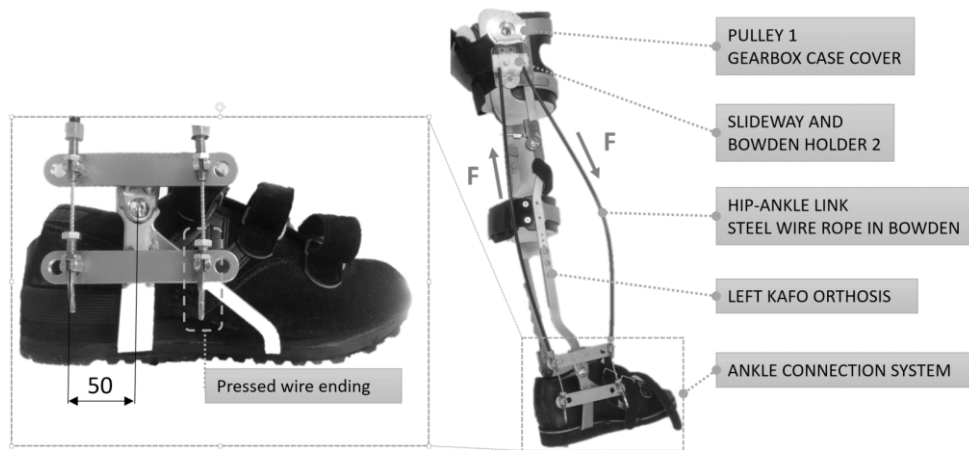
Figure 6.9 Steel wire rope and Bowden assembly

6.4.5 Slider and Oil Free Slide Plates combination

In order to prevent high bending forces on the main shaft, the Slider from POM material was used in combination with Oil-Free Slide Plates. The Plates have special multi-layer coating (Filler Added Polytetrafluoroethylene Layer, Sintered Bronze Layer, and Back Metal Layer) which does not require any kind of lubrication and works with a very low coefficient of friction.

This system was tested on nearly 1000 cycles during high loads and the result was satisfactory, abrasion of POM material was negligible and Oil-Free Slide Plates had no signs of losing coating structure.
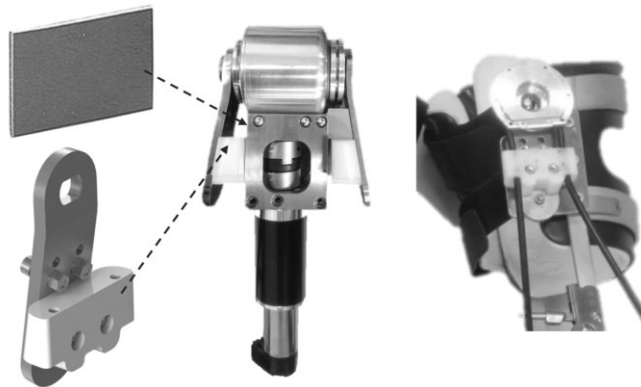

Figure 6.10 POM Slider and Oil Free Slide Plate combination

6.5   *@halo* control unit

Motor control hardware, connection layout and software are presented in this subchapter. The connection layout of the motor control unit is in Figure 6.11. The three main components of the system are PC with communication cards from company Interface corp., 4-Q-EC Servoamplifier DES 70/10 from company Maxon and Electronic Commutation (EC) Servomotor from company Maxon. The DES (Digital EC Servoamplifier) is the efficient digital servoamplifier with sinusoidal current commutation for the control of EC motors.

The PC is equipped by ADDA (analogue/digital, digital/analogue) board PCI-360116, counter, timer and digital input/output (DIO) card LPC-632104. The PC executes a motor control program and sends

the command signal to the servoamplifier via ADDA board. ADDA board is connected to servoamplifier via differential input "Set value" which is set to range -10 … +10 V. The analogue signal is amplified by the servoamplifier and from there sent to the motor. Such a way the motor can be driven or regulated.

A motor choke is inserted between the motor and servoamplifier to prevent overcurrent. There is just one motor, thus one actuated DOF, and two movements (dorsiflexion and plantarflexion) to be controlled. This is done by altering clockwise and counter-clockwise direction of the rotation of the motor output shaft.

In order to obtain information about speed, angle, and direction of rotation, the servomotor is equipped with the incremental encoder. To monitor this variables encoder is connected to servoamplifier by special port dedicated to encoder itself. For a closed loop position control (control method is discussed later in this chapter), the encoder is connected directly to the counter board as well. The pulse signal is received by the counter board and processed by a control program which converts this signal to angle value.

The output torque estimation is done from the monitored output current of the motor. This current is multiplied by torque constant obtained from the motor datasheet and the estimated torque is a result which is presented in chapter 5.

The servoamplifier was set for speed control during preliminary experiments, current control mode was however tested as well. If the "Digital 2" input is connected to a voltage higher than 2.4 VDC the servoamplifier is configured to speed controller mode. If the "Digital 2" input is connected to Gnd the servoamplifier is configured to current (torque) mode. If the "Digital 1" input is connected to Gnd the actual motor speed is given to the "Monitor" output. If a voltage is given at "Digital 1", the actual motor current is given to the "Monitor" output. The 3-Position Selector Switch is connected to "Digital 1", "Digital 2" and to "Enable" input for switching between control modes and for ON/OFF motor command, see Figure 6.15. The "Digital 2" button was switched on (connected to auxiliary voltage 5VDC) and speed control mode was activated during preliminary experiments. The "Digital 1" button was switched on (connected to auxiliary voltage 5VDC) and the actual motor current was monitored, received via ADDA board and processed by motor control program. Motor torque was estimated and evaluated from actual motor current value and the torque constant.

 An emergency button was installed and connected to "STOP" input of servoamplifier for the case of emergency. If a voltage is given at "STOP", the motor speed will be stopped with maximum deceleration until motor shaft stands still.

As an alternative, configuration and commanding of the servoamplifier also is possible over the PC using RS232 or CAN. This functionality was used and servoamplifier was connected via RS232 to PC in order to set quickly reproducibly and numerically parameters such as maximal speed, offset, gain or maximal current.

There is OS Windows XP installed in the PC and program Visual C ++ 2010 was used to create motor control program to process input and output data collectively in the timer loop of sampling frequency 100 [Hz] and sampling interval 100000 [ms].
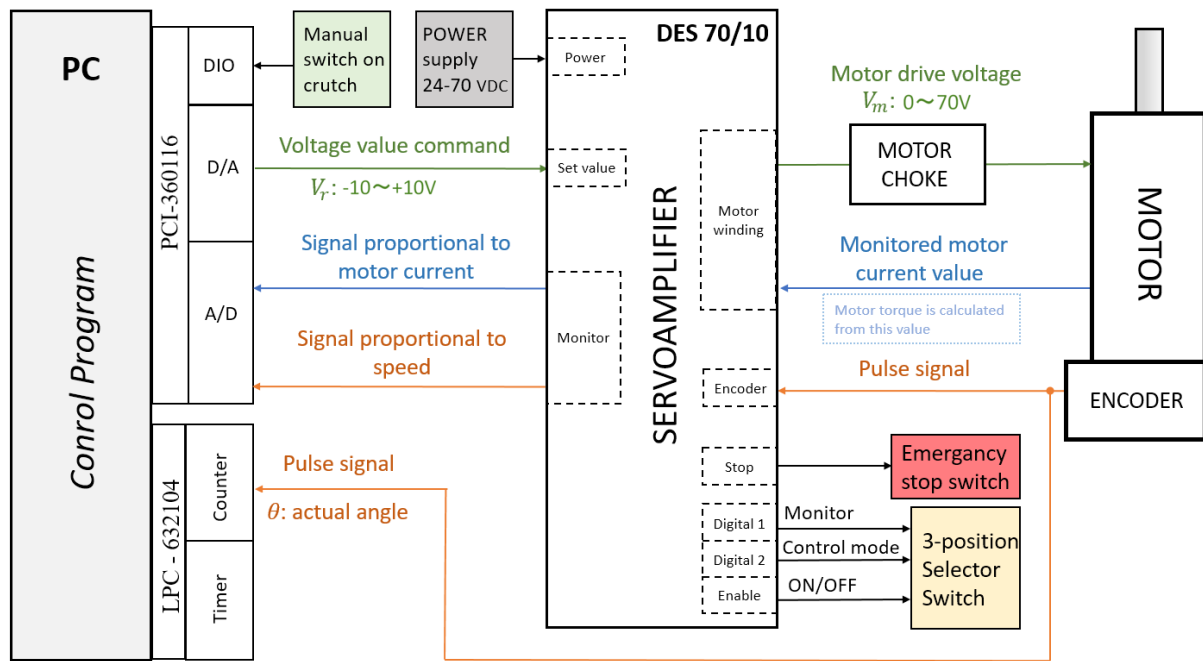
Figure 6.11 Connection layout of @halo control unit

The ADDA conversion board connected to PC's motherboard are shown in Figure 6.13, and the specifications of these conversion boards are presented in Table 6.11. The counter board by which the speed information was received is in Figure 6.13, and the specification of this board is shown in Table 6.12. The counter board can be set as an interval timer.

All system of the @halo prototype is stationary, connected to the mobile exoskeleton through a set of wires and terminal boards. This kind of setting is not practical for real application and absolutely inadequate for everyday use. One of the main directions of future development is a creation of a compact mobile control unit powered by a battery pack and embedded directly into the exoskeleton. As for testing purpose and proof of functionality of the idea however the prototype with the stationary system was satisfactory.

6.5.1   Servoamplifier

As already mentioned 4-Q-EC Servoamplifier DES 70 / 10 from Maxon company was used in the motor control system. The main advantage of this amplifier is the possibility of switching between speed and current control modes. Speed control mode was used during preliminary experiments and the current was monitored and stored. More details about control are discussed later in this chapter and in chapter 5 as well. The specifications of the servo amplifier are summarized in Table 6.10. Exact connection layout is presented in Figure 6.12 – picture extracted from Maxon datasheet. Servoamplifier DES 70 / 10 was chosen due to economical reasons, for the future development, use of different controller should be considered, the reasonable solution is for instance Maxon controller EPOS series.

Table 6.10 4-Q-EC Servoamplifier DES 70/10 specification

Characteristics	value
Operating voltage VCC	24 - 70 VDC
Max. output voltage	0.9 x VCC
Max. output current Imax	30 A

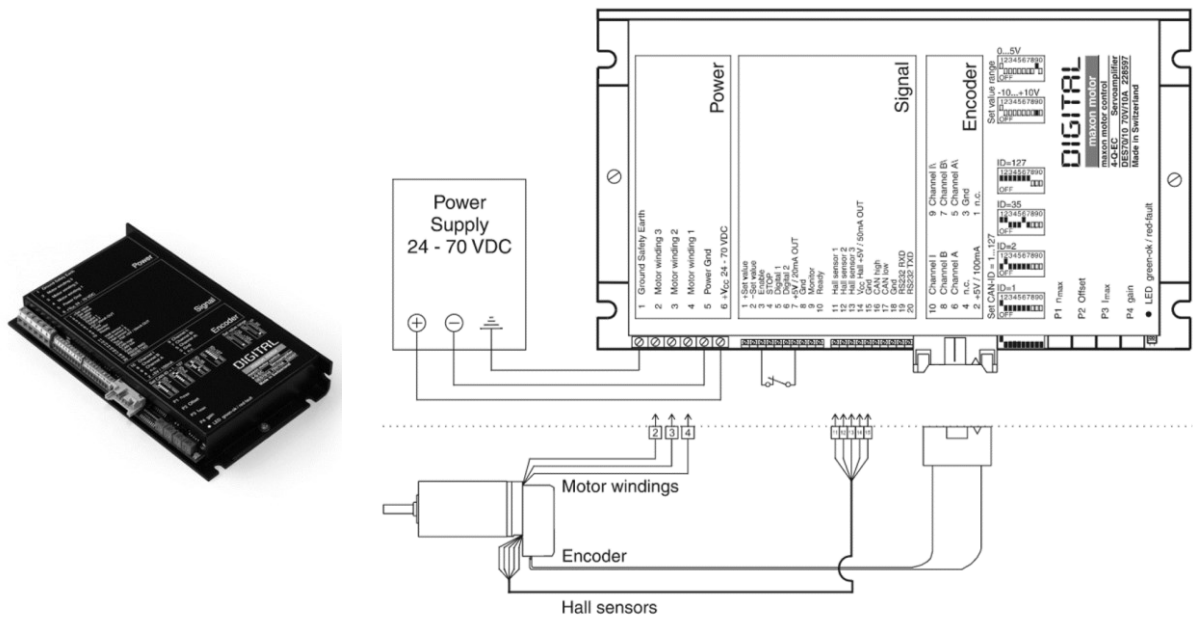| Continuous output current Icont	10 A
Max. speed (1 pole pair)	25 000 rpm
weight	400 g

Figure 6.12 4-Q-EC Servoamplifier DES 70/10 and connection layout with EC motor – pictures from Maxon Datasheet

6.5.2   Interface boards

Two interface boards were used for signal processing. The LPC-632104 is counter board which provides four 32-bit multi-function counters. As each counter is isolated, it can be used for different functions. The PCI - 360116 is a high - speed 16 - bit ADDA board compatible with the PCI bus. The AD conversion time is about 1 µs.
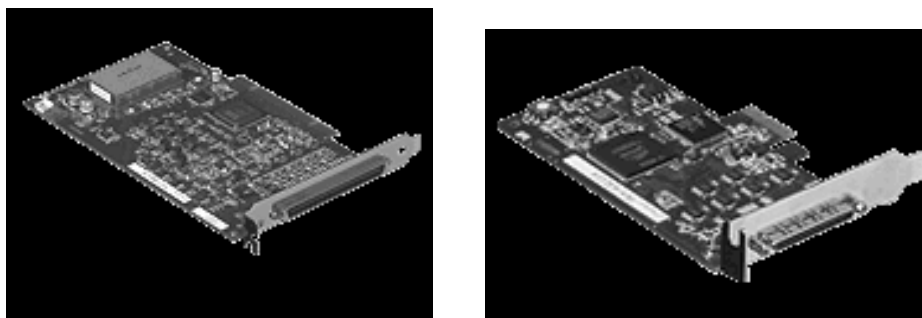

Figure 6.13 ADDA board and counter board

Table 6.11 ADDA board (PCI-360116) specification

Characteristics	value
A/D (ch)	8
D/A (ch)	2
Resolution (bit)	16
bipolar (V)	±10

64

Table 6.12 counter board (LPC - 632104) specification

Characteristics	value
max input frequency (MHz)	10
Counter (ch)	4
Resolution (bit)	32
bipolar (V)	±10

6.5.3 Choke

A choke is an inductor connected in series with the EC motor in order to block higher-frequency alternating current (AC) in an electrical circuit, while passing lower-frequency or direct current (DC). EC motor used for powering *@halo* exoskeleton is low inductance motor which enables design to be very slim and compact. However low inductance means low electrical time constants and this leads to high amount of a motor's current ripples and higher peaks, this results in high running current value which heats the motor up. In order to protect the motor, it is necessary to add a choke coil as additional inductance for attenuating the current spikes. The behaviour of the motor does not change, because the generated motor torque is proportional to the average value of the current and additional inductance in the electric circuit improves the stability of the current controller.

When the inductance of the motor is 0.4 mH or less, the choke needs to be added. The terminal inductance phase to phase value of the used EC motor is 0.0295 mH, see Table 6.2 Motor maxon data (EC-powermax30), this means there is necessary to include the choke, specific type which was used is on .
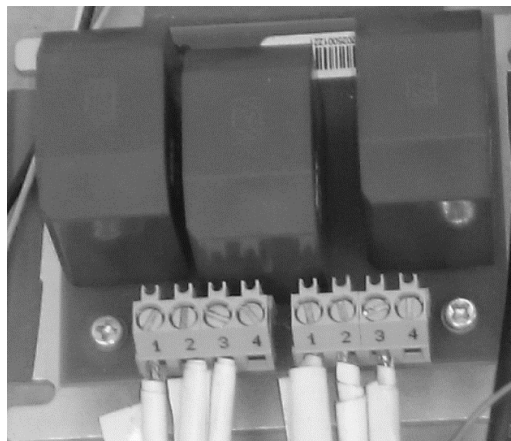

Figure 6.14 Choke

6.5.4 Buttons and switches

The 3-Position Selector Switch was used for switching between control settings and for turning the actuator ON and OFF. The emergency button was placed in near proximity of operator of the control unit during preliminary experiments, buttons are in Figure 6.15.

Figure 6.15 The 3-Position Selector Switch and emergency STOP button

6.6 Lofstrand crutch and integrated manual switch

The user wearing the *@halo* exoskeleton controls this device manually by pressing the switch integrated inside a moulded handpiece of the Lofstrand crutch, see Figure 6.16. This Manual switch is connected by wires directly to DIO card inside PC.

Force sensitive resistors (FSR) were integrated in shoe insoles of *@halo* exoskeleton as optional control method. This functionality was however not used during preliminary experiments. The manual switch button in crutch for its simplicity and easy-to-use benefits was selected as the safest and the most convenient.

Figure 6.16 Forearm crutch with integrated manual switch (DS-663)

6.7 Control system of actuator

Control system is discussed in this section, a block diagram of a closed loop position control and PI controller are described as well as the motor control program and specific modes which user can use during walking with the *@halo* exoskeleton.

6.7.1 Block diagram of control system

The closed loop position control system with a PI controller for less steady state error and smooth response is used for the motor control, the block diagram of the control system is presented in Figure

6.17. The controller gains Kp, Ki, and Ks were tuned for a good tracking performance by Ziegler-Nichols Ultimate Gain method (Lee et al. 2015).The system controls hip angle by referring to the target angle.
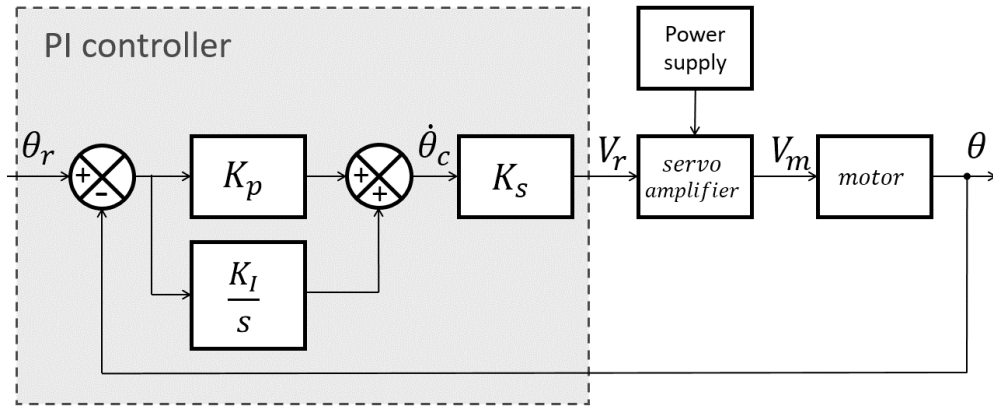

Figure 6.17 Block diagram of the @halo control system

Procedure of calculating control signal output V_r from PI controller is described in equations (6.4-8). Equation 6.7 represents PI controller, there is sum of two terms: a proportional term that is proportional to the error, an integral term that is proportional to the integral of the error.

$$\theta(t) = \frac{C_p \cdot 360}{N_{ppr} \cdot i_{gh} \cdot i_{bg} \cdot i_{wm}} => \dot{\theta}(t) = \frac{d\theta(t)}{dt} \tag{6.4}$$

$$\theta_r(t) = \frac{\theta_{r\_data} \cdot i_{gh} \cdot i_{bg} \cdot i_{wm}}{\eta_m \cdot \eta_{gh} \cdot \eta_{bg} \cdot \eta_{wm}} => \dot{\theta}_r(t) = \frac{d\theta_r(t)}{dt} \tag{6.5}$$

$$e_{\dot{\theta}}(t) = \frac{\dot{\theta}(t) - \dot{\theta}_r(t)}{F_{smpl}} \tag{6.6}$$

$$\dot{\theta}_c(t) = K_p \cdot e_{\dot{\theta}}(t) + K_i \int_0^t e_{\dot{\theta}}(t)dt \tag{6.7}$$

$$V_r(t) = \left(\frac{\dot{\theta}_r(t)}{\dot{\theta}_{max}}\right) \cdot 10 \tag{6.8}$$

Where θ_r: reference angle [deg], θ: actual angle [deg], $\dot{\theta}_r$: reference angular velocity

$\dot{\theta}_c$: control angular velocity [rpm], θ_{r_data}: loaded angle reference data, $e_{\dot{\theta}}$: control error,

K_p: Proportional gain, K_I: integral gain, K_s: voltage conversion gain, N_{ppr}: pulse encoder signal

V_r: Voltage value command [V], V_m: Motor drive voltage [V], F_{smpl}: Sampling frequency

$\eta_m, \eta_{gh}, \eta_{bg}, \eta_{wm}$: Efficiency of motor, planetary gearhead, bevel gear, wire mechanism

i_{gh}, i_{bg}, i_{wm}: gear ratio of planetary gearhead, bevel gear, wire mechanism

6.7.2 Control parameters of PI controller

In order to use the PI controller, it is necessary to set proportional gain K_p and integral gain K_I. In this study, Ziegler-Nichols Ultimate Gain method was used to find these parameters.

The first step of Ziegler-Nichols method is to find Ultimate gain K_u. We start with a closed-loop system with only proportional controller and gain K_c (critical gain), integral gain K_I is set to zero. K_c is set to very low value and gradually is increased until a steady-state oscillation occurs, such a way the gain called Ultimate gain K_u is obtained. For our application there was measured K_u= 1.8 with the period of oscillation T_u = 0.321. Based on these values, the control parameters are defined from Table 6.13.

As the result the gains K_p=0.54 with T_I = 0.27 and K_I= 0.1 were used.

Table 6.13 Ziegler-Nichols Ultimate Gain method

Controller	K_p	T_I	T_D
P	0.5 K_u		
PI	0.45 K_u	0.83 T_u	
PID	0.6 K_u	0.5 T_u	0.125 T_u

6.7.3 Control modes

Device *@halo* comes together with Loftstrand crutches as described in previous chapters. The left crutch is equipped with a switch, see Figure 6.16. The device can be controlled by the user either in semi-automatic mode or manual mode. Users press and hold the switch during the whole walking period in the semi-automatic mode for continuous walking. This serves as a safety feature, in a case of lost balance or instability, the switch is released and the motor stops at the next reference point. In manual mode the button has to be pushed after each step, this second option was used during preliminary experiments. The first prototype control system does not provide with an option of changing a speed of walking. Turning left and right is possible while standing both feet on the ground. This function, however, requires special modification of soles and was not tested, only forward walking was examined during the preliminary experiments.

6.7.4 Control program

Control programme structure, features and control logic is briefly discussed in this section.

Initialization of the ADDA and counter boards and calibration of the encoder are performed as the first step after turning on the control unit. In order to calibrate the Incremental encoder it is necessary to adjust the offset for angle detection. For the sake of accuracy, so all experiments begin in the same position, the users were instructed to stand on double support with legs in parallel so the toe tips are aligned and in this posture was set 0°. Left leg was then moved backward for 30° and this was the initial position for preliminary experiments. The serial communication via RS232 was established by connecting the servoamplifier and the PC, so described initialization process and data files creation and export can be done simply through programmed user interface, see Figure 6.18.

The file with the target reference angle is externally created. The period of the angle reference consists of rapid increase by +60° following by decrease to -60° and this is equal to one gait cycle. First

half period in positive direction is then equal to one step and this is equal to 90° counterclockwise rotation of the shaft of actuator. Second half period in negative direction is then equal to second step and this is equal to 90° clockwise rotation of the shaft of actuator. All file is loaded at once and the data are synchronized with the sample data number controlled by counter. Sample data number is the time length of the half period. In practice, one press of the manual switch runs one step. If the button is not released and user holds the button, then the program does not stop and reads second half of period, thus second step of the gait cycle is continuously initiated. This cycle is then set in a loop, it means while holding the manual switch walking does not stop, for more about gait cycle of the preliminary experiments see chapter 5.

Control program has following functions:

- Track target angle file and open it
- Target angle data input – load target angle reference data
- determination of the assist switch ON · OFF
  - start cycle of the right switch ON
  - set condition of the right switch OFF
- Calculate error from comparing target angle and actual angle data
- Sending error to PI controller and setting new output angle data for motor
- Differentiation of angle data and converting to voltage output for the servoamplifier
- Hip joint range of motion restriction ± 45° – user safety feature
- Set range of current restriction max ± 10 A – Servoamplifier safety feature
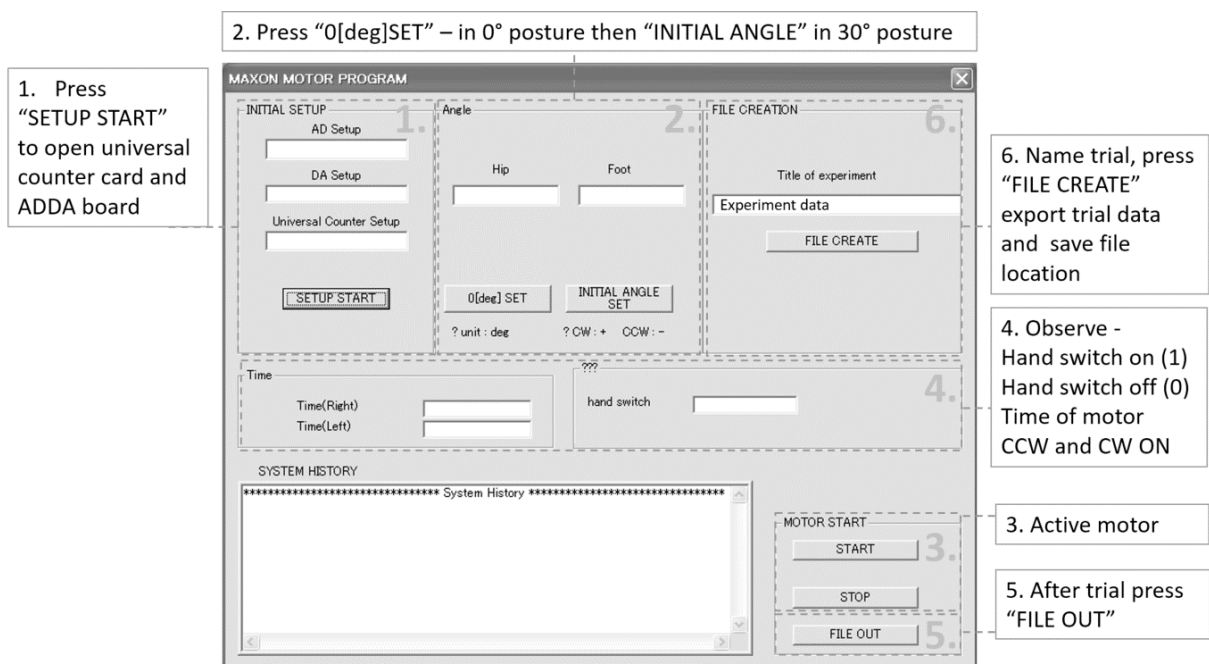
Figure 6.18 User interface for initialization, data file creation and export with description of each steps

7 Experiment procedure and set up

Exoskeleton which meets requirements from the requirement list and which fits better the aims of this work is selected. Exoskeleton *@halo* was chosen as better solution. Walking with active *@halo* device and passive *Halo* orthosis was tested during preliminary experiments. All necessary details about experiments such as experimental set up, experimental trials, data acquisition techniques and description of equipment used during experiments are presented in this chapter.

7.1 Selection of Exoskeleton for further research

The better solution for further experiments with able-bodied subjects was selected according significance of requirement and degree of fulfilling requirement of each solution. Device *@halo* has nearly twice higher score in comparison with Ortholeg 2.0, according Table 7.1.

Table 7.1 Selection of solution

i	Requirement	Value or description	Significance of req.	@halo	Ortholeg 2.0
1	**Mediolateral stability**	Walking independently without assistance	**2**	2	0
2	**Anteroposterior stability**	Walking independently without assistance	**2**	2	1
3	**Price**	max 10000 USD	**2**	2	0
4	**Weight of device**	max 8 Kg	**2**	2	1
5	**Weight of user**	up to 70 Kg	**2**	2	2
6	**Energy consumption of user**	Evaluated from vertical elevation of CoG	**2**	1	2
7	**Don/Doff directly from a wheelchair**	YES	**1**	2	0
8	**Modularity**	Possibility of switching to passive option	**1**	2	1
9	**Walking pattern**	Natural pattern similar to normal walking	**1**	0	2
Result = $\sum_{i=1}^{9}$ Significance $*$ Degree of fulfilling requirement				**26**	**15**

Table 7.2 Degree of fulfilling requirement

Degree of fulfilling requirement	Description
0	Does not satisfy requirement
1	Partially satisfy requirement
2	Completely satisfy requirement

7.2 Walking with *Halo* and *@halo*

Experimental trials were conducted in order to verify the assist effect of @halo. The main aim of data analysis and acquisition from trials was the comparison of the gait parameters between passive Halo setting and actuated @halo setting. The preliminary experiments were conducted with **two able-bodied subjects**, their parameter are summarized in Table 7.3.

Table 7.3 Subjects

Parameters	Subject 1	Subject 2
Height	1.724m	1.790m
Weight	63 kg	65 kg
Age	21	29

Each subject conducted 30 trials with Halo and 30 trials with powered @halo. One trial consists of the full gait cycle, of one stride. The trial starts in posture one leg in front of another with approximately 30 degrees between legs. The data obtained from experiments were processed and evaluated in chapter 8.

Due to specific HALO gait, there were many (hundreds) of trials conducted before recording evaluated strides. The subjects were trained by professional staff to adopt the walking style with Halo in order to simulate the authentic movement of the lower and upper body, as it was performed by patients. The @halo exoskeleton was adjusted according to the height of subjects before the start of the experiments. There was no big difference between subjects' heights, therefore the device was set for one configuration during all trials.

7.3 Experimental setup

The subjects accomplished experiments in an area which was monitored by six infrared motion tracking cameras Mac3D (Motion Analysis corp.) at the frequency of 60 Hz. Four Kistler force plates with six DOF were situated in the middle of the room in order to measure the ground reaction forces (GRF) of both legs and both crutches. Twenty-five reflective markers were placed on anatomical landmarks of the subjects in a modified Helen-Hayes marker arrangement. Software Cortex was used to track trajectories of markers and the GRFs during experiments.

Listed main components used during experiments are described in following subchapters, as illustrated in Figure 7.1:

    I.   Motion tracking cameras Mac3D (Motion Analysis corp.)

    II.   Control stand 1 - PC with cortex software for preprocessing of data

    III.   Kistler force plates with six DOF

    IV.   Control stand 2 – PC with *@halo* control hardware and software
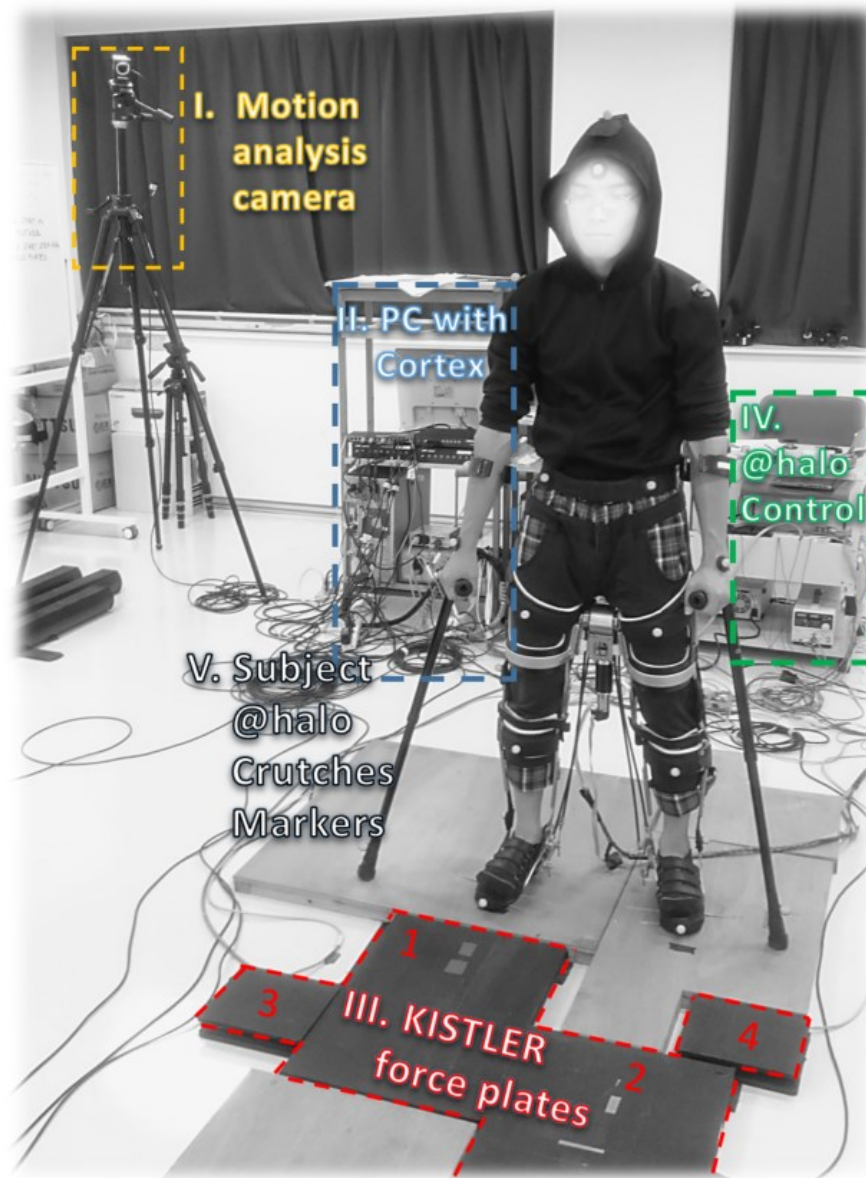
    V.   Tested device with user and crutches

Figure 7.1 Experimental setup

7.4   Motion capture system MAC3D

When any kind of motion needs to be analysed a motion capture system can be used. This technique of motion analysis is widely used for instance to evaluate correct running pattern of athletes in order to increase a performance or correct batting of baseball or golf players. The most common use by researchers is for analysing of the walking patterns during a rehabilitation in order to quantify and identify mistakes done by patients, this leads to creation of efficient plan for improvement. A motion capture technology can be broadly divided according of tracking technique to optical, mechanical, and magnetic. An optical motion capture system is the most suitable one for complicated movement tracking and it is widely used in clinical practice.

7.5 Digital camera Hawk and tracking markers

MAC3D System (Motion Analysis corp.) was used during experiments. MAC3D system is a digital real-time optical motion capture system for measuring the motion of the body in capture room. A capture room is monitored space which lays in capture range of cameras, see Figure 7.2, and in which the whole experiment is performed. Human motion is recorded and measured by tracking 3D position of a marker attached to the body in the capture room. The markers are spots attached on body landmarks. The markers are from reflective materials with narrow reflection angle (similar to safety reflective tapes). Infrared light from the multiple cameras is reflected by this spot markers to identify and record the position of the measurement point of the body in the capture space during all trial. Image of reflected light from the marker is identified, isolated, processed and other ambient noise is suppressed, so only the markers can be captured and position stored in time series datasets.

Recorded 2D position data of markers form each camera are sent through an Ethernet hub to the PC with the MAC3D control software Cortex, see connection layout in Figure 7.3. The 2D data are instantaneously constructed in this software into 3D representation and so the three-dimensional motion of the body can be evaluated in real-time.

Cortex is a control system that can perform necessary data processing such as camera control, camera calibration, collection of marker data, reconstruction of 3D data, collection of analogue data from force-plates, tracking of objects or calculation of virtual points etc., about Cortex see next subchapter.

Six infrared digital cameras Hawk (see Figure 7.4) with FPGA that can convert marker data to 2D digital position data in real time were used during experiments. Hawk high-performance digital cameras can minimize background noise and track markers with high accuracy. The specifications of the camera are shown in Table 7.4.
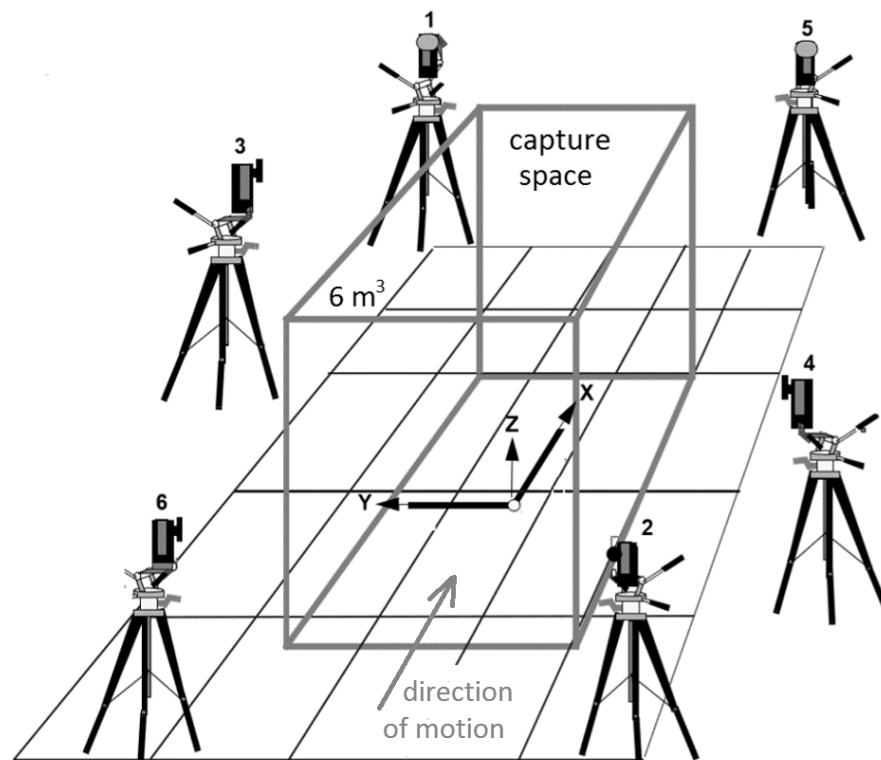

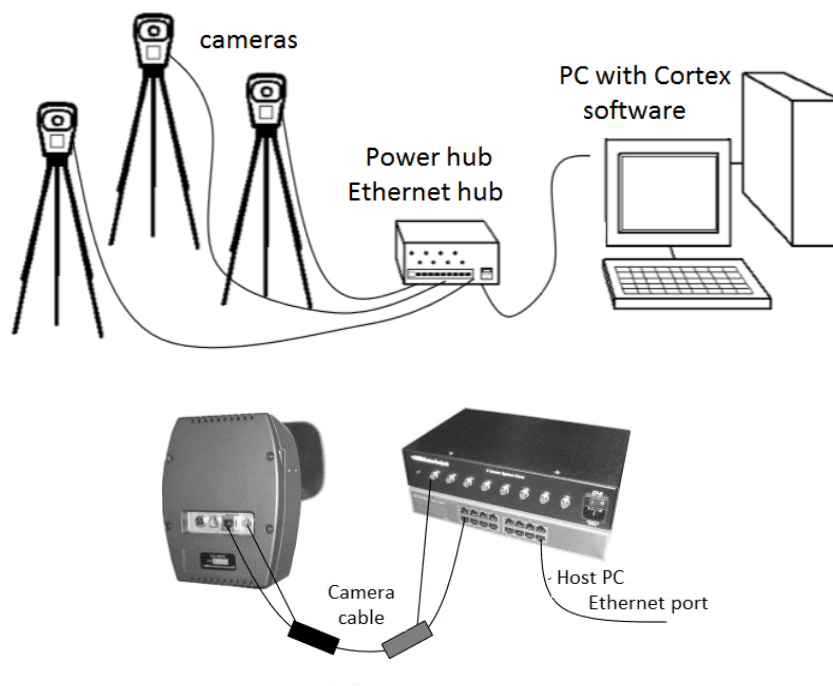*Figure 7.2 Disposition layout of Motion tracking cameras Mac3D during experiments*

Figure 7.3 Connection layout of motion tracking cameras Mac3D and PC

Table 7.4 Parameter of Hawk Digital Camera

Motion Analysis Hawk Digital Camera	
Sensor	CMOS
Resolution	640 x 480 [pixel]
Number of pixels	300,000 pixels
Shooting cycle	1 to 200 [Hz]
Maximum shooting speed at full resolution	200 [Hz]
Maximum number of cameras connected	64
Zoom lens	None

Figure 7.4 Hawk Digital Camera on stand and traditional reflective markers

7.5.1   Software Cortex

Cortex is a complete package, capable of meeting demanding requirements of the motion capture industry. The output is generated in real-time making Cortex a suitable engine for a number of widely used 3D animation packages as well as custom applications created using the supplied Software Developers Kit (SDK). Being a real-time application, the results of a motion capture session can be viewed instantly while simultaneously saved in several file formats. In addition, you can graphically edit data with a complete suite of tools without resorting to other off-the-shelf software packages.

Cortex handles image data from systems comprised of up to 250 cameras. System setup and calibration are fast with immediate feedback and a high degree of accuracy and precision. The motion capture sessions are managed using directory and file access tools. Post-processing data is accomplished graphically using controls integrated with mouse and keyboard functions for fast and easy editing. Model Edit features give the access to the properties of the current set of named markers, virtual markers, linkages, and skeletal segments.

Cortex combines three major functions:

    I.   Calibration of capture space

    II.   Tracking and identifying marker locations in your calibrated 3D space

    III.   Post processing tools for tracking, editing, and preparing the data for Other processing

This chapter is not a manual for Cortex software, but important notes from this three major functions which were used during analysis and should not be omitted are briefly discussed. Calibration of capture space procedure is discussed in the following subchapter. For the tracking and identifying marker location, the marker set template needs to be created.

- *Building a template from the range of motion trial in software Cortex*

A template is what is used to automatically identify markers in real time. In saving the template, the software stores the minimum and maximum distances that can exist between markers that have linkages. It is necessary to allow the software to identify each marker in each frame. The template information is saved in the capture (.cap) file. Before a template can be created, a marker set that will apply to the subject being captured must exist. Each subject has his own unique template, which is loaded and recognised before each trial. This procedure ensures all experimental trials has nearly identical measured points' locations, and serves as a checking feature of correct marker placement. In the post processing interface measured data were checked, in case of some major gabs (momentary missing marker artefact) were data interpolated using cubic joint and smoothed.

Figure 7.5 Cortex post-processing interface and description

Data were exported into three files for each trial:

- *Kinematic data of each marker in format – (.ts) File - position, velocity, acceleration*

- *Hierarchical Translation and Rotation - (.htr) file – Translation and rotation of the segments*

- *Force data file - (.forces) file - All components of the forces from four force plates, position of the centre of pressure and moment about Z axis*

These data were after used for further processing using Python packages.

Figure 7.6 Analysis of the first step of the experimental trial presented on skeleton model in Cortex software

7.6 Force plates and GRF measurement

Besides of the motion analysis, the GRFs were recorded and analysed. There were four force plates used during experiments, see Figure 7.7. Two Kistler portable multicomponent force plates for recording right and left foot GRFs and two smaller 6 DOF force plates to record reaction forces from crutches. Four wooden platforms were installed to align with an upper surface of the force plates and thus make the ground safe and easy to walk on.
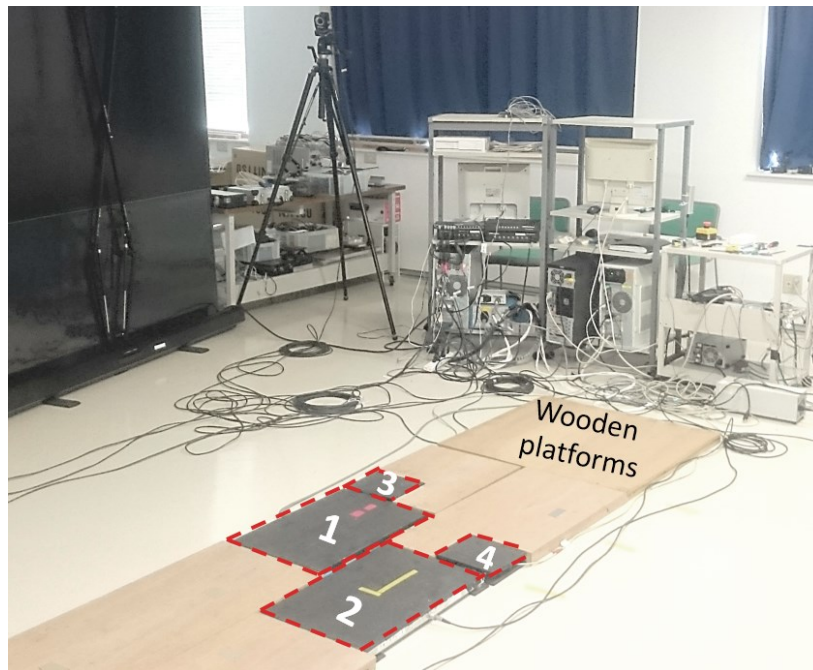
Figure 7.7 Capture space with marked force plates

7.6.1 Kistler portable multicomponent force plates

Kistler portable multicomponent force plates, see Figure 7.8, with aluminium top plate for measuring ground reaction forces, moments and the centre of pressure in biomechanics has following advantages:

- *Excellent accuracy of centre of pressure (COP)*

- *Very wide measuring range, Threshold Fz <250 mN*

- *Easy mounting and flexible, mobile application*

The Kistler forceplates use a built-in or external charge amplifier. Table X shows the specifications of the Kistler forceplates.

Figure 7.8 Kistler portable multicomponent force plate

Table 7.5 Kistler portable multicomponent force plate parameters

Parameter		Units	Value
Model number			9286A
Dimensions		mm	600 × 400 × 35
Weight		Kg	17.5
Measuring range	Fx, Fy	kN	-2.5 to 2.5
	Fz	kN	0 to 10
Linearity		%FSO	<±0,5
Hysteresis		%FSO	<0,5
Crosstalk	Fx <–> Fy	%	<±1,5
	F x, Fy –> Fz	%	<±2,0
	F z –> Fx, Fy	%	<±0,5

7.6.2   6 DOF force sensor

The specifications and picture of 6 DOF force/torque sensor used to measure the GRF of both crutches are shown in Table 4 and Figure 7.9.
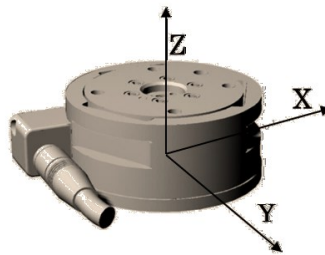
Figure 7.9 6 DOF force/torque sensor

Table 7.6 Specifications of a 6 DOF force/torque sensor

Parameter		Units	Value
6-axis force sense sensor			NITTA Corporation
Model			IFS-67M25A50-I40-ANA
Measuring range	Fx, Fy	± N	200
	Fz	± N	400
Torque	Tx, Ty, Tz	± Nm	13
Weight of main body approximately		kg	0.18

7.7   Characteristics of measurement

There was necessary to perform a calibration of the motion capture system and the force recording devices before all measurements and data processing. This calibration description together with a results are presented in this section.

7.7.1 Motion capture measurement accuracy

The motion capture system setting needs to be calibrated before the experiments in order to obtain correct 3D position data of markers. First, an origin and axes directions of the global coordinate system are defined by using L shape frame with markers see Figure 7.11. This frame was placed on the first Kistler force palate with a corner marker matching a corner of this force plate, showing X direction as travelling (anteroposterior) direction and Y as mediolateral direction. Calibration of capture space was done by a wand, equipped with three markers, see Figure 7.10. Between two end markers of the wand is distance 0.5 m this distance represents wand length. The calibration is performed by waving by the wand in a horizontal and vertical direction through all capture space for 2 minutes. The volume of capture space is about 6 m^3 3D residuals represents the measurement accuracy error and for this volume should be about 1.0 mm. Wand length deviation should be between 499 to 501 mm. The measurement accuracy obtained as a result of the calibration before experiments is shown in Table 7.7, according to results the measurement accuracy in this experiment is considered to be sufficient. The calibration was done before every new set of experiments and was always within 0.01% of measurement accuracy, which was sufficient and obtained data were considered accurate.
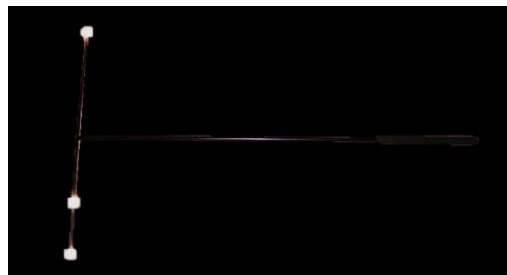
Figure 7.10 Calibration wand with markers

Table 7.7 Measurement accuracy

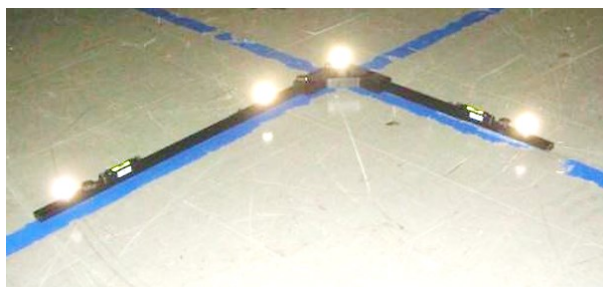| 3D Residuals [mm]		Wand Length	
Avarage	0.23	Avarage	499.99
Deviation	0.11	Deviation	0.41
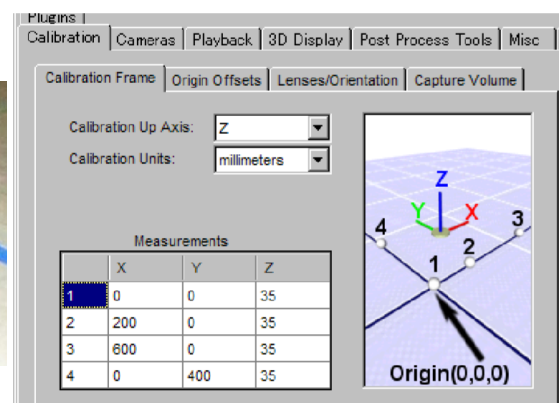
Figure 7.11 L shape frame and calibration setting in Cortex software with set axis directions

7.7.2 Markers position – modified Helen Hayes Marker Set

The markers were attached according to the Helen Hayes Marker Set, see Figure 7.12, with modifications. I addition to Helen Hayes Marker Set, there were two markers attached to the back one in lumbar part and another to the level of 6th thoracic vertebrae. Other extra markers were added in order to monitor the movement of exoskeleton itself. There were extra markers added to both thigh bands and shank bands of Halo device. To be able to record the movement of crutches another four markers were added, two markers on the back side of the left and right crutch cuff and two markers on the tips of the crutches, for complete final markers placement see Figure 7.13.
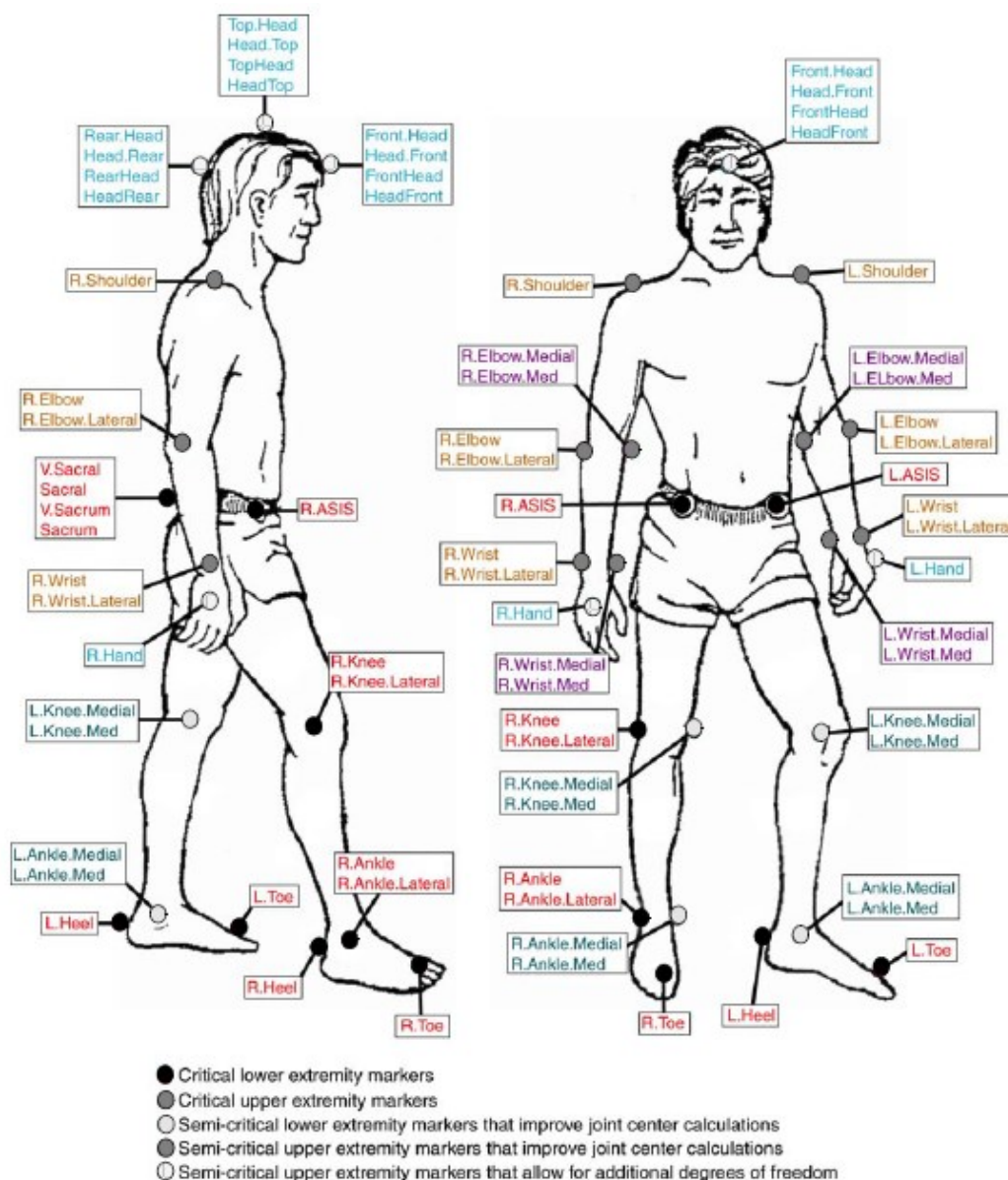
Figure 7.12 Helen Hayes Marker Set

Figure 7.13 Modified Helen Hayes Marker Set marker set distribution

Table 7.8 Description of the markers

	Marker name		Marker name
a	Top.Head	r	R.Thigh
b	Front.Head	s	L.Thigh
c	Rear.Head	t	R.Knee.Lateral
d	Back.T6	t'	R.Knee.Medial
e	R.Shoulder	u	L.Knee.Lateral
f	L.Shoulder	u'	L.Knee.Medial
g	R.Elbow	v	R.Shank
h	L.Elbow	v'	L.Shank
i	R.Wrist	w	R.Ankle.Lateral
j	L.Wrist	w'	R.Ankle.Medial
k	Back.Lumbar	x	L.Ankle.Lateral
l	R.ASIS	x'	L.Ankle.Medial
m	L.ASIS	y	R.Toe
n	R.Crutch.Up	y'	R.Heel
o	L.Crutch.UP	z	L.Toe
p	R.Crutch.Down	z'	L.Heel
q	L.Crutch.Down		

7.7.3 Ground reaction force plate Kistler

The ground reaction force plate Kistler has four strain gauges attached in the four corners of the aluminium plate. Components of the force (Fx, Fy, Fz) in three directions are calculated from these four force sensors. The force sensor outputs is electric charge which is converted to a voltage [V] proportional to this charge using a charge amplifier, see Table 7.9. Voltage range of the charge amplifier is -10 to +10 [V] for the external amplifier and -5 to 5 [V] for the built-in type, which corresponds to the binary output of 0 to 4096 from the ground reaction force plate. Equation 7.1 represents the conversion formula for external amplifier. The value of sensitivity of each component of the force at the amplifier's range of 5000 pC is listed together with other specifications in Table 7.9. Equations 7.2, 7.3 and 7.4 represent calculation of components of ground reaction forces, taken from multicomponent force plate datasheet of Kistler Group.

Table 7.9 Charge Amplifier Specifications

Manufacturer	Kistler
Model number	9865E1Y28
Output voltage (external)	± 10 [V]
Accuracy (all channels)	± 1%
Sensitivity F_{sx} , F_{sy}	-7.8 [pC/N]
Sensitivity F_{sz}	-3.6 [pC/N]

$$V_{(x,y,z)} = \frac{20}{4095} * \left(D_{(x,y,z)} - 2048 \right) + 10 \tag{7.1}$$

Where $V_{(x,y,z)}$ is output voltage from charge amplifier and *D* binary number output from forceplate.

$$GRF_x = -V_x * \frac{5000/F_{sx}}{10} \text{ [N]} \tag{7.2}$$

$$GRF_y = -V_y * \frac{5000/F_{sy}}{10} \text{ [N]} \tag{7.3}$$

$$GRF_z = -V_z * \frac{5000/F_{sz}}{10} \text{ [N]} \tag{7.4}$$

Where GRF_x, GRF_y, GRF_z are components of the ground reaction forces which are used for further analysis and evaluation of loads acting on the body.

- *An accuracy test of the Kistler force plates*

An accuracy test of the Kistler force plates were conducted in past, but results and accuracy verification experiment needs to be done as follows.

First, the position of the centre of pressure of the GRF was measured by MAC3D calculation based on Kistler force plate calculation formulas. After, Load on the force plate was applied with a stick which coordinate position was compared with the results calculated by MAC3D, see Table 7.10. An error of maximum about 5 mm was the result of this experiment and it was noticed the error increases and accuracy decreases towards the ends of the force plates.

Table 7.10 Ground reaction force pressure centre position accuracy in [mm]

	X	Y	X	Y	X	Y	X	Y	X	Y
Measured Point of action	506	200	506	100	506	0	506	-100	506	-200
Average	504.67	201.98	504.57	96.69	504.55	4.09	509.51	-96.79	511.02	-201.5
Standard Deviation	1.89	2.9	1.52	1.82	1.02	1.95	1.66	2.87	3.52	2.51
average difference	1.33	-1.98	1.43	3.31	1.45	-4.09	-3.51	-3.21	-5.02	1.52

7.7.4   6 DOF force sensor

The 6 DOF force sensor is equipped with semiconductor strain gauges attached to beams. The beams are deformed while force or torque is applied, this deformation cases a resistance change in the strain gauge as it bands. The change of resistance is read as voltage value and it is converted into force and torque values by using the calibration matrix. The voltage obtained from the six strain gages is V1 to V6 and the forces and torques in the X, Y, Z directions are Fx , Fy, Fz, Tx, Ty, Tz, a 6-row, 6-column calibration matrix is used, force and torque are calculated based on the formula 7.5. Specific numerical values of the calibration matrix are shown in Table 7.11 and Table 7.12.

$$
\begin{bmatrix} F_x \\ F_y \\ F_z \\ T_x \\ T_y \\ T_z \end{bmatrix} = \begin{bmatrix} m_{11} & m_{12} & \text{L} & m_{16} \\ m_{21} & \text{O} & & \text{M} \\ \text{M} & & & \\ m_{61} & \text{L} & & m_{66} \end{bmatrix} \begin{bmatrix} V1 \\ V2 \\ \text{M} \\ V6 \end{bmatrix}
\tag{7.5}
$$

Table 7.11 Calibration matrix （NITTA sensor 3072）

	i					
j	84.585	2.418	0.035	-6.256	0.975	1.085
	0.835	85.827	-2.235	3.387	-5.055	1.037
	-2.847	4.674	171.267	-3.501	-4.299	-20.142
	0.139	0.004	-0.062	5.611	0.607	0.147
	-0.098	0.231	-0.025	-0.462	5.721	-0.162
	0.003	-0.099	0.11	-0.031	0.083	5.724

Table 7.12 Calibration matrix （NITTA sensor 3649）

	i					
j	88.245	-1.009	-1.206	-3.403	-3.687	2.344
	0.464	-90.818	-1.24	-0.643	1.47	1.062
	0.432	2.519	171.272	0.064	-4.196	0.827
	0.011	0.091	0.024	5.652	0.701	-0.054
	-0.148	-0.063	-0.102	-0.498	5.712	-0.066
	-0.098	0.018	0.012	0.099	-0.034	5.938

7.8 Description of experiment trial

A detailed description of one stride trial together with the actuator activation pattern is explained in Figure 7.14. Start of the trial was set from the heel/toe off of the left leg to the heel/toe off of the same leg. The angular velocity output in Figure 7.14 is matching the phases of the stride and represents counterclockwise and clockwise spinning of the shaft of the actuator.

A switch button is pressed between double support and heel off during preswing phase, this indicates partial assistance of the actuator for push off from the ground and altering of the momentum of the body for the forward progression. Anterior shift of the total body COG is thanks to this assistance easier and smoother than in passive walking, this prevents backward bend and keeps upper body always forward. Users can feel safer and fear from falling is partially eliminated.
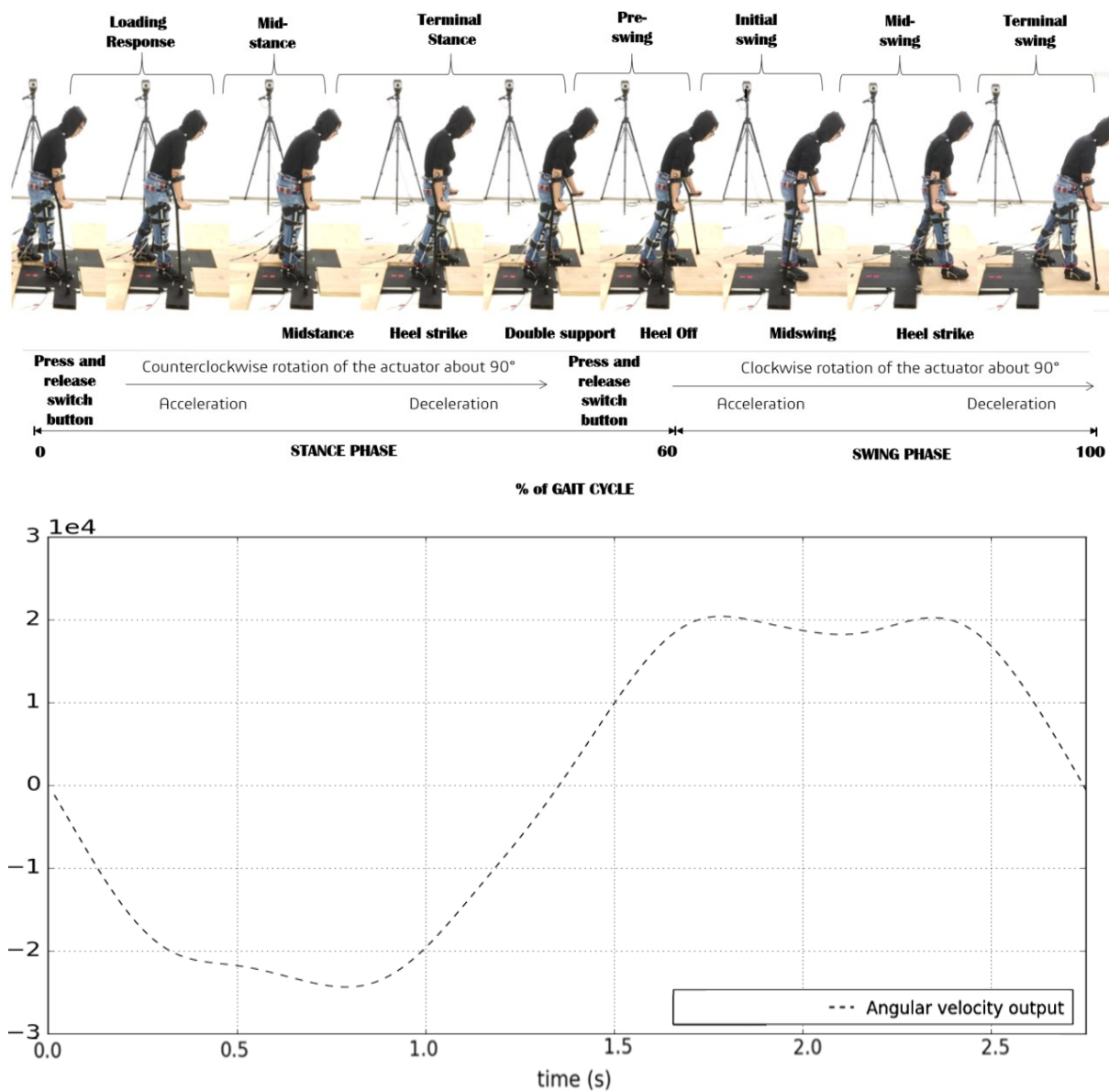
Figure 7.14 Preliminary experimental trial phases with motor activation pattern

7.9   Actuator output data during actuated gait cycle

The Servomotor of the *@halo* device was programmed to follow angular velocity reference trajectory. The duration time of gait cycle was set to 2.8 s, in this time the motor spun about 90° clockwise and another 90° counterclockwise with the average torque 15Nm estimated from the motor current. The bevel gearbox with gear ratio 1.5 distributes and magnify this torque to the left and right KAFO.

The generated torque at hip joint was increased to 22Nm in average, and the leg swung about 60 degrees during half gait cycle. Starting position of trials was set to approximately 30°, a controlled swing of the leg then reached midswing phase (MS) in 0° and continued to -30° until double support (DS) where the motor changed the direction of rotation and the opposite leg continued gait cycle in the same fashion. While legs were passing each other, KAFO connector plate was entering sideway and thus axis of joint was subtly unloaded, this produced little drops of torque during MS as it is presented in Figure 7.15. Description and detailed analysis of the results from experiments conducted in the Department of Robotics Science & Engineering of Chubu University, Japan, are presented in next chapter.
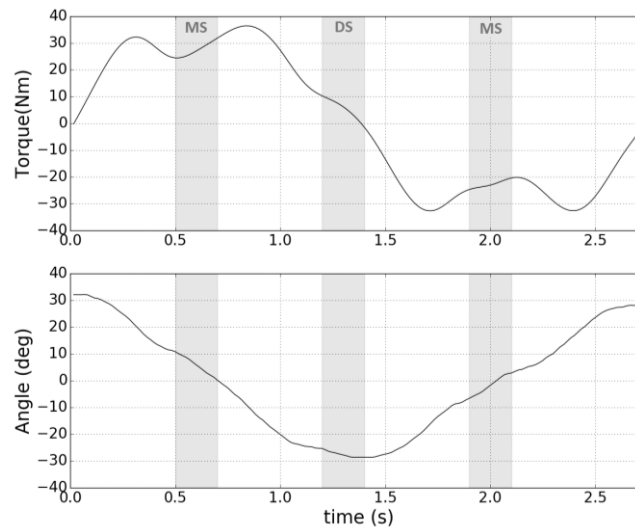
Figure 7.15 Torque and angle in hip joint during one cycle with @halo device

8   *Halo* and *@halo* gait analysis

Evaluation of walking pattern and gait parameters and processing of data obtained from software Cortex are presented in this chapter.

8.1   Motion analysis and data processing

Thirty trials with *Halo* and *@halo* device were conducted by two subjects. **Position, velocity and acceleration data** for each marker were obtained and pre-processed using software **Cortex**. In order to combine and pool data across all trials and from both users an **ensemble average** was introduced, (Robertson et al. 2004). The full trial cycle was defined from left foot toe-off to same foot toe-off. As first the movement time was normalized, by resampling, it was done separately for *Halo* and *@halo* device in different times. Data were after resampling interpolated. Interpolation was done by quintic splining. Data obtained after interpolation were smoothed using Butterworth filter. All ensemble average was done manually in Python using functions either newly created or standard, defined in different packages (pandas, scipy).

Data processing procedure of *ensemble average* using Python:

a)   Loading of raw data from Cortex software

b)   Split of data into three lists according axes X, Y, Z

c)   Standardization of movement time - resampling

d)   Interpolation – splining (quintic splines)

e)   Filtering – low pass 2nd order Butterworth filter

>   *Python - SciPy library:* scipy.signal.butter(N, Wn, btype='low', analogue=False, output='ba'),

- Butterworth filter is widely used in motion analysis
- Can be modeled as 2nd order differential equation
- Cut-off frequency was set $\omega_0 = 5\text{Hz}$

f)   Mean of all sixty normalised trials (each subject 30 trials) in three directions X, Y, Z.

g)   Result is *ensemble averaged (3 lists* X, Y, Z*)* of all trials separately for *Halo* and *@halo*.
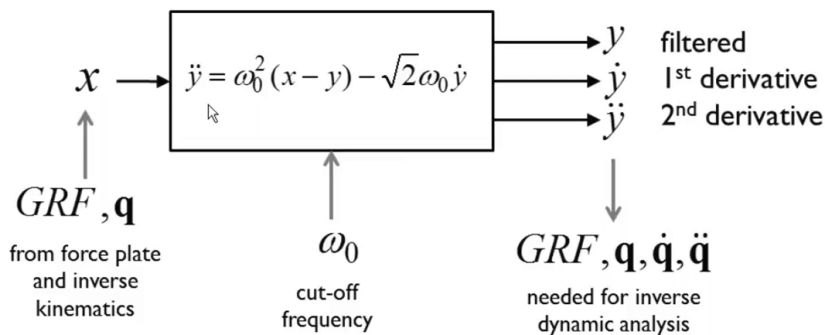
Figure 8.1 Butterworth filter can be modeled as 2nd order differential equation

8.2   Step length

The average step length for *@halo* was 23.82±1.42% of body height (%BH) and for *Halo* was 22.31±3.87%BH. The step length of *@halo* was primarily controlled by the device. It is possible to adjust step duration by modifying the trajectory and period of actuation. This attribute gives active device advantage in significantly smaller deviations (p < 0.05). The comparison of lengths with S.D. is presented in Figure 8.2.
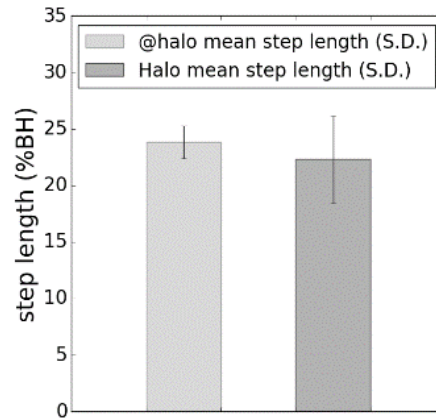
Figure 8.2 Step length comparison (p<0.05)

8.3   Velocities

Walking with *Halo* was faster, the average velocity was 0.3±0.045 m/s. It took 2.7s for the stride. Actuated walking average speed was 0.27±0.022 m/s and the stride was done in 3s. The standard deviation with *@halo* was twice smaller (p < 0.05), and similar in comparison with data reported by (Oberg et al. 1993). Such findings can be interpreted such as stability of walking with *@halo* exoskeleton evaluated from velocity variations is comparable with slow walking of able-bodied individuals.
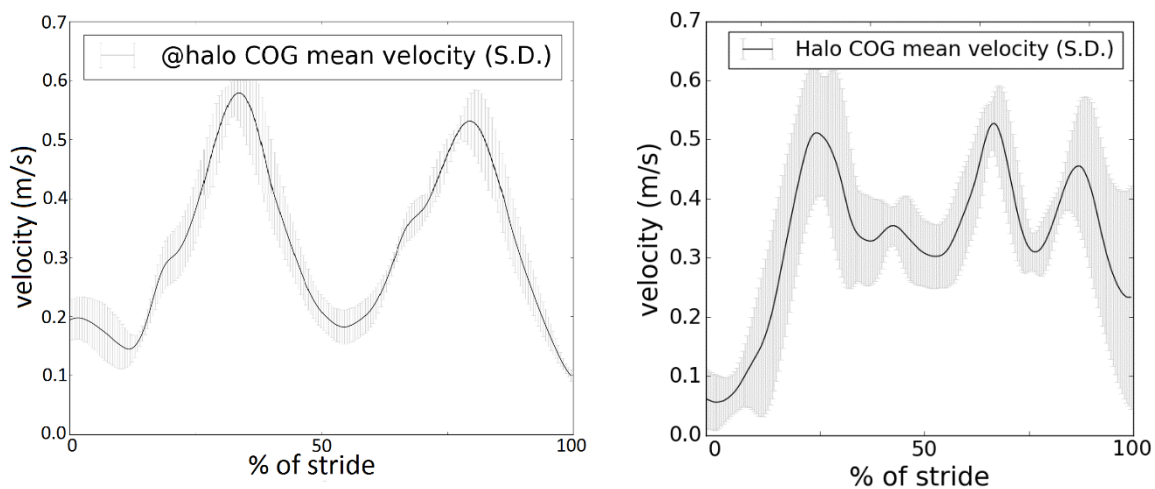
Figure 8.3 Total average velocity of walking with @halo and Halo

8.4 Center of Gravity displacement

As first a description of centre of gravity (CoG) calculation is presented in this subchapter, as next results of the CoG position during trials in all directions are discussed.

8.4.1 CoG calculation procedure

Quantitative biomechanical analysis of human movement, requires an estimate of body segment inertial properties (BSIPs) such as mass, position of the centre of gravity, principal radii of gyration, or moments of inertia. If the only known anthropomorphic parameters for our subjects are total mass and stature we can estimate mass properties and location of CoG of each segment from means obtained measuring cadavers of elderly males, for this work position of centres of gravity of each segment were calculated from bone lengths and average estimated locations as explained in (de Leva 1996) and mass properties of each segment from total mass of subject and percentage of total mass as presented in Table 8.1, (de Leva 1996).

Table 8.1 Adjusted parameters for females and males, Segment masses are relative to body mass

Segment	Endpoints Origin	Other	Longitudinal length (mm) F	M	Mass* (%) F§	M¶	Longitudinal CM position (%) F	M	Sagittal r (%) F	M	Transverse r (%) F	M	Longitudinal r (%) F	M
Head	VERT†	MIDG†	200.2	203.3	6.68	6.94	58.94	59.76	33.0	36.2	35.9	37.6	31.8	31.2
Trunk	SUPR†	MIDH‡	529.3	531.9	42.57	43.46	41.51	44.86	35.7	37.2	33.9	34.7	17.1	19.1
UPT	SUPR†	XYPH†	142.5	170.7	15.45	15.96	20.77	29.99	74.6	71.6	50.2	45.4	71.8	65.9
MPT*	XYPH†	OMPH†	205.3	215.5	14.65	16.33	45.12	45.02	43.3	48.2	35.4	38.3	41.5	46.8
LPT	OMPH†	MIDH‡	181.5	145.7	12.47	11.17	49.20	61.15	43.3	61.5	40.2	55.1	44.4	58.7
Upper arm	SJC‡	EJC‡	275.1	281.7	2.55	2.71	57.54	57.72	27.8	28.5	26.0	26.9	14.8	15.8
Forearm	EJC‡	WJC‡	264.3	268.9	1.38	1.62	45.59	45.74	26.1	27.6	25.7	26.5	9.4	12.1
Hand	WJC‡	MET3†	78.0	86.2	0.56	0.61	74.74	79.00	53.1	62.8	45.4	51.3	33.5	40.1
Thigh	HJC‡	KJC‡	368.5	422.2	14.78	14.16	36.12	40.95	36.9	32.9	36.4	32.9	16.2	14.9
Shank	KJC‡	LMAL†	432.3	434.0	4.81	4.33	44.16	44.59	27.1	25.5	26.7	24.9	9.3	10.3
Foot*	HEEL†	TTIP†	228.3	258.1	1.29	1.37	40.14	44.15	29.9	25.7	27.9	24.5	13.9	12.4
Using alternative endpoints:														
Head*	VERT†	CERV†	243.7	242.9	6.68	6.94	48.41	50.02	27.1	30.3	29.5	31.5	26.1	26.1
Trunk	CERV†	MIDH‡	614.8	603.3	42.57	43.46	49.64	51.38	30.7	32.8	29.2	30.6	14.7	16.9
Trunk	MIDS‡	MIDH‡	497.9	515.5	42.57	43.46	37.82	43.10	37.9	38.4	36.1	35.8	18.2	19.7
UPT*	CERV†	XYPH†	228.0	242.1	15.45	15.96	50.50	50.66	46.6	50.5	31.4	32.0	44.9	46.5
Forearm	EJC‡	STYL†	262.4	266.9	1.38	1.62	45.92	46.08	26.3	27.8	25.9	26.7	9.5	12.2
Hand	WJC‡	DAC3‡	170.1	187.9	0.56	0.61	34.27	36.24	24.4	28.8	20.8	23.5	15.4	18.4
Hand*	STYL†	DAC3‡	172.0	189.9	0.56	0.61	35.02	36.91	24.1	28.5	20.6	23.3	15.2	18.2
Hand	STYL†	MET3†	79.9	88.2	0.56	0.61	75.34	79.48	51.9	61.4	44.3	50.2	32.7	39.2
Shank	KJC‡	AJC‡	438.6	440.3	4.81	4.33	43.52	43.95	26.7	25.1	26.3	24.6	9.2	10.2
Shank	KJC‡	SPHY†	426.0	427.7	4.81	4.33	44.81	45.24	27.5	25.8	27.1	25.3	9.4	10.5

* Not adjusted values.
† Normal projection on the segment longitudinal axis.
‡ Assumed to lay on the segment longitudinal axis.
§ Zatsiorsky *et al.* (1990a).
¶ Zatsiorsky *et al.* (1990b, 1993).

Total body CoG location is consecutively calculated from the position of each segment's CoG and masses according equation (8.1), this equation is for walking with *@halo* device.

$$CoG_{total} = \frac{\sum_{i=1}^{17} m_i \cdot \overrightarrow{x_i}}{m_{total}}$$

(8.1)

Where m_i is mass of a segment, $\overrightarrow{x_i}$ is position vector of CoG of the segment and m_{total} is total mass of the subject together with device.

There are 17 segments considered in case of *@halo* device and 16 segments for *Halo* setting. The extra segment for *@halo* represents actuator unit. In order to be as precise in calculations as possible there was the actuator unit position of CoG measured and added to calculation of total body CoG as separate segment. The masses of KAFO orthoses were added to thigh, leg and foot segments masses.

Same procedure was used for calculation of upper body (UB) CoG and lower body (LB) CoG, considering only segments included in these portions of the body.

8.4.2 Evaluation of CoG displacement

The CoG of total body (TB), lower body (LB) – including the weight of orthosis and upper body (UB) were examined. CoG was calculated by the segmental method, from known position vectors of centers of each segment calculated in motion analysis software Cortex and from the segment inertia parameters (de Leva 1996). The initial position of subjects for stride trials was examined from the moment just after standing both legs on the floor with right leg in front and left leg backward. Thus the stride began just after first double support phase (DS). Second and final double support phases are indicated in Figure 8.4 by yellow vertical stripes.

The change of CoG position in the anteroposterior (Sagittal) direction is shown in the first row of Figure 8.4. In the case of both actuated and passive settings, the CoG of LB is leveled off during double support period and the CoG of UB indicates steeper upward slope, this means trunk was tilted forward to balance out lower body onward movement, this is important prevention against falling backward. There is, however, a difference between the CoGs of LB of *@halo* and *Halo* during DS. The active torque in hip resulted in a smoother transition between single and double support phase by following the CoG of UB similar as it is in the case of normal walking where upper and lower body CoGs have almost identical trend.

Wavier profile of *@halo* is due to short delay caused by manual servomotor activation. The standard deviation of the CoG of TB was more than twice smaller with the actuated configuration, (p<0.0001).

The variation of CoG position of TB in horizontal direction or waddling was about 15.2±1.68% without actuator and 9.1±0.51% of body height (%BH) with the *@halo* device. It is not possible that the waddling decreases to the level of normal walking since the walking manner is associated with locked knees and is essential in order to secure safe foot clearance from the floor. The CoGs of UB and LB with *Halo* were oscillating with larger offset from the CoG of TB. It means deeper tilting on the sides, which resulted in a need to apply bigger forces on the crutches. This is proven in the next chapter. The standard deviation significantly decreased with *@halo* (p<0.0001). This means promising stabilization in the longer distance walking with *@halo*. Unfortunately, small time delay caused by the activation of servomotor was disturbing and prolonging trajectory just immediately after double support (DS) phase, see the second row of graphs of Figure 8.4. The vertical displacement of the CoG of TB during stride with *Halo* was 2.29±0.4%BH and it was decreased to 1.36±0.15%BH during actuator-assisted walking, (p<0.0001) and this is close to a normal slow walking according to results from the study by (Orendurff et al. 2004).

In the case of walking with *Halo,* the CoG displacement of LB was nearly constant during first DS period, but UB fell rapidly down to forward bend to prepare for the next step. The following acceleration of upper body and thus increase of its momentum was then utilized by force impulse from the crutch and this was the result of the high increase of power in upper limbs. This enabled fast return of upper body in upright posture together with lower limb which continued to midswing and then to another DS period. Such big impulse from the crutches was not required while walking with *@halo.* It was due to active torque in hip and linkage mechanism which slightly augmented plantar and dorsiflexion of ankles in the later stage of DS period. It resulted in smaller forward and backward tilting of UB and smoother forward movement of TB as it is evident from the last row of Figure 8.4.
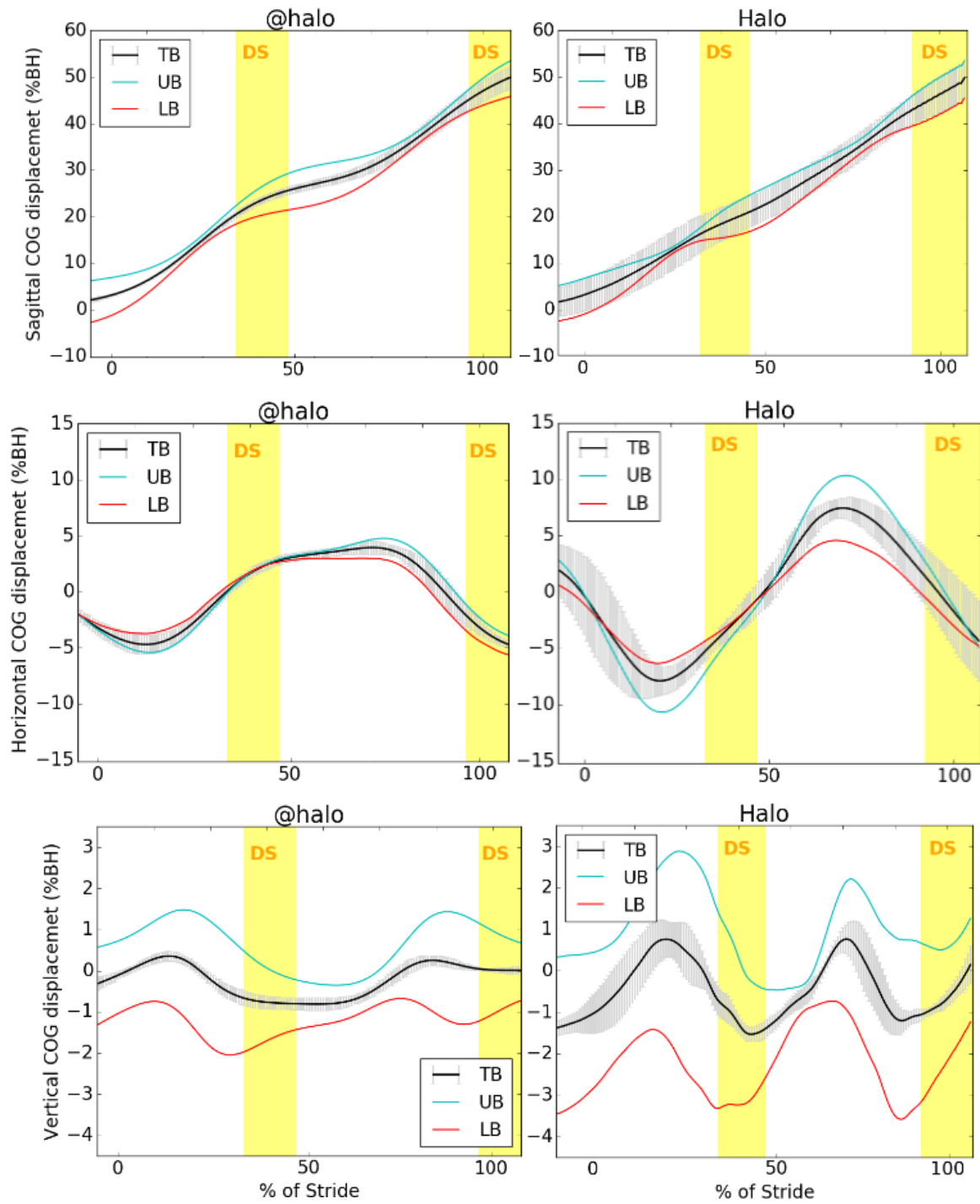
Figure 8.4 Sagittal, horizontal and vertical CoG displacement

8.5 Linear force impulse from crutches and GRF

Four force plates recorded ground reaction forces during the gait cycle. Two force plates were set for the right foot (RF) and the left foot (LF) and another two for the right crutch (RC) and the left crutch (LC). Results were analysed to compare the distribution of reaction forces acting on the lower limbs and extra forces which user has to apply on the crutches in order to stabilize the body. In this subchapter the ground reaction forces and their impulses are calculated and evaluated.

8.5.1 Calculation of linear force impulse from crutches and GRF

The linear impulse of force is defined as the integral of force over its period of application, this impulse changes the momentum of the body. The linear impulse is the area under a force history, it means it depends not only on amplitude, but as well on duration, (Robertson et al. 2004).

$$linear\ impulse = \int F\ dt \tag{8.2}$$

8.5.2 Linear force impulse from crutches and GRF evaluation

The GRF of the right foot was positive before the middle of the cycle, see Figure 8.5. Right foot acted as an accelerator of the walk with *@halo* due to active torque from the actuator. It helped easily overcome negative breaking GRF of LF caused by heel strike an instant before the middle of the cycle. No big assistance of the crutches was needed during this process in anteroposterior (AP) direction. In the case of *Halo*, the accelerating force was much smaller and the right foot together with the left foot were breaking during the middle of the stride. It was done due to forward leaning of the upper body. Peaks of the GRF in the crutches during actuator-assisted walking were almost twice smaller, but breaking and accelerating GRF impulses of limbs were larger due to active torque in the hip joint.

The shift of body from left to the right tilt caused increase of the GRF of RF at the beginning of stride with *Halo* which can be seen in Figure 8.6. Left crutch then boosted this movement so the GRF vector of RF turned to positive direction and LF could leave the ground. During midswing, the right crutch impulse acted in opposite direction in order to return the body back to the center position. During heal-strike of LF, load on RF was continuously declining due to intensification of force in RC. These results were caused by excessive waddling, which was compensated by the crutches.

It can be noticed that very different trend is found in the GRF of RC in the case of *@halo*. There was smaller impulse needed to balance the body in mediolateral (ML) direction. In the single leg support period, the GRF trend of the feet was more stabilized and less oscillating with *@halo*. It means the stability in the stance phase was better with *@halo*.

Vertical GRF with *@halo* had smooth transition between right and left foot in the middle of stride, see Figure 8.7. There was the uniform decrease of the reaction force from the left crutch and gradual increase in the right crutch, while no significant increase was recorded during period from LF heal strike to RF toe-off. It represents absence of need using the crutch impulse to alter the momentum of the body for its forward progression. This is done by energy coming from the actuator. The drawback is, however, bigger heel strike forces which is corresponding to results in anteroposterior direction. Walking with *Halo* is clearly more demanding, due to insufficient load transfer from the right to left foot. In order to shift body ahead big increase of the GRF of the right crutch just before the middle of the stride was required as can be seen in Figure 8.7.
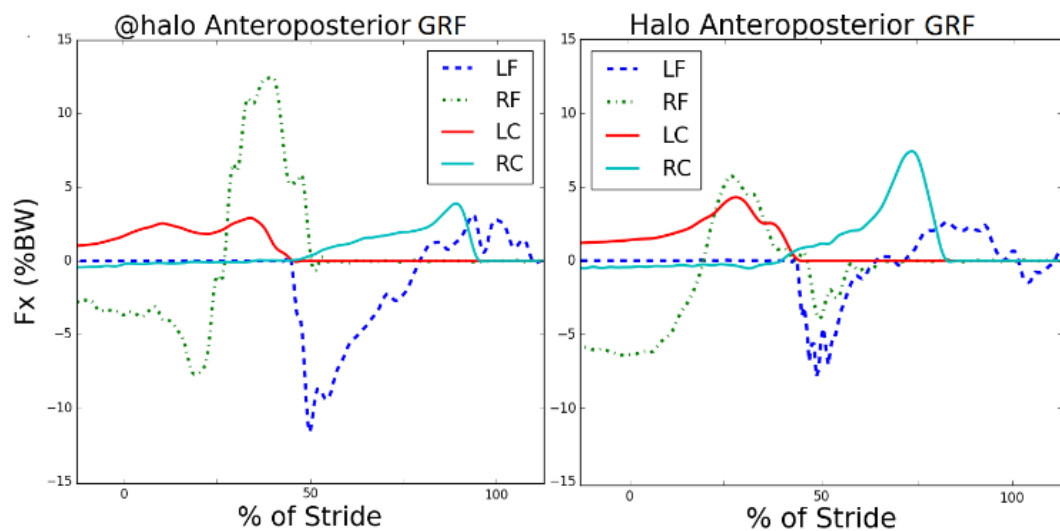
Figure 8.5 Anteroposterior GRF
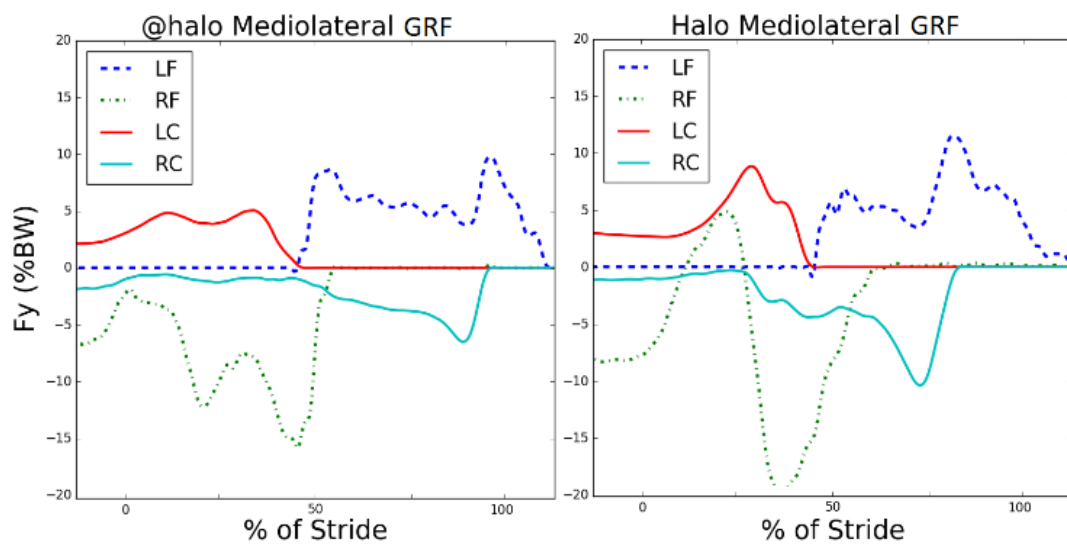
Figure 8.6 Mediolateral GRF
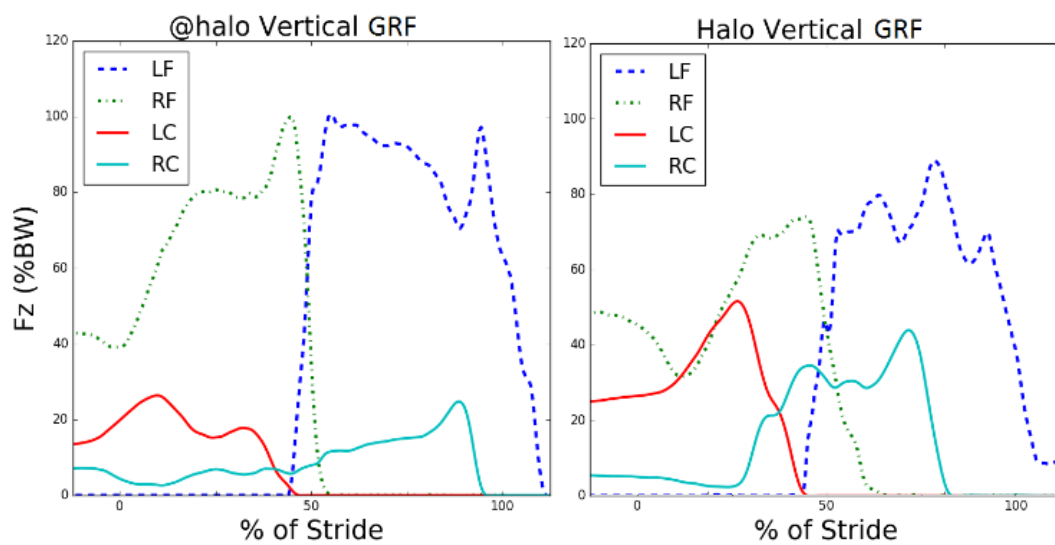
Figure 8.7 Vertical GRF

92

There is a significant difference between GRF S.D. from crutches of trials with *Halo* and *@halo*, (p<0.05). These values together with total impulses per stride are presented in the three directions in Table 8.2.

Table 8.2 Forces and total impulses in crutches

Device configuration		Mean F [%BW]	S.D. [%BW]	max F [%BW]	Impulse [%BWs]	total impulse per stride		
@halo	left	-2	0.3	-2.91	3.32	**5.97**		AP direction
	right	-1.81	0.31	-3.89	2.65			
Halo	left	-2.34	0.96	-4.98	3.3	**6.54**		
	right	-2.39	0.93	-6.98	3.24			
@halo	left	3.7	0.5	5.05	6.2	**11.38**		ML direction
	right	3.9	0.58	6.5	-5.18			
Halo	left	4.01	0.67	8.84	5.83	**12.5**		
	right	5.01	1.2	9.33	-6.67			
@halo	left	17.6	2.1	26.3	29.24	**49.56**		Vertical direct.
	right	15.21	1.96	24.7	20.32			
Halo	left	32.99	4.95	52.4	44.33	**80.58**		
	right	29	7.25	43.2	36.25			

8.6 Moments and forces in glenohumeral joint

HALO walking pattern, and walking patterns of any passive and active orthoses or exoskeletons which require crutch assistance is causing excessive loads in upper extremities, and especially in the glenohumeral joint. Patients are often complaining about overloading shoulders during rehabilitation. It is essential, to investigate this conditions in order to be able to reduce the forces and moments applied to the upper extremities musculature and thus decrease the incidence of some diseases as well as shoulder pain.

8.6.1 Inverse dynamics model of the human upper extremity

The right-hand side of the equation of motion in a form normally used for robotics (8.3) represents known variables. Moments of inertia of all segments as well its Coriolis and gravitational forces are known and GRF are measured using force plates as described in the previous subchapter.

$$Joint\ torques \left\{ \begin{bmatrix} \tau_1 \\ \cdots \\ \tau_x \end{bmatrix} = \underbrace{M(q)\ddot{q}}_{\text{Inertia}} + \underbrace{C(q,\dot{q})\dot{q}}_{\text{Coriolis}} + \underbrace{G(q)}_{\text{Gravity}} + B(q)\underbrace{\begin{bmatrix} GRF_1 \\ \cdots \\ GRF_x \end{bmatrix}}_{\substack{\text{Measured} \\ \text{forces}}} \tag{8.3}$$

An inverse dynamic model of the upper extremity with crutch was formulated after measuring GRFs from the crutches, (Requejo et al. 2005) and (Slavens et al. 2010). Using this model we can determine load in glenohumeral joint of upper extremities during crutch-assisted gait with active setting *@halo* and passive setting *Halo.* After calculation of the moments and forces, comparison and evaluation of actuated and passive walking impact on shoulders can be done. The result will indicate the suitability of long-term usage of devices.
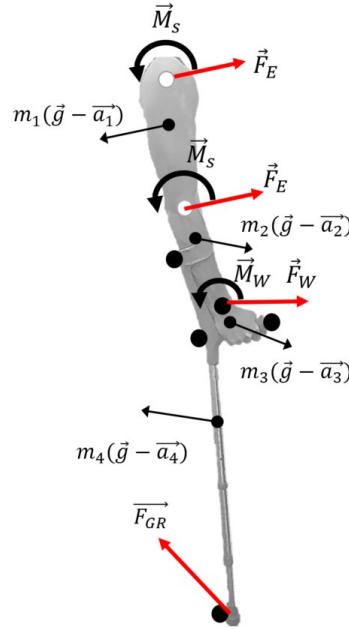
Figure 8.8 Upper extremity with crutch - inverse dynamic model

Loads in glenohumeral joint Fs and Ms can be calculated using following equations:

$$\vec{F}_s = \vec{F}_{GR} + \sum_{i=1}^{4} m_i(\vec{g} - \vec{a}_i) \tag{8.4}$$

$$\vec{M}_s = \vec{r}_{SGR} \times \vec{F}_{GR} + \sum_{i=1}^{4} \vec{r}_i \times m_i(\vec{g} - \vec{a}_i) - \sum_{i=1}^{4} \vec{M}_{Ii} \tag{8.5}$$

Where the ground reaction force was obtained from measurement, m_i is i^{th} segment mass, a_i and g are inertial and gravitational accelerations, $\vec{r}_{SGR}$ is position vector from the glenohumeral joint to the marker on the tip of the crutch (black spot) and $\vec{r}_i$ is position vector from the glenohumeral joint to the ith segment center of gravity and finally $\vec{M}_{Ii}$ is inertial moment due to i^{th} segment, see Figure 8.8.

This equations were defined as functions in Python and loads in the left and right shoulder were calculated. During calculations, there was found out, movement of the shoulder with the crutch during loading phase is such slow, that can be considered as quasi-static. Resultant moments and forces calculated with inertial moments were almost same as those where these moments were omitted.

Force results are in % of body weight (%BW) and moments are in % of the body weight times body height (%BW*BH).

8.6.2 Results and Evaluation of forces in Glenohumeral joint

As it can be seen on Figure 8.9, forces in the glenohumeral joint are not very different from GRFs presented earlier in this chapter.
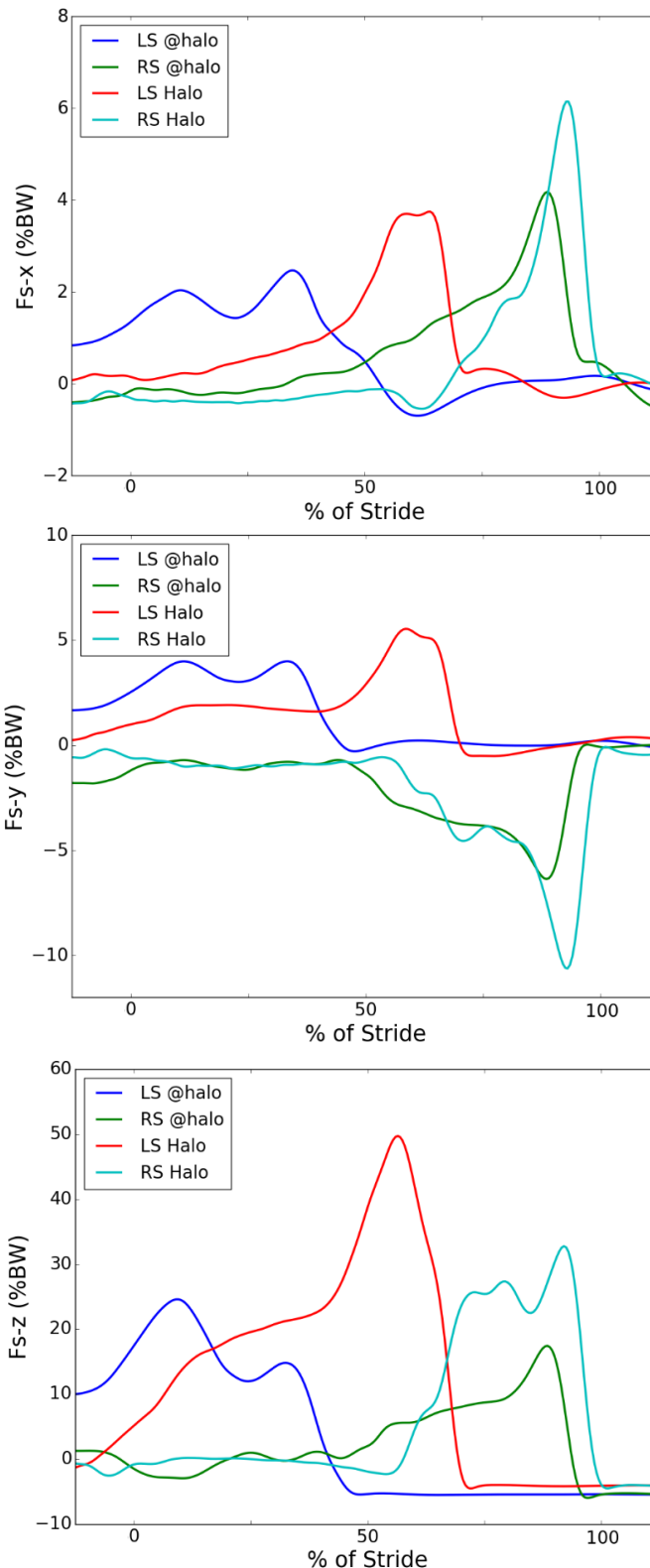
Anteroposterior forces in the glenohumeral joint are larger with the steeper increase and sharper peaks during walking with Halo. Left shoulder undergoes nearly twice smaller forces in this direction while wearing @halo powered exoskeleton. About 1/3 larger excessive forces acting on right shoulder while walking with Halo.

A similar situation is in mediolateral direction. Force peaks are more than 1/3 larger and sharper, with uncomfortable steep, fast increase.

As it was presented previously, the reaction forces in the vertical direction will the most significantly influence long-term use comfort and safety. As can be noticed Left shoulder is overloaded by nearly twice larger force peak while walking with Halo, this may have negative effect on trapezius muscles.

Figure 8.9 Joint reaction forces in anteroposterior, mediolateral and vertical direction in left shoulder (LS) joint and right shoulder (RS) joint during walking with Halo and @halo device

8.6.3 Results and Evaluation of moments in Glenohumeral joint

In this subchapter will be briefly presented how the moments in the glenohumeral joints affected upper limbs musculature differently with the actuated and with the passive device, see Figure 8.10.
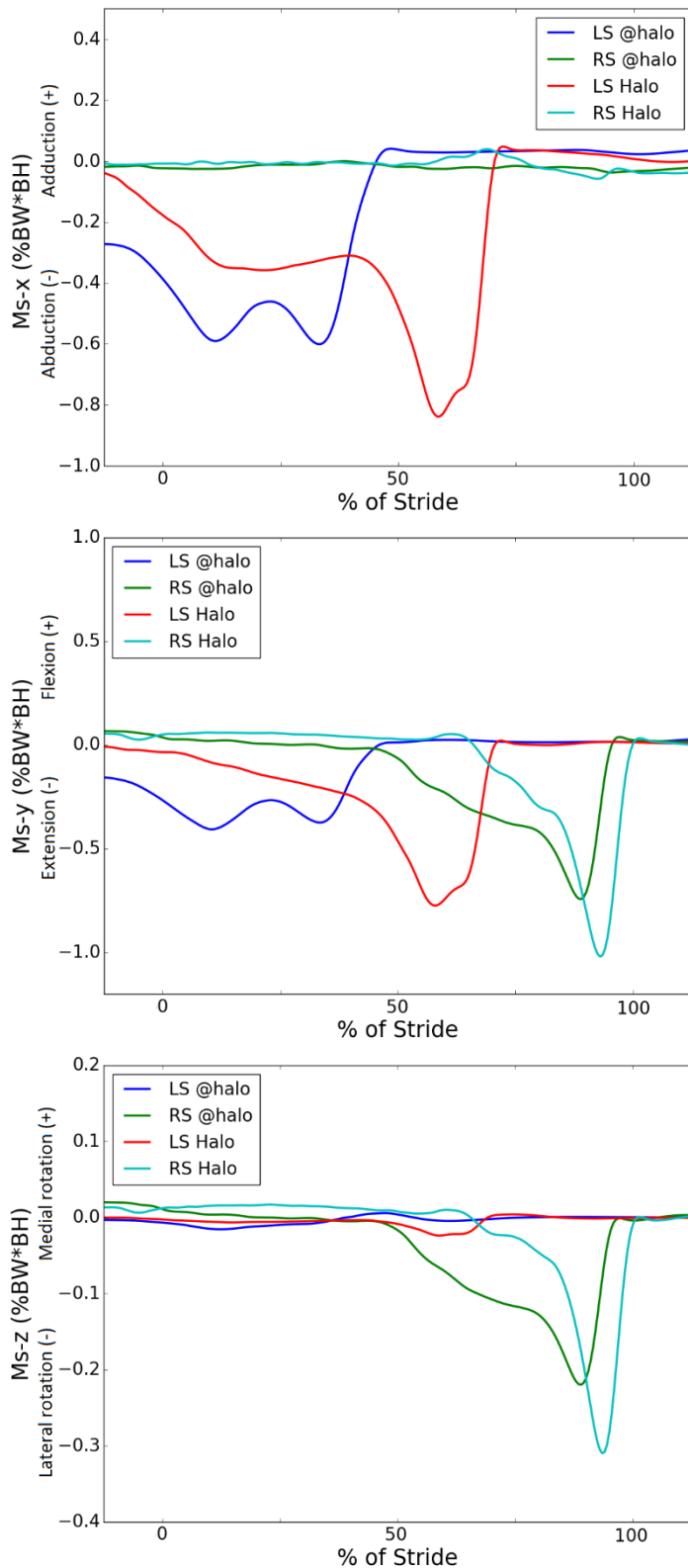
Abduction moment in the left shoulder joint is larger with the steeper increase and sharper peak, this negatively influences the functionality of deltoid muscles and may cause their continuous tiring during every-day use.

The smoother trend can be seen while wearing @halo.

Extension moment acts in shoulder joint while supporting the body in a forward progression. Nearly twice larger extension moments were calculated while walking without the actuator. This fact may cause pain or overloading of latissimus dorsi muscles during everyday use.

The excessive lateral rotation was calculated in right glenohumeral joint during terminal swing. Rotation occurs due to excessive waddling which is larger in case of walking with the *Halo* orthosis. As well here is obvious smoother trend and smaller peak while using active *@halo* exoskeleton.

Figure 8.10 Joint reaction moments about anteroposterior, horizontal a vertical axis in left shoulder (LS) joint and right shoulder (RS) joint during walking with Halo and @halo device

8.7 Glenohumeral joint power

Glenohumeral joint power represents the rate of work at which shoulder muscles remove or add energy to the system. If resultant power is positive, then muscles are adding energy to the system, muscles are contracting, and negative power means removing energy, (Robertson et al. 2004). By calculating power in the shoulder, we can compare the energy consumption of the upper extremities while walking with powered or with the passive orthosis.

8.7.1 Calculation of Glenohumeral Joint Power

Shoulder joint power is given by equation:

$$\vec{P}_S = P_{proximal} + P_{distal} \tag{8.6}$$

Where $P_{proximal}$ is the power of the proximal segment of the joint at the shoulder joint, which is trunk segment and P_{distal} is the power of the distal segment of the joint at the shoulder joint, which is upper arm segment. Now, after application of Newton's third law of equal and opposite forces and moments on both sides, we got following equation:

$$\vec{P}_S = \left(\vec{F}_S \cdot \vec{v}_{proximal}\right) + \left(\vec{\tau}_S \cdot \vec{\omega}_{proximal}\right) + \left(-\vec{F}_S \cdot \vec{v}_{distal} - \vec{\tau}_S \cdot \vec{\omega}_{distal}\right) \tag{8.7}$$

If we simplify this equation by assumption there is **no** shoulder dislocation and thus $\vec{v}_{proximal} = \vec{v}_{distal}$ (for our purpose of comparison between two similar walking patterns this assumption is considered to be sufficient), then we can further simplify to

$$\vec{P}_S = \left(\vec{\tau}_S \cdot \vec{\omega}_{proximal}\right) + \left(-\vec{\tau}_S \cdot \vec{\omega}_{distal}\right) \quad => \quad \vec{P}_S = \vec{\tau}_S \cdot \left(\vec{\omega}_{proximal} - \vec{\omega}_{distal}\right) \tag{8.8}$$

This equation can be further simplified to final simple equation:

$$\vec{P}_S = \vec{\tau}_S \cdot \vec{\omega}_s \tag{8.9}$$

Where $\vec{\omega}_s$ is angular velocity in glenohumeral joint and $\vec{\tau}_S = \vec{M}_S$ (moment in shoulder calculated in previous subchapter).

Data of angle values in each time frame were obtained from all trials from software Cortex, angular velocity was calculated in python using simple discrete difference:

$$\vec{\omega}_s = \frac{\Delta\vec{\theta}_s}{\Delta t} \tag{8.10}$$

Python – SciPy library

numpy.diff (a, n=1, axis=-1)

8.7.2   Results and Evaluation of Glenohumeral joint Power

Work done by muscles and power needed to give an impulse, alter momentum and push the body forward to another step was calculated. Muscles activation and distribution of power in glenohumeral joint is presented and discussed in Figure 8.11.
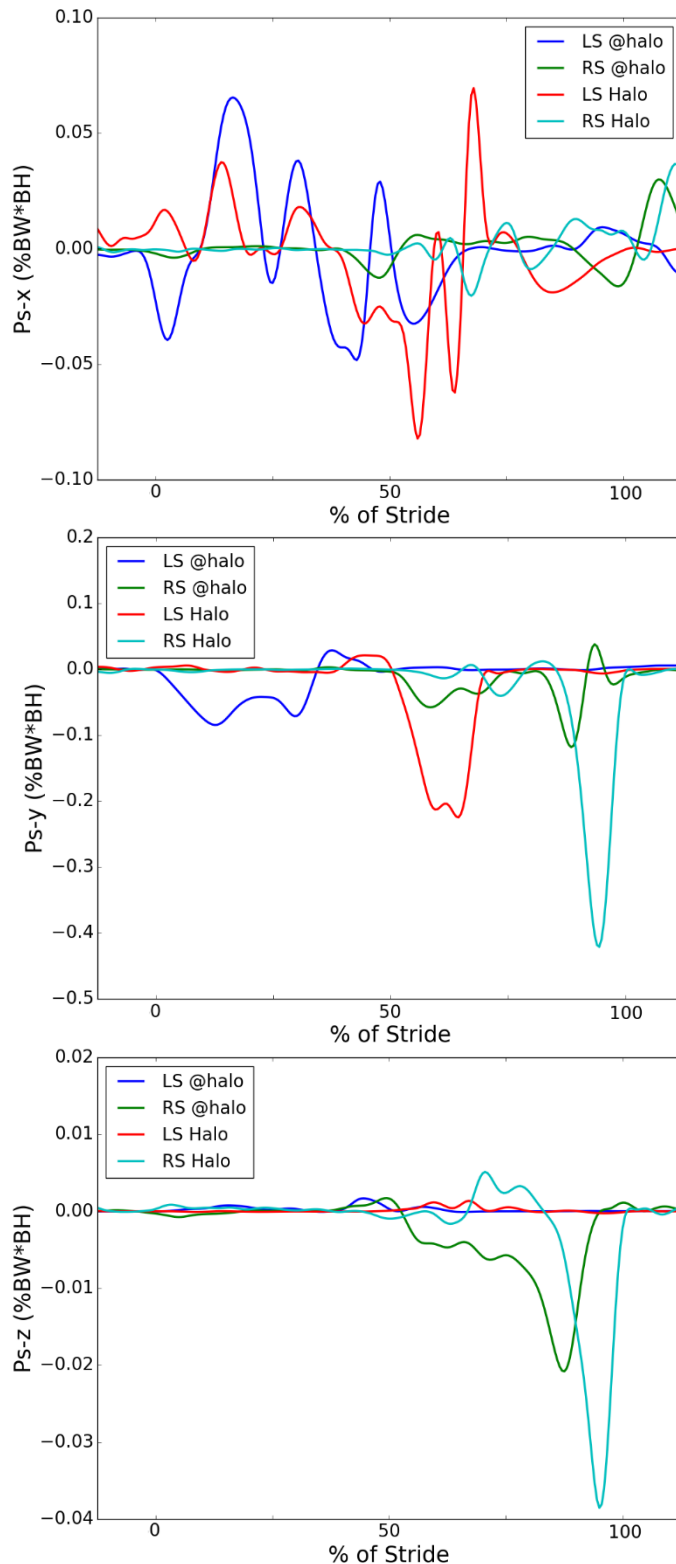
There were small fluctuations measured in the anteroposterior direction and overall no big difference in power consumption generated in shoulders while wearing both *Halo* and *@halo.*

Higher joint power values in mediolateral direction are associated with work of deltoid muscles. Excessive waddling is larger for Halo walking, thus bigger power is needed to stabilize body.

Minor energy consumption was demonstrated while walking with the powered *@halo* device.

Energy consumption and power calculated in vertical direction is mainly associated with the work of trapezius muscles due to sudden elevation and following retraction of shoulders while leaning on the crutches during the swing phase. Engaging of these muscles is more aggressive while walking passively without actuator and costs user more energy.

Figure 8.11 Joint Power in anteroposterior, horizontal a vertical axis in left shoulder (LS) joint and right shoulder (RS) joint during walking with Halo and @halo device

9 Conclusions

Two new lower limbs exoskeletons for paraplegics were presented in this study, the main aim was to find the solution which is affordable, lightweight, stable, with low energy consumption and easy to don/doff directly from a wheelchair. These attributes were entirely matching with the *@halo*. This was the reason, why *@halo* device was further tested with able-bodied subjects and its performance was evaluated in the details. Brief conclusion about ORTHOLEG 2.0 and more detailed conclusion about *@halo* device is discussed in this chapter.

9.1 Exoskeleton ORTHOLEG 2.0

The main objective of redesign of ORTHOLEG was the development of lighter lower limbs exoskeleton which construction will decrease battery consumption and increase users comfort during walking. The weight of the whole device was decreased by 1/3 from original prototype to 11,5 kg while the weight of user allowed to wear Ortholeg 2.0 was increased by 10 kg to 70 kg. Gait cycle is now smoother and more natural thanks to new shoe inserts made from strong but flexible prepreg carbon. Energy transfer from exoskeleton to users legs and body was improved thanks to better fixtures made from prepreg carbon and Kydex polymer. Wires from actuators and sensory subsystem (for future implementation) connected to control electronics in the backpack can be easily hidden thanks to the construction of main frame made from pipes. The modular knee concept was implemented in order to test differences in power consumption and user's comfort during walking with passive or actuated knee. After manufacturing of all components, experiments on both settings and power consumption are planned as well as testing of gait cycle algorithms in order to determine the impact of design on walking patterns.

9.2 Exoskeleton @halo

The novel powered exoskeleton *@halo* was invented based on the passive HALO orthosis walking pattern principle. The New *@halo* exoskeleton has just one powered DOF and its structure is modular. The user can simply remove actuator unit and walk passively without motor assistance, the passive setting without actuator was for better differentiating called *Halo*. In order to examine the performance of active *@halo*, there were preliminary experiments with able-bodied subject conducted and walking patterns of *Halo* and *@halo* were compared and evaluated.

Walking with *Halo* was faster than with *@halo* but step length was slightly longer with active configuration. Standard deviations, however, were remarkably higher while walking without the actuator. This is due to partially predetermined walking patterns of *@halo*, influenced by constant actuated periods. These results can be summarized as walking with the actuator is expected to be more stable for longer distances and probability of fall is expected to be lower, (SHINODA et al. 2008).

Ranges of vertical excursion of CoG during stride are compared and summarized in Table 9.1 with overall significance ($p<0.0001$). There is 40% decrease of excessive up-down movement in case of *@halo*. If we simplify energy consumption assessment we can calculate decrease of the power consumption per moving distance due to smaller up-down movement from the vertical excursion, Equation (9.1), (Lee et al. 2015).

$$P = \frac{m \cdot g \cdot z}{T} \ [Nm/s] \tag{9.1}$$

Where z is the vertical excursion, $m \cdot g$ is weight and T is the time period of the cycle. Average weight was constant, thus can be excluded from equation and calculation can be for comparison reasons further simplified to the vertical excursion in %BH per second. The results show that walking with actuator required 51.65% less energy spent by the user, see Table 9.1. The range of waddling during walking with *@halo* was decreased by 40% in comparison with *Halo* configuration. Waddling is still about twice larger than during normal slow walking (Orendurff et al. 2004), this is however not possible to diminish due to the construction of medial-hip-joint orthosis with locked knees.

Table 9.1 Ranges of COG displacement and energy consumption

Device	Waddling (%BH)	vertical excursion (%BH)	%BH/s
halo	15.32	2.29	0.848
@halo	9.16	1.36	0.438
comparison	-40.21%	-40.61%	-51.65%

There was measured 38.5% bigger impulse in crutches in the vertical direction while walking without the motor. This difference was greatly compensated by upper limbs excessive energy expenditure. This was proven by calculating and evaluating moments and joint power in the glenohumeral joint. Abduction moment in the left shoulder joint may negatively influences functionality of deltoid muscles and may cause their continuous tiring during every-day use, the prove is calculated higher joint power values in mediolateral direction, this can be significantly eliminated by switching to powered *@halo.* Nearly twice larger extension moments were calculated while walking without the actuator. This fact may cause pain or overloading of latissimus dorsi muscles during everyday use. After calculating power in vertical direction there was found out engaging of trapezius muscles is more aggressive while walking passively without actuator and costs user more energy. After calculation of the power flow in the glenohumeral joint it can be summarized, all main muscle groups are engaged more aggressively and indicate more energy consumption. Walking with *@halo* means significant reduction of the forces applied on the upper extremities musculature and thus decrease the incidence of some diseases as well as shoulder pain.

9.3   Contribution for scientific discipline

New designs of two exoskeletons were discussed and exoskeleton *@halo* has been chosen. Mechanical design of *@halo*, electronic hardware and software were newly created in order to be able to conduct evaluation of the first functional prototype. The core of this evaluation consists of biomechanical methods described in details step by step in this work. Over 500 experimental trials were conducted in the laboratory setting. A specified data collection using motion analysis system and their further processing was demonstrated. Data processing was done in the programming language Python after pre-processing in software cortex, new code was written for this purpose. Different kinds of scientific approaches were considered. As specifically, all processes to obtain the ensemble averages were described and applied to investigate the displacement of the COG of the body and GRF applied on the crutches. The inverse dynamics approach was chosen and explained to calculate and investigate the loads applied on the upper extremities during preliminary experiments.

To conclude, this work contains complete and unique methodology of inventing new product from the field of assistive and medical robotics and validating its functionality, efficiency and safety for the end-users.

9.4 Contribution for practice

The main two advantages and features of @halo are affordability and stability, and the most important factor for the user of this device is the intensity of usage.

The first two attributes are in technical contradiction because to make exoskeleton for lower limbs stable requires more control advancements and usually more degrees of freedom and thus more expensive components. The new device was designed for people with paraplegia. As it was discussed in the introduction of this chapter the life of the people with some form of paraplegia or tetraplegia changes rapidly, school enrolment and employment rate drop significantly with a global unemployment rate of more than 60% and substantial individual and societal costs emerge. From this statistical report done by World Health Organisation, it's obvious, that the key factor is the price of the device. The second key element is stability. Fear of falling due to low stability was reported as another factor of giving up regular independent walking as discussed in the introduction chapter.

To conclude, @halo is an economical solution due to maximal reduction of powered DOF and control complexity and due to unique construction is at the same time performing well in the terms of stable walking patterns. This makes @halo good candidate for practical everyday home use and thus increases the intensity of actually walking and being in the upright posture, which is so important for the better overall health of people with paraplegia.

9.5 Recommendation for further research

There is not possible to consider this system plugged in the stationary external controller as it is now. Compact lightweight embedded control unit with the battery pack as a part of portable exoskeleton needs to designed and programed as the first step of further development.

The crucial is testing of the device with actual aiming group. Walking patterns of the able-bodied subjects wearing *@halo* exoskeleton were deeply examined during the preliminary experiments. Even though subjects were trained by professional staff to simulate walking patterns accordingly big difference is expected in use by actual people with paraplegia.

The continuity of gait cycle with *@halo* was affected by the short time delay caused by pressing of the manual switch button in order to activate the motor for the next step, disturbance is evident from Figure 8.4. In order to investigate smoothness of the walking, the trajectories of CoG of the body without time dependency in sagittal and horizontal planes during one gait cycle using @halo exoskeleton were plotted and trajectory graphs show smooth history without disturbances, see Figure 9.1. In order to eliminate this delay pressure sensors were sealed in soles of the *@halo* device, these sensors were not used in preliminary experiments. Fully automated walking without the necessity of activating motor by the button is expected while these sensors will be operational. This new functionality will improve smoothness and continuity of walking pattern, this, however, needs to be further tested.
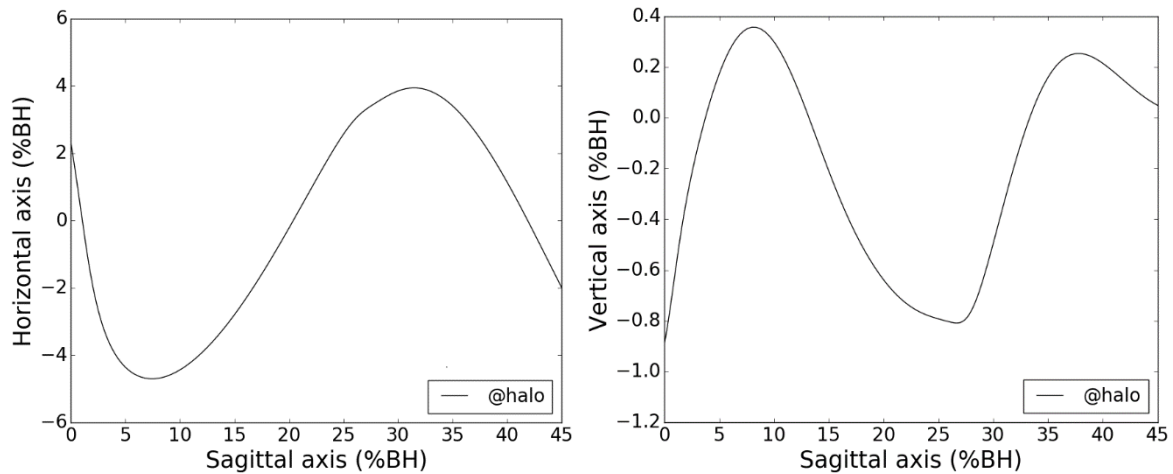
Figure 9.1 Trajectories of CoG in horizontal plane and sagittal plane

The ground reaction force of foot during the heal strike acts partially against velocity vector *v* of the total body CoG, see Figure 9.2. This causes dissipative negative work, which has to be compensated and extra effort needs to be done to continue in forward movement (Kuo and Donelan 2010). Bigger dissipation of energy was noticed during evaluation of GRF in case of active device *@halo*. This dissipation is caused by inertial forces acting on the body during deceleration of the actuator, this effect helps the user easily overcome redirection phase (from one step to another) with minimum effort, but on the other hand, heel impact is less comfortable. To diminish this effect softer cushion insole similar to running shoes can be implemented or completely new design of shoe can be considered (Suzuki et al. 2005). Another approach is the change of trend of reference angle trajectory of the actuator which was experimentally tested, comparison and outputs from this tests should be extended and further examined.
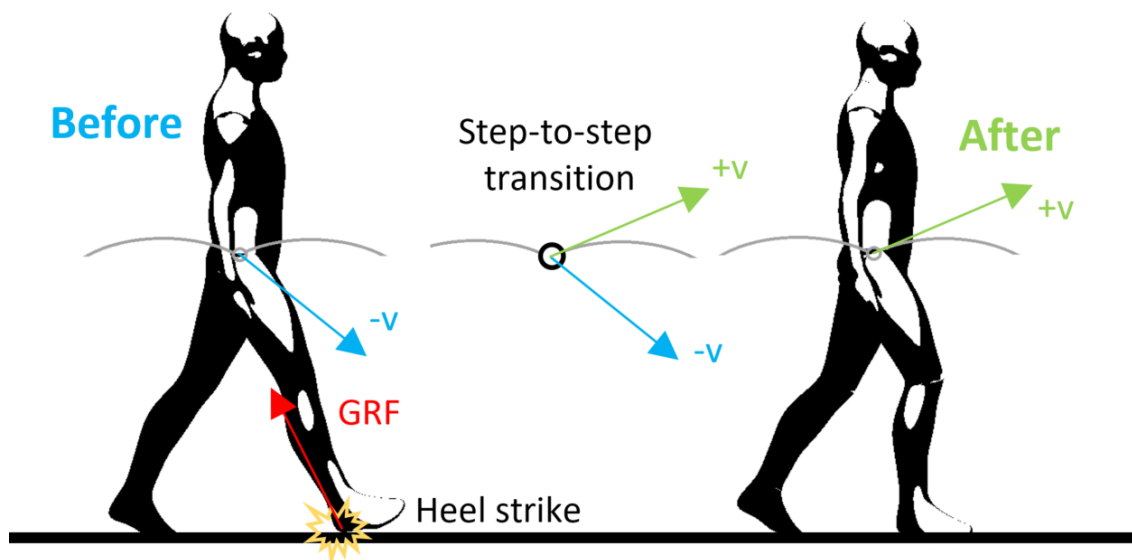
Figure 9.2 Step-to-step transition and redirection of velocity vector

10 Závěry

Dva nové mnou navržené exoskelety aplikovatelné na dolní končetiny a určené pro lidi s paraplegií byly představeny v této práci. Hlavním cílem bylo nalezení ekonomického, odlehčeného a stabilního řešení se sníženou uživatelskou energetickou náročností. Další prioritou je jednoduchá manipulace, obsluha a jednoduché nasazení zařízení na dolní končetiny přímo z invalidního vozíku. Tyto atributy byly v naprosté shodě s benefity *@halo* a proto byl tento exoskelet podroben detailnímu testování na zdravých subjektech a správnost funkce byla vyhodnocována. V této kapitole je popsán krátký závěr z vývoje exoskeletu ORTHOLEG 2.0 a detailní zhodnocení systému *@halo.*

- *Exoskelet ORTHOLEG 2.0*

Hlavním cílem redesignu exoskeletu ORTHOLEG bylo vyvinutí odlehčené verze, jejichž konstrukce sníží spotřebu energie a zvýší pohodlí uživatelů při chůzi. Hmotnost celého zařízení byla snížena o 1/3 na 11,5 kg, zatímco povolená váha uživatele byla zvýšena o 10 kg na 70 kg. Chůze je nyní plynulejší a přirozenější díky novým karbonovým vložkám do bot vyrobeným ze silného, ale pružného prepreg kompozitu z uhlíkových vláken. Přenos energie z ortézy na dolní končetiny a tělo uživatelů byl vylepšen díky novým fixačním prvkům taktéž z prepreg kompozitu z uhlíkových vláken a polymeru Kydex. Kabeláž z pohonů a senzoriky lze jednoduše skrýt do rámu exoskeletu, který je navrhnut z trubkových profilů. Koncepce modulárního kolenního kloubu byla navržena za účelem testování rozdílů ve spotřebě energie a pohodlí uživatele při chůzi s pasivním nebo poháněným kolenním kloubem.

Experimenty s uživateli jsou prioritním dalším krokem, bude se testovat chůze s pasivním, zamknutým a poháněným kolenním kloubem přičemž uživatelská energetická náročnost bude měřena a vyhodnocována stejně jako testování řídících algoritmů chůze.

- *Exoskelet @halo*

Nový aktivní exoskelet *@halo* byl vynalezen na základě principu pasivní ortézy HALO. Nový exoskelet *@halo* má pouze jeden poháněný stupeň volnosti (DOF) a jeho konstrukce je modulární. Uživatel může jednoduše odebrat pohonnou jednotku a chodit pasivně bez pomoci pohonu, pasivní nastavení bez pohonu bylo pro lepší odlišení nazváno *Halo*. Předběžné experimenty se zdravými subjekty byly provedeny za účelem vyhodnocení funkčnosti aktivního systému *@halo* a za účelem porovnání a vyhodnocení chůze mezi pasivní verzí *Halo* a aktivním exoskeletem *@halo*.

Chůze s *Halo* byla rychlejší než s *@halo*, ale délka kroku byla s aktivní verzí mírně delší. Standardní odchylky byly však výrazně vyšší při chůzi bez pohonu. To je částečně způsobeno předem stanoveným cyklem řídícího programu aktivního exoskeletu, ovlivněným konstantními periodami aktivace pohonu. Tyto výsledky lze vyhodnotit následně: Chůze s pohonem je stabilnější pro delší vzdálenosti a pravděpodobnost pádu je výrazně snížena, (SHINODA et al. 2008).

Rozsahy vertikální výchylky CoG během krokového cyklu jsou porovnávány a shrnuty v tabulce 9.1 s celkovou významností (p <0,0001). Nadměrný pohyb nahoru-dolů byl redukován v případě chůze s *@halo* o 40%. Pokud zjednodušíme posouzení spotřeby energie uživatelem, můžeme pak vypočítat pokles spotřeby energie na ušlou vzdálenost v důsledku menších pohybů ve vertikálním směru podle rovnice (9.1), (Lee et al. 2015).

$$P = \frac{m \cdot g \cdot z}{T} \ [Nm/s] \qquad\qquad (9.2)$$

Kde *z* je vertikální odchylka, *m · g* je tíha a *T* je perioda cyklu chůze. Hodnota průměrné tíhy byla konstantní, může být vyloučena z rovnice a výpočet může být z důvodů srovnání dále zjednodušen na výsledek ve vertikální odchylce v jednotkách % BH za sekundu. Výsledky ukazují, že chůze s pohonem vyžaduje 51,65% méně energie spotřebované uživatelem, viz Tabulka 9.1. Rozsah kolébání se při chůzi s pohonem ze strany na stranu byl snížen o 40% ve srovnání s konfigurací *Halo*. Kolébavost chůze je stále asi dvakrát větší než během normální pomalé chůze (Orendurff et al. 2004), nicméně toto nelze eliminovat z důvodu konstrukčního řešení ortézy se zamčenými kolenními klouby.

Během chůze bez motoru byl naměřen o 38,5% větší silový impuls v berlích ve svislém směru než v případě chůze s pohonem. Tento rozdíl byl výrazně kompenzován nadměrným zatížením horních končetin. To bylo dokázáno výpočtem a vyhodnocením krouticích momentů a sil v glenohumerálním kloubu. Zvýšený moment ve směru abdukce v ramenním kloubu může negativně ovlivnit funkčnost deltových svalu a může způsobit jejich pravidelnou únavu při každodenním zatěžování, důkazem je vypočtená hodnota výkonu v kloubu v mediolaterálním směru, což může být výrazně eliminováno při chůzi s aktivním systémem *@halo*. Téměř dvakrát větší extenzní momenty v rameni byly vypočítány při chůzi bez pohonu. Tato skutečnost může během každodenního užívání způsobit bolest nebo přetížení svalů latissimus dorsi.

Po výpočtu síly ve vertikálním směru bylo zjištěno, že dochází k agresivnějšímu zapojení trapézových svalů při pasivní chůzi bez pohonu, tato svalová skupina tedy spotřebovává více energie. Po výpočtu výkonu v glenohumerálním kloubu, můžeme souhrnně říci, že všechny hlavní svalové skupiny jsou agresivněji zapojeny a indikují větší spotřebu energie. Chůze s exoskeletem *@halo* znamená výraznou redukci silového působení na svaly horních končetin a tím snížení pravděpodobnosti výskytu některých onemocnění či bolesti a únavy ramen.

10.1 Přínos pro vědní obor

Byly popsány mnou navržené konstrukční řešení dvou exoskeletů pro paraplegiky a zařízení *@halo* bylo vybráno k podrobnějšímu rozboru. Bylo zhotoveno kompletní konstrukční řešení, návrh elektroniky a softwaru za účelem testování a vyhodnocení prvního funkčního prototypu. Jádrem tohoto vyhodnocení jsou biomechanické metody popsané podrobně krok za krokem v této práci, jejich souhrnné použití reprezentuje unikátní předlohu pro stanovení vhodnosti a bezpečnosti použití daného zařízení cílovou skupinou. V laboratoři bylo provedeno více než 500 experimentálních zkoušek. Byly popsány detailní postupy sběru dat za použití systému analýzy pohybu a jejich dalšího zpracování. V rámci experimentů bylo pro detailnější vyšetření horních a dolních končetin navrženo unikátní modifikované rozložení markerů vycházející z rozložení podle Helen-Hayes. Data byla první předběžně zpracována v programu Cortex a poté vyhodnocena za pomocí programovacího jazyku Python, pro tento účel byl vytvořen nový kód.

Konkrétně byl popsán mnou navržený specifický postup výpočtu takzvaných "ensemble averages", které byly použity k vyšetření pohybu těžiště těla a k analýze reakčních sil působících při chůzi na berle. Pro vyšetření zatížení horních končetin během předběžných experimentů byl popsán a aplikován model inverzní dynamiky.

Tato práce obsahuje kompletní a unikátní metodiku návrhu nového produktu z oblasti asistenčních zdravotnických technologií a ověření jeho funkčnosti, účinnosti a bezpečnosti pro koncové uživatele.

10.2 Přínos pro praxi

Hlavní dvě výhody systému *@halo* jsou cenová dostupnost a stabilita. Nejdůležitějším faktorem pro uživatele tohoto zařízení je intenzita používání. První dva atributy jsou v technickém rozporu, protože pro návrh stabilního exoskeletu je zapotřebí pokročilé řízení a obvykle více stupňů volnosti a tím i dražších komponenty. Nové zařízení bylo navrženo pro lidi s paraplegií. Jak bylo uvedeno v úvodu této práce, život lidí s nějakou formou paraplegie nebo tetraplegie se po nehodě rychle mění, školní docházka a míra zaměstnanosti výrazně klesají, celková míra nezaměstnanosti přesahuje 60%, a objevují se značně navýšené individuální a společenské náklady. Z této statistické zprávy provedené světovou zdravotnickou organizací (WHO) je zřejmé, že klíčovým faktorem zůstává cena zařízení. Druhým klíčovým prvkem je stabilita. Strach z pádu kvůli nízké stabilitě je většinou důvod k tomu vzdát to a místo roboticky asistované chůze se vrátit zpátky na invalidní vozík.

@halo je ekonomicky dostupné řešení díky maximální redukci poháněných stupňů volnosti a zjednodušenému řídicímu systému. Unikátní konstrukční řešení navíc zabezpečuje poměrně vysokou stabilitu chůze. Díky těmto výsledkům může být *@halo* vhodný kandidát pro praktické každodenní používáni z pohodlí domova, čímž také dojde ke zvýšení intenzity chůze a života ve vzpřímené poloze. Následně pak může dojít k celkovému zlepšení zdraví lidí s paraplegií.

10.3 Doporučení pro další výzkum

Současné řešení řídicího systému bylo navrženo z ekonomických důvodů k pouhému ověření funkčnosti zařízení. Takto navřená stacionární řídící jednotka je neslučitelná s praktickým používáním konečného produktu. Proto jako první krok dalšího vývoje je návrh a naprogramování kompaktní odlehčené vestavěné řídicí jednotky s baterií jako součásti přenosného exoskeletu.

Zásadní a neméně důležité je testování zařízení se skutečnou cílovou skupinou. Během předběžných experimentů došlo k detailní analýze chůze s exoskeletem *@halo* pouze se zdravými subjekty. Pro patřičnou simulaci specifické chůze byly subjekty proškoleny profesionálním personálem, i přesto lze však očekávat vysokou odlišnost chůze v porovnání s chůzí paraplegiků.

Kontinuita cyklu chůze se zařízením *@halo* byla ovlivněna krátkým časovým zpožděním způsobeným nepatrnou prodlevou mezi stisknutími ručně ovládaného tlačítka, pro aktivaci motoru k dalšímu kroku, toto narušení kontinuity je patrné z analýzy pohybu těžiště těla diskutované v kapitole 8. Za účelem zkoumání kontinuity chůze byly trajektorie těžiště těla zavedeny do grafů bez závislosti na časech. Byly vytvořeny grafy jednoho cyklu chůze s použitím exoskeletu *@halo* v sagitální a horizontální rovině. Z těchto grafů je patrný hladký průběh bez narušení kontinuity.

Pro eliminaci těchto časových prodlev byly navrženy tlakové senzory (FSR) implementované do podrážek exoskeletu *@halo.* Během předběžných experimentů tyto senzory však nebyly zapojeny a testovány. Po zapojení senzorů do systému lze očekávat plně automatickou chůzi, bez nutnosti manuální aktivace pohonu tlačítkem, tato nová automatická funkce pak zlepší plynulost chůze, toto je však nutné podložit reálnými experimenty. Reakční síly (GRF) chodidla během počátečního kontaktu se zemí částečně působí proti vektoru rychlosti těžiště těla, viz obrázek 9.2. To způsobuje disipativní negativní práci, která pak musí být kompenzována a je třeba vynaložit další úsilí na pokračování v pohybu vpřed (Kuo and Donelan 2010).

Při posuzování reakčních sil v případě aktivního přístroje *@halo* byla zjištěna větší zmařená energie během počátečního kontaktu chodidla se zemí. Tato ztráta je způsobena inerciálními silami působícími na tělo při zpomalování pohonu, což pomáhá uživateli snadno překonat fázi přesměrování (z jednoho kroku na druhý) s minimálním úsilím, ale na druhou stranu je náraz paty při počátečním kontaktu méně komfortní. Pro snížení tohoto účinku lze použít měkkou odpruženou podrážku podobnou běžeckým botám nebo lze přistoupit k zcela novému návrhu ortopedické boty (Suzuki et al. 2005). Další možností jak ovlivnit snížení reakčních sil je změna trendu referenční úhlové trajektorie pohonu, různé úhly rozběhu a zpomalení pohonné jednotky byly experimentálně testovány, porovnání a výstupy z těchto zkoušek by měly být rozšířeny a dále zkoumány.

11 References

ARAÚJO, Marcio Valerio, Pablo Javier ALSINA, Valber Cesar CAVALCANTI ROZA a Nicholas Bastos MELO, 2015. Powered orthosis ortholeg: Design and development. *IEEE Latin America Transactions* [online]. ISSN 15480992. Dostupné z: doi:10.1109/TLA.2015.7040633

BAARDMAN, G, M J LTZERMAN, H J HERMENS, P H VELTINK, H B K BOOM a G ZILVOLD, 1997. The influence of the reciprocal hip joint link in the Advanced Reciprocating Gait Orthosis on standing performance in paraplegia. *Prosthetics and Orrhotics International*. **21**, 210–221.

BREGMAN, D.J.J. J J, M.M. M. VAN DER KROGT, V. DE GROOT, J. HARLAAR, M. WISSE a S.H. H. COLLINS, 2011. The effect of ankle foot orthosis stiffness on the energy cost of walking: A simulation study. *Clinical Biomechanics* [online]. ISSN 02680033. Dostupné z: doi:10.1016/j.clinbiomech.2011.05.007

CUCCURULLO, Sarah J, 2015. *Physical Medicine and Rehabilitation Board Review*. B.m.: Demos Medical Publishing,. ISBN 978-1-620700-39-6.

DE LEVA, Paolo, 1996. Adjustments to Zatsiorsky-Seluyanov's segment inertia parameters. *Journal of Biomechanics* [online]. **29**(9), 1223–1230. ISSN 00219290. Dostupné z: doi:10.1016/0021-9290(95)00178-6

DOLLAR, Aaron M a Hugh HERR, 2008. Lower Extremity Exoskeletons and Active Orthoses: Challenges and State-of-the-Art. *IEEE TRANSACTIONS ON ROBOTICS* [online]. **24**(1). Dostupné z: doi:10.1109/TRO.2008.915453

FAUSTINI, Mario C, RR NEPTUNE, Richard H CRAWFORD a Steven J STANHOPE, 2008. Manufacture of Passive Dynamic ankle-foot orthoses using selective laser sintering. *IEEE transactions on bio-medical engineering* [online]. ISSN 1558-2531. Dostupné z: doi:10.1109/TBME.2007.912638

GENDA, E, 2010. 対麻痺用新歩行装具HALO(Hip and Ankle Linked Orthosis)の歩行効率 [online]. **20**(1), 65–70. Dostupné z: doi:jspo1985.23.65

GENDA, E, K OOTA, Y SUZUKI, K KOYAMA a T KASAHARA, 2004. A new walking orthosis for paraplegics: hip and ankle linkage system. *Prosthetics and Orthotics International*. **28**, 69–74.

HAMILL, J a K M KNUTZEN, 2009. *Biomechanical basis of human movement*. ISBN 0781734053.

HARVEY, Lisa A., Glen M. DAVIS, Merrick B. SMITH a Stella ENGEL, 1998. Energy expenditure during gait using the walkabout and isocentric reciprocal gait orthoses in persons with paraplegia. *Archives of Physical Medicine and Rehabilitation* [online]. ISSN 00039993. Dostupné z: doi:10.1016/S0003-9993(98)90092-2

HIRANO, S., E. SAITOH, H. KAGAYA, Y. SHIMIZU, S. TANABE, M. KATOH a T. TAKEMITSU, 2012. *The energy consumption and the displacement of the center of gravity between primewalk and WPAL*. 2012. ISBN 1545-9683.

KIM, Jung Hoon, Jeong Woo HAN, Deog Young KIM a Yoon Su BAEK, 2013. Design of a walking assistance lower limb exoskeleton for paraplegic patients and hardware validation using CoP. *International Journal of Advanced Robotic Systems* [online]. ISSN 17298806. Dostupné z: doi:10.5772/55336

KUO, A. D. a J. M. DONELAN, 2010. Dynamic Principles of Gait and Their Clinical Implications. *Physical Therapy* [online]. ISSN 0031-9023. Dostupné z: doi:10.2522/ptj.20090125

LEE, Jaeryoung, Ryota MIZUMOTO, Goro OBINATA, Eiichi GENDA, Dimitar STEFANOV, Hirofumi AOKI a Yanling PEI, 2015. Gait generation for powered Hip-Ankle-Linkage-Orthosis. In: *Proceedings of the*

Annual International Conference of the IEEE Engineering in Medicine and Biology Society, EMBS [online]. ISBN 9781424492718. Dostupné z: doi:10.1109/EMBC.2015.7319694

M.T., Karimi, Mohammad Taghi KARIMI a Karimi M.T., 2011. Evidence-Based Evaluation of physiological effects of standing and walking in individuals with spinal cord injury. *Iranian Journal of Medical Sciences*. ISSN 0253-0716.

MARASOVIČ, Tea, Mojmil CECIČ a Vlasta ZANCHI, 2009. Analysis and interpretation of ground reaction forces in normal gait. *WSEAS Transactions on Systems*. ISSN 11092777.

MOORE, P. a J. STALLARD, 1991. A clinical review of adult paraplegic patients with complete lesions using the ORLAU parawalker. *Paraplegia* [online]. ISSN 00311758. Dostupné z: doi:10.1038/sc.1991.27

OBERG, Tommy, Alek KARSZNIA a Kurt OBERG, 1993. Basic gait parameters : Reference data for normal subjects, 10-79 years of age. *Journal of Rehabilitation Research and Development*. **30**(2), 210–223.

ONOGI, KEIKO MD, PHD, KONDO, IZUMI, MD, PHD, SAITOH, EIICHI, MD, DMSC, KATO, MASAKI, OYOBE, Tamaki, 2010. Comparison of the effects of sliding-type and hinge-type joints of knee-ankle-foot orthoses on temporal gait parameters in patients with paraplegia. *Jpn J Compr Rehabil Sci*. **1**.

ORENDURFF, Michael S., Ava D. SEGAL, Glenn K. KLUTE, Jocelyn S. BERGE, Eric S. ROHR a Nancy J. KADEL, 2004. The effect of walking speed on center of mass displacement. *The Journal of Rehabilitation Research and Development* [online]. **41**(6), 829. ISSN 0748-7711. Dostupné z: doi:10.1682/JRRD.2003.10.0150

REQUEJO, Philip S., David P. WAHL, Ernest L. BONTRAGER, Craig J. NEWSAM, JoAnne K. GRONLEY, Sara J. MULROY a Jacquelin PERRY, 2005. Upper extremity kinetics during Lofstrand crutch-assisted gait. *Medical Engineering and Physics* [online]. ISSN 13504533. Dostupné z: doi:10.1016/j.medengphy.2004.08.008

ROBERTSON, Gordon, Graham CALDWELL, Joseph HAMILL, Gary KAMEN a Saunders WHITTLESEY, 2004. *Research methods in biomechanics*. ISBN 0736093400.

ROSE, G K, 1979. The principles and practice of hip guidance articulations. *Prosthetics and orthotics international* [online]. **3**(1), 37–43. ISSN 03093646. Dostupné z: doi:10.3109/03093647909164699

ROUHANI, H., J. FAVRE, X. CREVOISIER a K. AMINIAN, 2014. A wearable system for multi-segment foot kinetics measurement. *Journal of Biomechanics* [online]. ISSN 18732380. Dostupné z: doi:10.1016/j.jbiomech.2014.02.027

SAWICKI, G. S. a D. P. FERRIS, 2009. Powered ankle exoskeletons reveal the metabolic cost of plantar flexor mechanical work during walking with longer steps at constant step frequency. *Journal of Experimental Biology* [online]. ISSN 0022-0949. Dostupné z: doi:10.1242/jeb.017269

SHINODA, Hayato, Haruhiko SATO a Yoshikazu SUZUKI, 2008. *Evaluation of Gait Stability Based on Variability of Medio-Lateral Motion of the Center of Mass* [online]. 2008. ISSN 1341-1667. Dostupné z: doi:10.1589/rika.23.55

SHORTER, Kenneth Alex, Jicheng XIA, Elizabeth T. HSIAO-WECKSLER, William K. DURFEE a G??za F. KOGLER, 2013. *Technologies for powered ankle-foot orthotic systems: Possibilities and challenges* [online]. 2013. ISBN 1083-4435 VO - 18. Dostupné z: doi:10.1109/TMECH.2011.2174799

SHOWERS, David C, C P O MARTHA a L STRUNCK, 1985. Sheet Plastics and Their Applications in Orthotics and Prosthetics.

SLAVENS, Brooke A., Peter F. STURM a Gerald F. HARRIS, 2010. Upper extremity inverse dynamics model for crutch-assisted gait assessment. *Journal of Biomechanics* [online]. ISSN 00219290. Dostupné z: doi:10.1016/j.jbiomech.2010.03.026

SUZUKI, Toru, Shigeru SONODA, Eiichi SAITOH, Motonori MURATA, Akihito UNO, Yasuhiro SHIMIZU, Kayo MISAWA a Tomomitsu KOTAKE, 2005. Development of a novel type of shoe to improve the efficiency of knee-ankle-foot orthoses with a medial single hip joint (Primewalk orthoses): A novel type of shoe for Primewalk orthosis. *Prosthetics and Orthotics International* [online]. ISSN 03093646. Dostupné z: doi:10.1080/03093640500465195

TANABE, Shigeo, Eiichi SAITOH, Satoshi HIRANO, Masaki KATOH, Tomohiko TAKEMITSU, Akihito UNO, Yasuhiro SHIMIZU, Yoshihiro MURAOKA a Toru SUZUKI, 2013. Design of the Wearable Power-Assist Locomotor (WPAL) for paraplegic gait reconstruction. *Disability and Rehabilitation: Assistive Technology* [online]. ISSN 1748-3107. Dostupné z: doi:10.3109/17483107.2012.688238

TIMO BORCHERS, Elena Schumilin, 2010. Custom made shoes. *Orthopädieschuhtechnik* [online]. 20–21. Dostupné z: http://www.ostechnik.de

WALL, Anneli, Jörgen BORG a Susanne PALMCRANTZ, 2015. Clinical application of the Hybrid Assistive Limb (HAL) for gait training - a systematic review. *Frontiers in Systems Neuroscience* [online]. ISSN 1662-5137. Dostupné z: doi:10.3389/fnsys.2015.00048

WINCHESTER, P K, J J CAROLLO, R N PAREKH, L M LUTZ a J W ASTON, 1993. A comparison of paraplegic gait performance using two types of reciprocating gait orthoses. *Prosthetics and Orthotics International*. **17**, 101–106.

12 Published papers

GLOGER, Michal, Pablo J. ALSINA a Nicholas B. MELO, 2016. Ortholeg 2.0 - A new design for a lower limb active orthosis. In: *2015 International Symposium on Micro-NanoMechatronics and Human Science, MHS 2015* [online]. ISBN 9781479966783. Dostupné z: doi:10.1109/MHS.2015.7438347

BASTOS MELO, Nicholas, Carlos Eduardo DOREA, Pablo JAVIER ALSINA, Marcio Valerio ARAUJO a Michal GLOGER, 2017. Ortholeg 2.0 - Design of a Transparent Active Orthosis. *IEEE Latin America Transactions* [online]. **15**(10), 1869–1874. ISSN 1548-0992. Dostupné z: doi:10.1109/TLA.2017.8071229GLOGER,

Michal GLOGER, Goro OBINATA, Eiichi GENDA, Jan BABJAK a Yanling PEI, 2017. Active lower limb orthosis with one degree of freedom for people with paraplegia. In: *2017 International Conference on Rehabilitation Robotics (ICORR)* [online]. B.m.: IEEE, s. 258–263. ISBN 978-1-5386-2296-4. Dostupné z: doi:10.1109/ICORR.2017.8009256

Michal GLOGER, Goro OBINATA, Eiichi GENDA, 2017. Modular active orthosis for lower extremities with one degree of freedom for paraplegics. In: *16th ISPO World Congress 2017* Abstract Book, s. 330–331. ISBN 978-87-93486-01-0, EAN 9788793486010.

13 List of Figures and Tables

13.1 List of Figures

13.2   List of Tables